www.sciencemag.org/cgi/content/full/science.aaw4675/DC1

Supplementary Materials for

Concerted proton-electron transfer reactions in the Marcus inverted region

Giovanny A. Parada, Zachary K. Goldsmith, Scott Kolmar, Belinda Pettersson Rimgard, Brandon Q. Mercado, Leif Hammarström*, Sharon Hammes-Schiffer*, James M. Mayer*

*Corresponding author. Email: james.mayer@yale.edu (J.M.M.); sharon.hammes-schiffer@yale.edu (S.H.-S.); leif.hammarstrom@kemi.uu.se (L.H.)

Published 11 April 2019 on *Science* First Release
DOI: 10.1126/science.aaw4675

This PDF file includes:

Other Supplementary Material for this manuscript includes the following:
(available at www.sciencemag.org/cgi/content/full/science.aaw4675/DC1)

Data S1 and S2 (.xlsx)

Table of Contents

1. Synthesis.

General considerations: The syntheses of triads **1-8** was performed using modifications of our previous synthesis of **6** (*16*) (Figure S1). The first step of the sequence is the condensation of *para*-phenolate aldehydes and anthracenyl lithium reagents. In contrast to our previous synthesis, use of *para*-phenolate aldehydes instead of *para*-anisole aldehydes has the advantage that deprotection of the phenolic hydroxyl group in the last step of the sequence is not required. This results in higher overall yields and better functional group tolerance in the revised synthesis. In addition, switching from a Negishi to a Suzuki-Miyaura coupling with phenol-boryl nucleophiles enables the use of a range of commercially available bromo-pyridine electrophiles.

Materials: The following materials were used without any special purification. 3-bromo-4-hydroxybenzaldehyde (Sigma Aldrich), 9-bromo-anthracene (Sigma Aldrich), n-BuLi 1.6 M in hexane (Sigma Aldrich), triethylsilane (Sigma Aldrich), BF_3•Et_2O (Sigma Aldrich), bis(pinacolato)diboron (Alfa Aesar), $Pd_2(dba)_3$ (Aldrich), tricyclohexylphosphine (Sigma Aldrich), [$Pd(PPh_3)_4$] (Sigma Aldrich), 2-bromo-4- methylpyridine (Across Organics), 2-bromo-4-methoxypyridine (Santa Cruz Chemicals), 2-bromo-4-N-dimethylaminopyridine (Ark Pharm), 2-bromo-4-cyanopyridine (Alfa Aesar), 2-bromo-pyridine (Sigma Aldrich), 2-bromo-4-trifluoromethylpyridine (Alfa Aesar), 2-bromo-6-trifluoromethylpyridine (TCI Chemicals), 9-cyano-10-methyl anthracene (9-CN-10Me-AN) used as a reference for spectro-electrochemistry and transient spectroscopy was synthetized using the literature procedure reported by Torrado *et al.* (*27*). All solvents for synthetic procedures purified using a Glass Contour Solvent Purification System (Pure Process Technology, LLC, Nashua, NH) or purified by standard solvent purification methods (*28*). Colum chromatography was done using silica gel 230-400 mesh, Grade 6 (Fisher Scientific).

Instrumentation: NMR spectra were recorded on Bruker 400, 500 and 600 MHz spectrometers at room temperature. Spectra were referenced internally by the residual solvent proton signal for ^1H NMR and by the solvent signal for ^{13}C NMR spectra. Elemental analyses were performed by Robertson Microlit Laboratories, Ledgewood, NJ. Liquid chromatography mass spectrometry (LCMS) data was obtained on a Waters UPLC/ESI instrument. Samples were eluted over a reverse-phase C18 column (1.7 μm particle size, 2.1 × 50 mm) with a linear gradient of 5% acetonitrile−water containing 0.1% formic acid → 95% acetonitrile−water containing 0.1% formic acid over 1.6 min, followed by 100% acetonitrile containing 0.1% formic acid for 1 min, at a flow rate of 600 μL/min. High resolution mass spectroscopy (HRMS) data was obtained on an Orbitrap XL mass spectrometer (ThermoFisher Scientific) via API electrospray source. The ionization source parameters were: ESI voltage (4 kV); tube lens (125 V); capillary temperature (300 °C) and voltage (20 V); auxiliary and sheath gas flow rate (10 and 11, respectively). MS data were collected in profile mode at a resolution of 100,000 in the Orbitrap detector and for 10 scans in positive mode conditions. The resulting mass spectra are averages over 10 scans. Peak picking and analyses were carried out with Xcalibur Software (v. 2.6). Samples for high resolution mass spectrometry were prepared in acetonitrile with 0.05% formic acid. Solutions were directly injected (at 6 μL/min flow using a 500μL Hamilton Syringe).

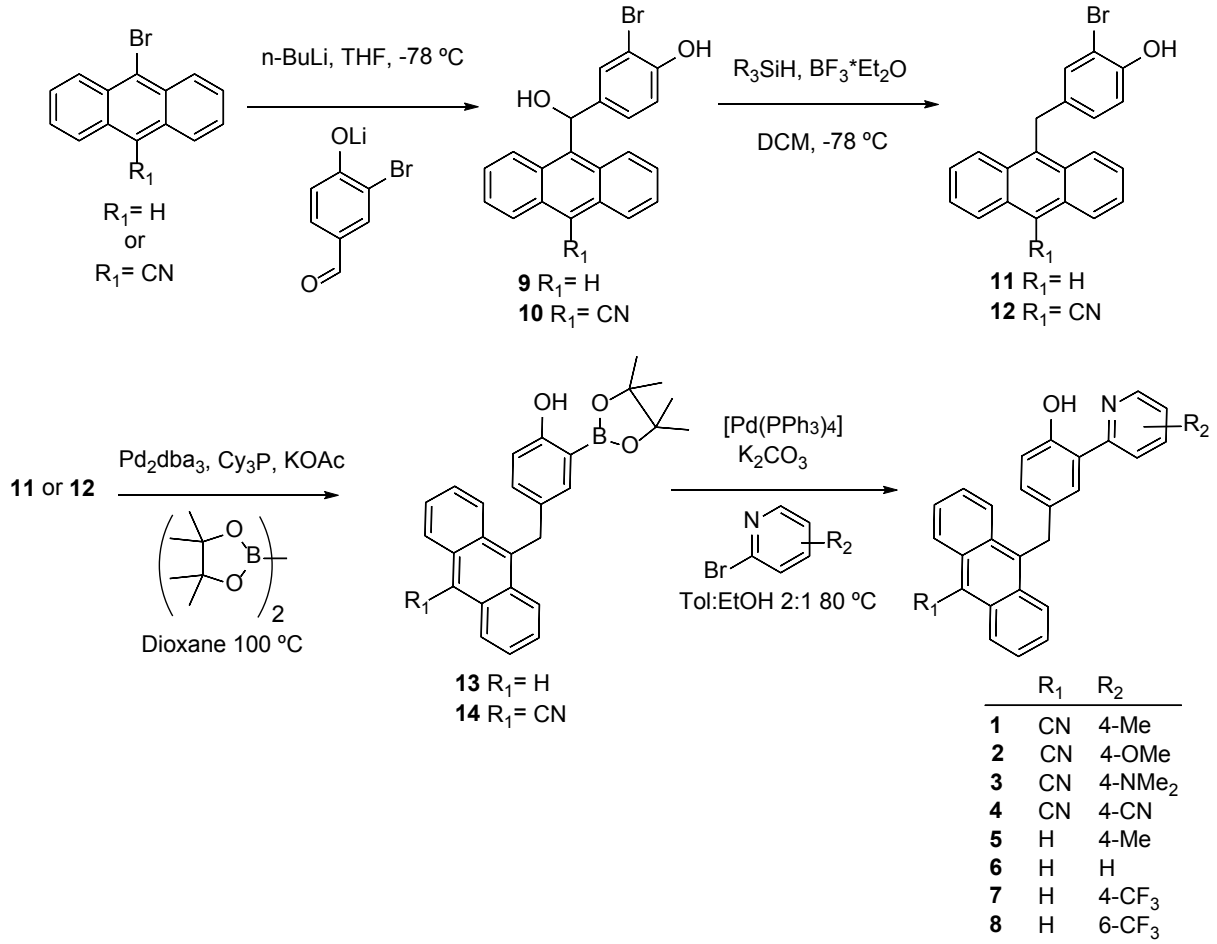

	R_1	R_2
1	CN	4-Me
2	CN	4-OMe
3	CN	4-NMe_2
4	CN	4-CN
5	H	4-Me
6	H	H
7	H	4-CF_3
8	H	6-CF_3

Figure S1. Synthetic route for triads **1**-**8**.

4-(anthracen-9-yl(hydroxy)methyl)-2-bromophenol (**9**): A flame dried Schlenk flask loaded with 2.31 g (11.5 mmol) of 3-bromo-4-hydroxybenzaldehyde and 30 ml of dry THF was cooled to -78 ºC in an acetone/dry ice slurry under nitrogen atmosphere. A second flame dried Schlenk flask was loaded with 2.95 g (11.5 mmol) of 9-bromo-anthracene and 30 ml of dry THF, and then the mixture was also cooled to -78 ºC in an acetone/dry ice slurry under nitrogen atmosphere. 7.9 ml of n-BuLi 1.6 M in hexane were added dropwise over 20 minutes to each of the mixtures. The formed slurries were stirred at -78 ºC for 30 minutes. Next, the slurry of the lithiated anthracenyl was transferred dropwise via a gauge 10 Teflon cannula into the solution of the lithium phenolate, both flasks at -78 ºC vigorously stirred. To aid completing the transfer, 30 ml of dry THF were added to the lithiated anthracenyl flask. Upon completion of the transference, the reaction was stirred overnight allowing it to reach room temperature under nitrogen atmosphere. 5 ml of saturated aqueous NH_4Cl were added. The solvent was evaporated under *vacuum* and the residue was extracted with dichloromethane and brine. The organic extract was dried over anhydrous $MgSO_4$ and concentrated under *vacuum* for further column chromatography on silica gel eluted with n-hexane/ethyl acetate 7:3. The title compound co-eluted in fractions with R_f = 0.25, which were concentrated under *vacuum* yielding 3.74 g of a red oil. The title compound was identified by ^{1}H-NMR and used in subsequent reactions without further purification. ^{1}H-NMR (400 MHz, 298 K, $CDCl_3$): δ 8.51 (s, 1H, Anth), 8.40 – 8.29 (m, 2H, Anth), 8.09 – 8.00 (m, 2H, Anth), 7.60 (dd, J = 2.2, 1.1 Hz, 1H, 3-PhOH), 7.51 – 7.39 (m, 4H, Anth), 7.10 (dd, J=8.4, 2.2, 1H, 5-PhOH), 6.88 (d, J = 8.4 Hz, 1H, 6-PhOH), 5.43 (s, 1H, -CH-), 3.54 (s, br, 1H, O*H*). MS (ESI): Calcd. for $C_{21}H_{14}BrO^+$ $[M\text{-}OH]^+$ 361.02, found 361.05(100%), 363.01(95%) m/z.

10-((3-bromo-4-hydroxyphenyl)(hydroxy)methyl)anthracene-9-carbonitrile (**10**): The title compound was synthetized similarly to **9** starting from 10-bromoanthracene-9-carbonitrile, (*29*) The product was isolated as pale yellow solid. Yield 0.326 g, 28%. ^{1}H-NMR (400 MHz, 298 K, $CDCl_3$): δ 8.50 (d, J = 8.6 Hz, 2H, Anth), 8.45 (d, J = 9.0 Hz, 2H, Anth), 7.70 (ddd, J = 9.0, 8.6, 0.8 Hz, 2H, Anth), 7.57 (s, 1H, OH), 7.55 (ddd, J = 9.0, 8.6, 1.2 Hz, 2H, Anth), 7.36 (d, J = 4.0 Hz, 1H, 3-PhOH), 7.06 (dd, J=8.37, 1.51, 1H, 5-PhOH), 6.90 (d, J = 8.5 Hz, 1H, 6-PhOH), 5.46 (s, 1H –CH-), 5.30 (s, 1H, OH). ^{13}C-NMR (151 MHz, 298 K, $CDCl_3$): δ 151.59, 140.43, 136.59, 133.42, 129.40, 129.21, 128.63, 127.12, 126.88, 126.48, 125.88, 117.39, 116.17, 110.75, 107.86, 69.64, corresponding to 20 aromatic carbon signals (only one set of signals for the peripheral anthracene benzene rings is resolved), and one methylene carbon. HRMS (ESI): Calcd. for $C_{22}H_{13}BrNO^+$ [M-HO]$^+$ 386.0175, found 386.0187(100%), 388.0178(95%) m/z.

4-(anthracen-9-ylmethyl)-2-bromophenol (**11**): A flame dried Schlenk flask loaded with 3.72 g (7.8 mmol, ca. 80% pure) of **9** and 200 ml of dry dichloromethane was cooled to -78 °C in an acetone/dry ice slurry under nitrogen atmosphere. 4.75 mL (30 mmol) of triethylsilane were added dropwise over 5 minutes followed by 3.75 mL (30 mL) of BF_3•Et_2O 48% w/v were added dropwise over 5 minutes. The formed slurry was stirred overnight and allowing it to reach room temperature under nitrogen atmosphere. After this, 5 ml of saturated aqueous NH_4Cl were added and then the mixture was extracted with brine. The organic extract was dried over anhydrous $MgSO_4$ and concentrated under *vacuum*. This yielded a red oil that solidified into a yellow solid standing on the bench. The solid was washed with pentane/diethylether 1:1. The title compound was isolated as pale yellow solid. Yield 1.95 g, 69%. ^{1}H-NMR (500 MHz, 298 K, $CDCl_3$): δ 8.45 (s, 1H, Anth), 8.21 – 8.12 (m, 2H, Anth), 8.09 – 8.00 (m, 2H, Anth), 7.51 – 7.43 (m, 4H, Anth), 7.20 (d, J = 2.2 Hz, 1H, 3-PhOH), 6.95 (dd, J = 8.4, 2.2 Hz, 1H, 5-PhOH), 6.85 (d, J = 8.4 Hz, 1H, 6-PhOH), 5.32 (s, br, 1H, OH), 4.92 (s, 2H, -CH_2-). ^{13}C-NMR (151 MHz, 298 K, $CDCl_3$): δ 150.41, 134.55, 131.64, 131.14, 131.12, 130.41, 129.20, 128.86, 126.84, 126.09, 124.97, 124.50, 115.94, 110.32, 32.33, corresponding to 20 aromatic carbon signals (only one set of signals for the peripheral anthracene benzene rings is resolved), and one methylene carbon. HRMS (ESI): Calcd. for $C_{21}H_{15}BrOH^+$ [M+H$^+$] 363.0379, found 363.0215(100%), 363.0391(95%) m/z.

10-(3-bromo-4-hydroxybenzyl)anthracene-9-carbonitrile (**12**): The title compound was synthetized similarly to **11**, which was isolated as pale yellow solid. Yield 0.205 g, 73%. ^{1}H-NMR (400 MHz, 298 K, $CDCl_3$): δ 8.51 (dt, J = 8.7, 1.1 Hz, 2H, Anth), 8.26 (dt, J = 8.9, 1.1 Hz, 2H, Anth), 7.73 (ddd, J = 8.7, 6.6, 1.1 Hz, 2H, Anth), 7.60 (ddd, J = 8.9, 6.6, 1.2 Hz, 2H, Anth), 7.16 (d, J = 2.0 Hz, 1H, 3-PhOH), 6.92 (dd, J = 8.4, 2.0 1H, 5-PhOH), 6.87 (d, J = 8.4 Hz, 1H, 6-PhOH), 5.35 (s, 1H, OH), 4.98 (s, 2H, -CH_2-). ^{13}C-NMR (151 MHz, 298 K, $CDCl_3$): δ 150.98, 138.84, 133.37, 131.24, 129.95, 128.93, 128.70, 127.24, 126.50, 125.49, 117.62, 116.38, 110.69, 106.11, 33.03, corresponding to 20 aromatic carbon signals (only one set of signals for the peripheral anthracene benzene rings is resolved), and one methylene carbon. HRMS (ESI): Calcd. for $C_{22}H_{14}BrNOH^+$ [M+H$^+$] 388.0332, found 388.0343 (100%), 390.0.323(95%) m/z. Crystals suitable for X-ray crystallography were obtained by slow evaporation of chloroform solutions.

4-(anthracen-9-ylmethyl)-2-(4,4,5,5-tetramethyl-1,3,2-dioxaborolan-2-yl)phenol (**13**): In the glovebox, a microwave vial was loaded with 0.5 g (1.4 mmol) of **10**, 0.387 g (1.5 mmol) of bis(pinacolato)diboron, 0.204 g (2.08 mmol) of potassium acetate, 0.038 g (0.041mmol) $Pd_2(dba)_3$, 0.054 g (0.192 mmol) of tricyclohexylphosphine and 7.5 mL of dioxane. The vial was sealed, brought outside the glovebox to be placed in an oil bath with stirring at 100 °C overnight. After this, the mixture was passed through a Celite filter while washed with dichloromethane. The mixture was

concentrated under *vacuum*. The concentrate was treated with pentane/diethylether 3:1 to yield a pale off-white powder. Attempting further purification by chromatography resulted on product decomposition, at least in part due to deborylation. Hence, the off-white powder obtained from pentane/diethylether 3:1 washing was dried under *vacuum* and used in subsequent reactions without further purification. Yield 0.201 g. ^{1}H-NMR (400 MHz, 298 K, $CDCl_3$): δ 8.42 (s, 1H, Anth), 8.25 – 8.16 (m, 2H, Anth), 8.07 – 7.98 (m, 2H, Anth), 7.71 (d, J = 2.4 Hz, 1H, 3-PhOh), 7.45 (dt, J = 6.5, 3.2 Hz, 4H, Anth), 6.76 (dd, J = 8.5, 2.4 Hz, 1H, 5-PhOH), 6.59 (d, J = 8.5 Hz, 1H, 6-PhOH), 4.93 (s, 2H, -CH_2-), 1.38 (s, 12H, -CH_3).

10-(4-hydroxy-3-(4,4,5,5-tetramethyl-1,3,2-dioxaborolan-2-yl)benzyl)anthracene-9-carbonitrile (**14**): The title compound was synthetized similarly to **13**. Likewise, it was isolated as yellow solid and used in subsequent reactions without further purification. Yield 0.147 g. ^{1}H-NMR (400 MHz, 298 K, $CDCl_3$): δ 8.49 (d, J = 8.7 Hz, 2H, Anth), 8.31 (d, J = 8.9 Hz, 2H, , Anth), 7.71 (ddd, J = 8.7, 6.5, 1.2 Hz, 2H, Anth), 7.63 (d, J = 2.1Hz, 1H, 3-PhOH), 7.57 (ddd, J = 8.9, 6.5, 1.2 Hz, 2H, Anth), 6.74 (dd, J = 8.5, 2.1 Hz, 1H, 5-PhOH), 6.63 (d, J = 8.5 Hz, 1H, 6-PhOH), 4.98 (s, 2H, -CH_2-), 1.37 (s, 12H, -CH_3).

10-(4-hydroxy-3-(4-methylpyridin-2-yl)benzyl)anthracene-9-carbonitrile (**1**): In the glovebox, a microwave vial was loaded with 0.042 g (0.097 mmol, ca. 80% pure) of **14**, 0.005 g (0.005 mmol) of [$Pd(PPh_3)_4$], 13.2 μL (0.116 mmol) of 2-bromo-4- methylpyridine and 3 mL of toluene/ethanol 2:1. The vial was sealed, brought outside the glovebox and 0.15 mL of 2M $K_2CO_{3(aq)}$ were added followed by $N_{2(g)}$ bubbling for 10 minutes. The vial was placed in an oil bath with stirring at 80 ^{o}C for 4 hours. After this, the mixture was extracted with ethyl acetate and water. The organic extract was dried over anhydrous $MgSO_4$ and concentrated under vacuum for further column chromatography on silica gel eluted with n-hexane/ethyl acetate 4:1. The compound was isolated as yellow solid. Yield 0.021 g, 54%. ^{1}H-NMR (500 MHz, 298 K, $CDCl_3$): δ 14.36 (s, 1H, PhO*H*), 8.51 (d, J = 8.6 Hz, 2H, Anth), 8.37 (d, J = 8.9 Hz, 2H, Anth), 8.32 (d, J = 5.2 Hz, 1H, 6-py), 7.72 (ddd, J = 8.6, 6.6, 0.9 Hz, 2H, Anth), 7.59 (ddd, J = 8.8, 6.6, 1.1 Hz, 2H, Anth), 7.59 (d, J = 2.1 Hz, 1H, 3-PhOH), 7.40 (s, 1H, 3-py), 7.02 (d, J = 5.2 Hz, 1H, 5-py), 6.92 (dd, J = 8.5, 2.1 Hz, 1H, 5-PhOH), 6.85 (d, J = 8.5 Hz, 1H, 6-PhOH), 5.04 (s, 2H, -CH_2-), 2.36 (s, 3H, -CH_3). ^{13}C-NMR (126 MHz, 298 K, $CDCl_3$) δ 158.82, 157.31, 149.13, 145.65, 139.95, 133.40, 131.00, 130.05, 129.60, 128.64, 127.01, 126.39, 125.82, 125.40, 122.86, 119.63, 119.02, 118.98, 117.76, 105.73, 33.66, 21.78 corresponding to 23 aromatic carbon signals (only one set of signals for the peripheral anthracene benzene rings is resolved), one methylene carbon, and one methyl carbon. Anal. Calcd. for $C_{28}H_{20}N_2O$: C 83.98; H 5.03; N 7.00, found C 83.49; H 5.11; N 6.92. HRMS (ESI): Calcd. for $C_{28}H_{20}N_2OH^+$ [M+H$^+$] 401.1654, found 401.1676 m/z. Crystals suitable for X-ray crystallography were obtained by slow evaporation of hexanes/ethyl acetate solutions.

10-(4-hydroxy-3-(4-methoxypyridin-2-yl)benzyl)anthracene-9-carbonitrile (**2**)**:** The title compound was synthetized similarly to **1** using intermediate **14** (ca. 80% pure) and 2-bromo-4-methoxypyridine. The purification was done using column chromatography on silica gel eluted with n-hexane/ethyl acetate 4:1.The compound was isolated as yellow solid. Yield 0.035 g, 62%. ^{1}H-NMR (400 MHz, 298 K, $CDCl_3$): δ. 14.39 (s, 1H, PhO*H*), 8.51 (dt, J = 8.7, 1.0 Hz, 2H, Anth), 8.37 (dt, J = 9.0, 1.0 Hz, 2H, Anth), 8.29 (d, J = 5.9 Hz, 1H, 6-py), 7.72 (ddd, J = 8.7, 6.6, 1.1 Hz, 2H, Anth), 7.60 (ddd, J = 8.9, 6.6, 1.3 Hz, 2H, Anth), 7.45 (d, J = 2.4 Hz, 1H, 3-PhOH), 6.97 (d, J = 2.4 Hz, 2H, 3,5-py), 6.86 (d, J = 8.4 Hz, 1H, 5-PhOH), 6.73 (dd, J=8.4, 2.4,1H, 6-PhOH), 5.05 (s, 2H, -CH_2-), 3.80 (s, 3H, -CH_3). ^{13}C-NMR (151 MHz, 298 K, $CDCl_3$) δ 139.32, 133.19, 133.12, 132.30, 131.12, 130.79, 129.81, 129.73, 128.56, 128.54, 127.50, 127.13, 127.03, 126.31, 126.15, 125.67,

125.40, 118.86, 117.50, 117.31, 109.40, 108.87, 105.61, 56.38, 33.06, corresponding to 25 aromatic carbon signals (only one set of signals for the peripheral anthracene benzene rings is resolved), one methylene carbon, and one methyl carbon. Anal. Calcd. for $C_{28}H_{20}N_2O_2$: C 80.75; H 4.84; N 6.73, found C 80.31; H 4.77; N 6.63. HRMS (ESI): Calcd. for $C_{28}H_{20}N_2O_2H^+$ 417.1603 [M+H$^+$], found 417.1628 m/z.

10-(3-(4-(dimethylamino)pyridin-2-yl)-4-hydroxybenzyl)anthracene-9-carbonitrile (**3**): The title compound was synthetized similarly to **1** using intermediate **14** (ca. 80% pure) and 2-bromo-4-N-dimethylaminopyridine. Regular column chromatography on silica gel eluting with hexanes / ethyl acetate mixtures were unsuccessful to isolate the product. Instead, a short silica plug of the reaction mixture concentrate (obtained in a similar workup as for **1**) was dry loaded and eluted with hexanes and ethyl acetate, this allowed elution of the deborylation and other unknown byproducts. This was followed by elution with ethyl acetate / triethylamine 2:1, this allowed desorption of the product from the silica. The organic fraction was concentrated under *vacuum* and further extracted with hot ethyl acetate. Upon cooling, the organic extract was discarded and the yellow precipitate isolated for further extraction with dichloromethane / water to remove triethylammonium salts. The organic extract was dried over anhydrous $MgSO_4$ and then concentrated under *vacuum*. The compound was isolated as yellow solid. Yield 0.018 g, 41%. ^{1}H-NMR (500 MHz, 298 K, CD_2Cl_2): δ 14.80 (s, br, 1H, PhO*H*), 8.46 (ddt, J = 13.0, 8.8, 1.0 Hz, 4H, Anth), 8.02 (d, J = 6.0 Hz, 1H, 6-py), 7.72 (ddd, J = 8.6, 6.6, 1.2 Hz, 2H, Anth), 7.62 (ddd, J = 8.9, 6.6, 1.4 Hz, 2H, Anth), 7.46 (d, J = 2.5 Hz, 1H, 3-PhOH), 6.98 (dd, J = 8.4, 2.3 Hz, 1H, 3-py), 6.74 (d, J = 8.5 Hz, 1H, 5-py), 6.57 (d, J = 2.6 Hz, 1H, 6-PhOH), 6.42 (dd, J = 6.2, 2.6 Hz, 1H, 5-PhOH), 5.06 (s, 2H, -CH_2-), 2.92 (s, 6H, -CH_3). ^{13}C-NMR (101 MHz, 298 K, CD_2Cl_2) δ 159.35, 157.42, 155.47, 145.89, 140.98, 133.64, 130.73, 130.22, 129.33, 128.90, 127.13, 126.45, 126.26, 125.75, 119.68, 118.69, 117.78, 105.80, 105.51, 100.55, 39.35, 33.51, corresponding to 25 aromatic carbon signals (only one set of signals for the peripheral anthracene benzene rings is resolved), one methylene carbon and two methyl carbons (only one methyl carbon is resolved). Anal. Calcd. for $C_{29}H_{23}N_3O$: C 81.09; H 5.40; N 9.78, found C 80.76; H 5.51; N 9.61. HRMS (ESI): Calcd. for $C_{29}H_{23}N_3OH^+$ [M+H$^+$] 430.1919, found 430.1942 m/z. Crystals suitable for X-ray crystallography were obtained by slow evaporation of dichloromethane solutions.

2-(5-((10-cyanoanthracen-9-yl)methyl)-2-hydroxyphenyl)isonicotinonitrile (**4**): The title compound was synthetized similarly to **1** using intermediate **14** (ca. 80% pure) and 2-bromo-4-cyanopyridine. The purification was done using column chromatography on silica gel eluted with n-hexane/ethyl acetate 4:1.The compound was isolated as yellow solid. Yield 0.038 g, 63%. ^{1}H-NMR (400 MHz, 298 K, $CDCl_3$): δ 13.17 (s, 1H, PhO*H*), 8.65 (dd, J = 5.2, 1.0 Hz, 1H, 6-py), 8.53 (dt, J = 8.7, 1.0 Hz, 2H, Anth), 8.33 (dt, J = 8.9, 1.0 Hz, 2H, Anth), 7.83 (t, J = 1.3 Hz, 1H, 3-py), 7.74 (ddd, J = 8.7, 6.6, 1.2 Hz, 2H, Anth), 7.61 (ddd, J = 9.0, 6.6, 1.3 Hz, 2H, Anth), 7.55 (d, J = 2.4 Hz, 1H, 3-PhOH), 7.42 (dd, J = 5.2, 1.4 Hz, 1H, 5-py), 7.02 (dd, J = 8.6, 2.3 Hz, 1H, 5-PhOH), 6.90 (d, J = 8.6 Hz, 1H, 6-PhOH), 5.06 (s, 2H, -CH_2-). ^{13}C-NMR (101 MHz, 298 K, $CDCl_3$) δ 159.03, 158.67, 147.45, 139.16, 133.41, 132.73, 130.65, 130.02, 128.73, 127.22, 126.59, 125.60, 125.56, 125.52, 122.60, 122.44, 121.53, 119.64, 117.63, 117.59, 116.27, 106.14, 33.56, corresponding to 25 aromatic carbon signals (only one set of signals for the peripheral anthracene benzene rings is resolved), and one methylene carbon. Anal. Calcd. for $C_{28}H_{17}N_3O$: C 81.73; H 4.16; N 10.21, found C 81.48; H 4.21; N 10.12. HRMS (ESI): Calcd. for $C_{28}H_{17}N_3OH^+$ [M+H$^+$] 412.1450, found 412.1477 m/z.

4-(anthracen-9-yl-methyl)-2-(4-methylpyridin-2-yl)phenol (**5**): The title compound was

synthetized similarly to **1** using **13** (ca. 90% pure) and 2-bromo-4-methylpyridine with purification employing column chromatography on silica gel eluted with n-hexane/ethyl acetate 8:1. The compound was isolated as an off-white solid. Yield 0.049 g, 31%. ^{1}H-NMR (400 MHz, 298 K, $CDCl_3$): δ 14.31 (s, 1H, PhO*H*), 8.45 (s, 1H, Anth), 8.34 – 8.23 (m, 3H, Anth, 6-py), 8.10 – 8.01 (m, 2H, Anth), 7.65 (d, J = 2.4 Hz, 1H, py), 7.52 – 7.42 (m, 5H, Anth, 3-PhOH), 7.03 – 6.94 (m, 2H, 5-py, 5-PhOH), 6.84 (d, J = 8.4 Hz, 1H, 6-PhOH), 5.00 (s, 2H, -CH_2-), 2.35 (s, 3H). ^{13}C-NMR (151 MHz, 298 K, $CDCl_3$) δ 156.06, 141.80, 132.86, 132.44, 131.77, 131.75, 130.60, 130.58, 129.26, 127.50, 126.82, 126.25, 125.15, 124.92, 123.67, 119.09, 117.19, 32.77, 22.25, corresponding to 25 aromatic carbon signals (only one set of signals for the peripheral anthracene benzene rings is resolved), one methylene carbon, and one methyl carbon. Anal. Calcd. for $C_{27}H_{21}NO$: C 86.37; H 5.64; N 3.73, found C 85.21; H 5.98; N 3.46. HRMS (ESI): Calcd. for $C_{27}H_{21}NOH^+$ [M+H^+] 376.1701, found 376.1723 m/z. Crystals suitable for X-ray crystallography were obtained by slow evaporation of chloroform solutions.

4-(anthracen-9-ylmethyl)-2-(pyridin-2-yl)phenol (**6**): The title compound was synthetized similarly to **1** using **13** (ca. 90% pure) and 2-bromo-pyridine with purification employing column chromatography on silica gel eluted with n-hexane/ethyl acetate 4:1. The title compound was isolated as an off-white power. Yield 0.089 g, 64 %. ^{1}H-NMR (500 MHz, 298 K, $CDCl_3$): δ 14.10 (s, 1H, PhO*H*), 8.48 – 8.41 (m, 2H, Anth, 6-py), 8.32 – 8.22 (m, 2H, Anth), 8.08 – 8.03 (m, 2H, Anth), 7.68 (td, J = 8.3, 1.8 Hz, 1H, py), 7.56 – 7.51 (m, 2H, 3-py, 3-PhOH), 7.51 – 7.44 (m, 4H, Anth), 7.16 (ddd, J = 7.6, 7.5, 0.8 Hz , 1H, py), 7.08 (dd, J = 8.5, 2.0 Hz, 1H, 5-PhOH), 6.88 (d, J = 8.5 Hz, 1H, 6-PhOH), 5.00 (s, 2H, -CH_2-). ^{1}H-NMR (126 MHz, 298 K, $CDCl_3$): δ 158.40, 158.01, 145.97, 137.73, 132.24, 131.93, 131.55, 131.05, 130.76, 129.31, 126.73, 126.09, 125.58, 125.11, 124.98, 121.44, 119.18, 118.84, 118.82, 33.08, corresponding to 25 aromatic carbon signals (only one set of signals for the peripheral anthracene benzene rings is resolved), and one methylene carbon. All of the spectra match literature values (*16*).

4-(anthracen-9-ylmethyl)-2-(4-(trifluoromethyl)pyridin-2-yl)phenol (**7**): The title compound was synthetized similarly to **1** using **13** (ca. 90% pure) and 2-bromo-4- trifluoromethylpyridine. The title compound was synthetized similarly to **1** with purification employing column chromatography on silica gel eluted with n-hexane/ethyl acetate7:3. The compound was isolated as an off-white solid. Yield 0.049 g, 30%. ^{1}H-NMR (500 MHz, 298 K, $CDCl_3$): δ 13.30 (s, 1H, PhO*H*), 8.64 (d, J = 5.2 Hz, 1H, 6-py), 8.46 (s, 1H, Anth), 8.31 – 8.22 (m, 2H, Anth), 8.09 – 8.03 (m, 2H, Anth), 7.83 (s, 1H, 3-py), 7.69 (d, J = 2.3 Hz, 1H, 3-PhOH), 7.48 (m, 4H, Anth), 7.40 (d, J = 5.2, 1H, 5-py), 7.01 (dd, J = 8.6, 2.3 Hz, 1H, 5-PhOH), 6.85 (d, J = 8.5 Hz, 1H, 6-PhOH), 5.02 (s, 2H, -CH_2-). ^{13}C-NMR (151 MHz, 298 K, $CDCl_3$) δ 159.30, 158.24, 147.39, 140.27, 140.04, 139.82, 139.59, 132.45, 131.88, 131.85, 131.53, 130.60, 129.37, 126.88, 126.17, 125.93, 125.11, 124.76, 123.59, 121.78, 119.05, 117.92, 116.96, 116.91, 116.89, 115.14, 32.80, corresponding to 25 aromatic carbon signals (only one set of signals for the peripheral anthracene benzene rings is resolved), one –CF_3 (quartet), and one methylene carbon. Anal. Calcd. for $C_{27}H_{18}F_3NO$: C 75.52; H 4.23; N 3.26, found C 75.08; H 4.31; N 3.58. HRMS (ESI): Calcd. for $C_{27}H_{18}F_3NOH^+$ [M+H^+] 430.1419, found 430.1444 m/z.

4-(anthracen-9-ylmethyl)-2-(6-(trifluoromethyl)pyridin-2-yl)phenol (**8**): The title compound was synthetized similarly to **1** using **13** (ca. 90% pure) and 2-bromo-6- trifluoromethylpyridine. The title compound was synthetized similarly to **1** with purification employing column chromatography on silica gel eluted with n-hexane/ethyl acetate 7:3. The compound was isolated as an off-white solid. Yield 0.035 g, 33%. ^{1}H-NMR (500 MHz, 298 K, $CDCl_3$): δ 12.64 (s, 1H, PhO*H*), 8.46 (s, 1H, Anth), 8.28 – 8.21 (m, 2H, Anth), 8.10 – 8.03 (m, 2H, Anth), 7.83 (dd, J = 8.4, 8.1 Hz, 1H, 4-py),

7.64 (d, J = 8.4 Hz, 1H, *m*-py), 7.51 (d, J = 8.1 Hz, 1H, *m*-py), 7.50 – 7.45 (m, 5H, Anth, 3-PhOH), 7.17 (dd, J = 8.5, 2.3 Hz, 1H, 5-PhOH), 6.93 (d, J = 8.4 Hz, 1H, 6-PhOH), 5.00 (s, 2H, -CH_2-). ^{13}C-NMR (101 MHz, 298 K, $CDCl_3$) δ 158.33, 157.94, 145.74, 145.39, 145.03, 144.68, 139.01, 132.59, 131.85, 131.83, 131.67, 130.67, 129.35, 126.86, 126.19, 125.95, 125.15, 124.81, 122.17, 119.16, 118.01, 117.98, 117.95, 117.92, 29.86, corresponding to 25 aromatic carbon signals (only one set of signals for the peripheral anthracene benzene rings is resolved), one –CF_3 (quartet), and one methylene carbon. Anal. Calcd. for $C_{27}H_{18}F_3NO$: C 75.52; H 4.23; N 3.26, found 74.63; H 4.47; N 3.08. HRMS (ESI): Calcd. for $C_{27}H_{18}F_3NOH^+$ [M+H^+] 430.1419, found 430.1444 m/z.

2. NMR Spectra.

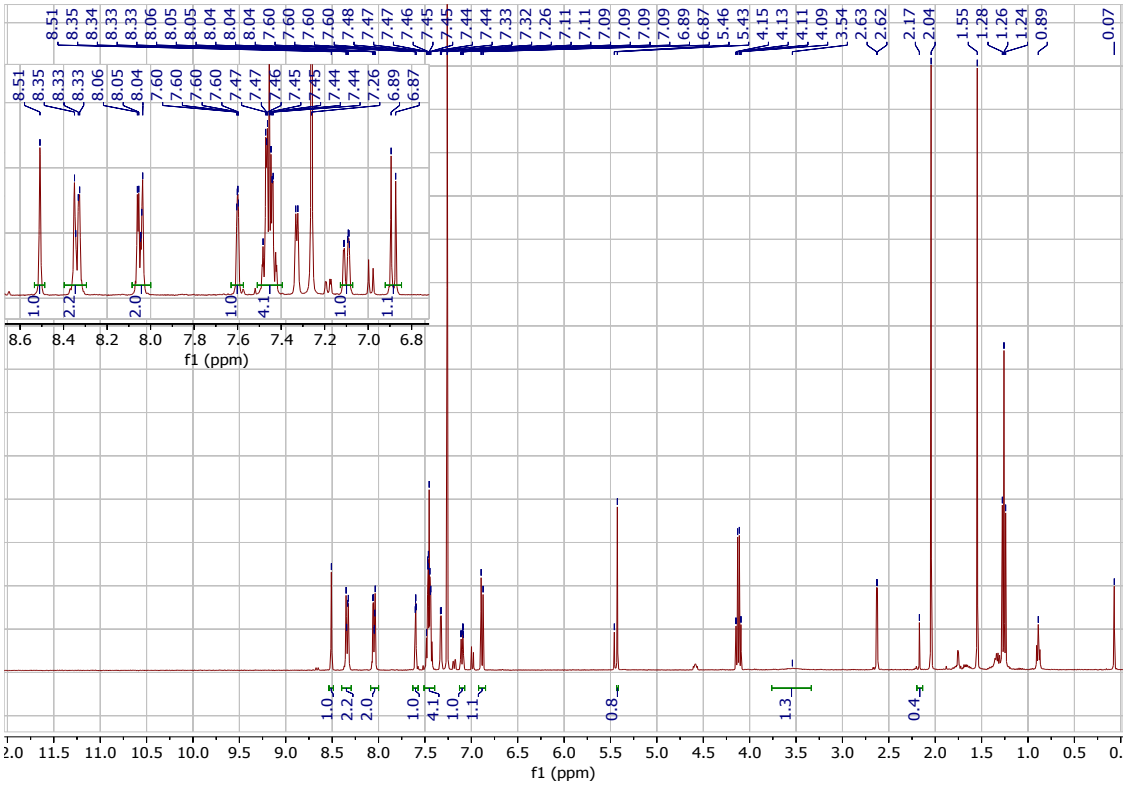

Figure S2. ^{1}H-NMR $CDCl_3$ 4-(anthracen-9-yl(hydroxy)methyl)-2-bromophenol (**9**).

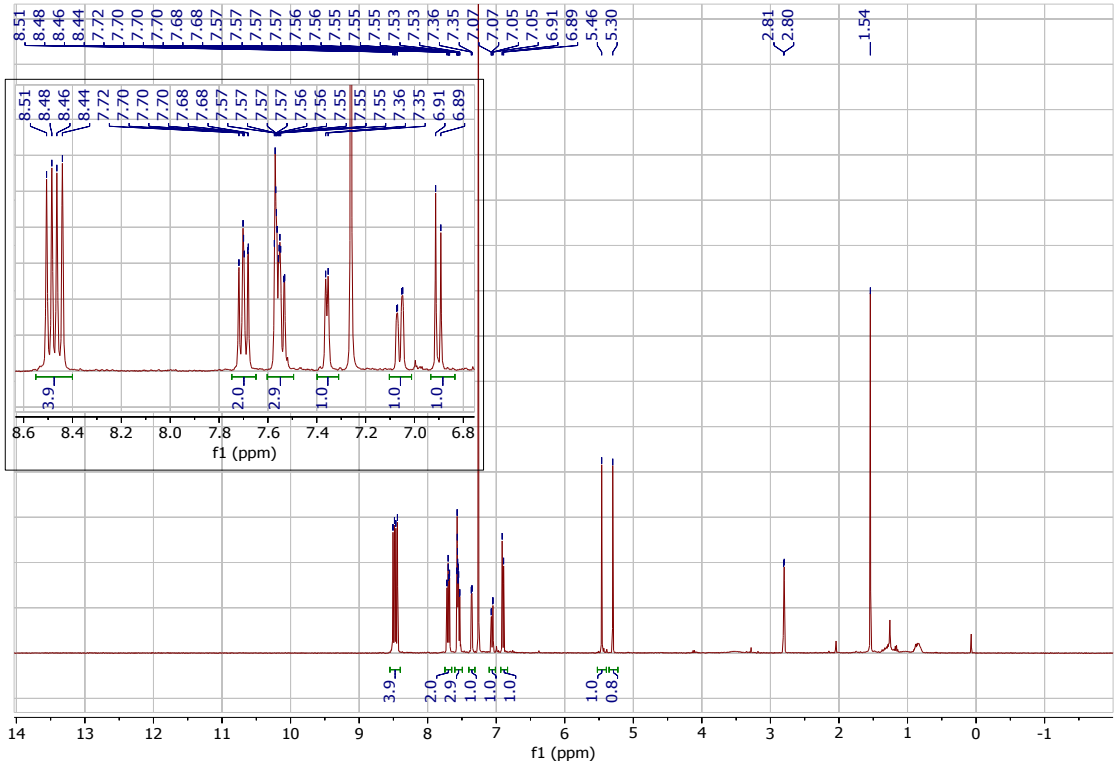

Figure S3. ^{1}H-NMR $CDCl_3$ 10-((3-bromo-4-hydroxyphenyl)(hydroxy)methyl)anthracene-9-carbonitrile (**10**).

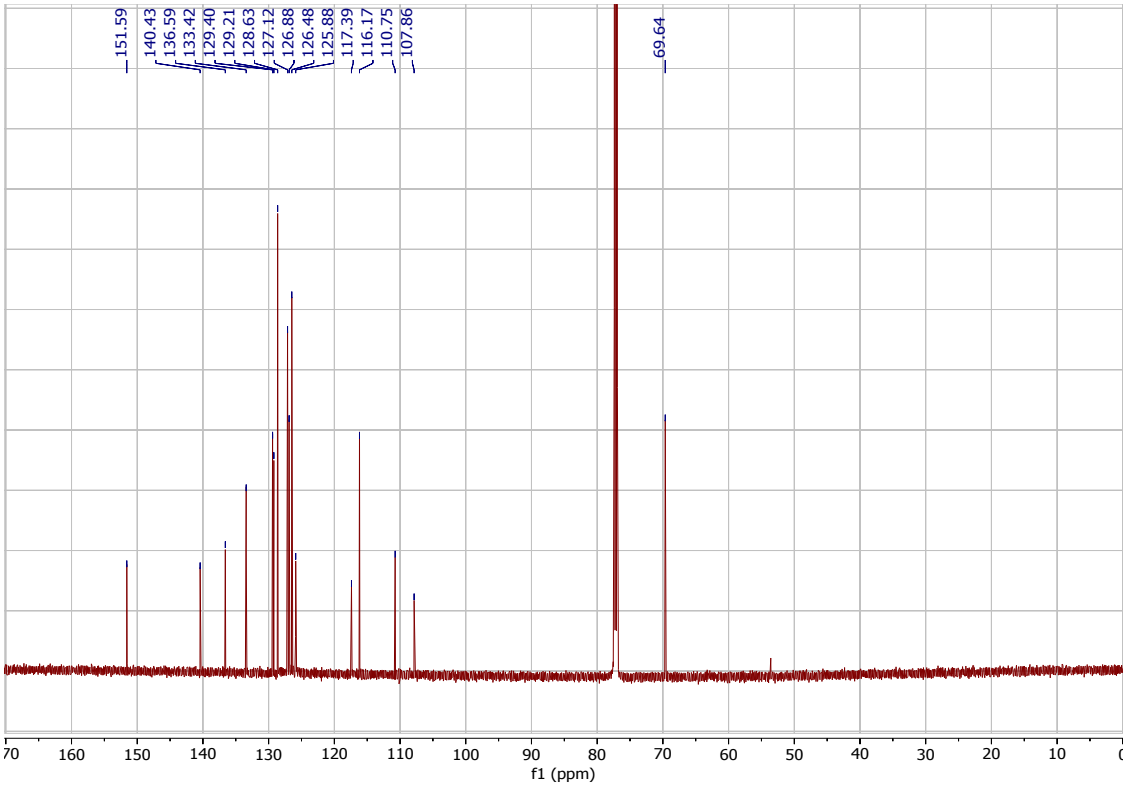

Figure S4. ^{13}C-NMR $CDCl_3$ 10-((3-bromo-4-hydroxyphenyl)(hydroxy)methyl)anthracene-9-carbonitrile (**10**).

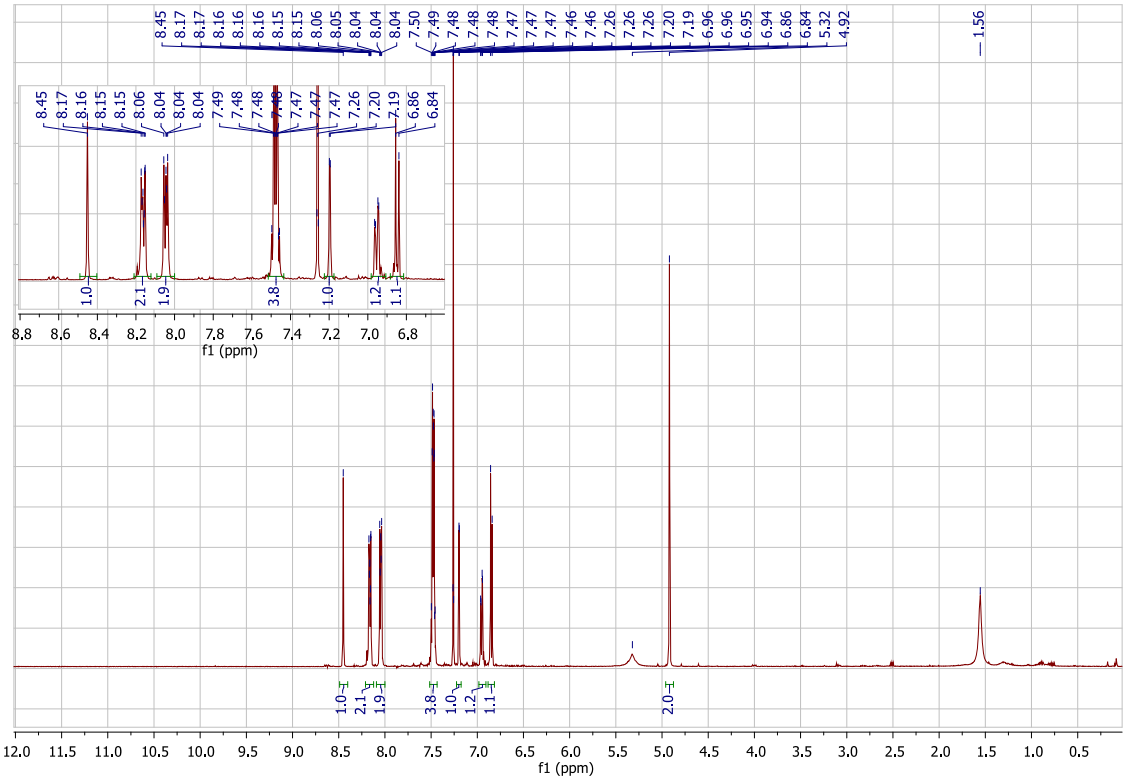

Figure S5. ^{1}H-NMR $CDCl_3$ 4-(anthracen-9-ylmethyl)-2-bromophenol (**11**).

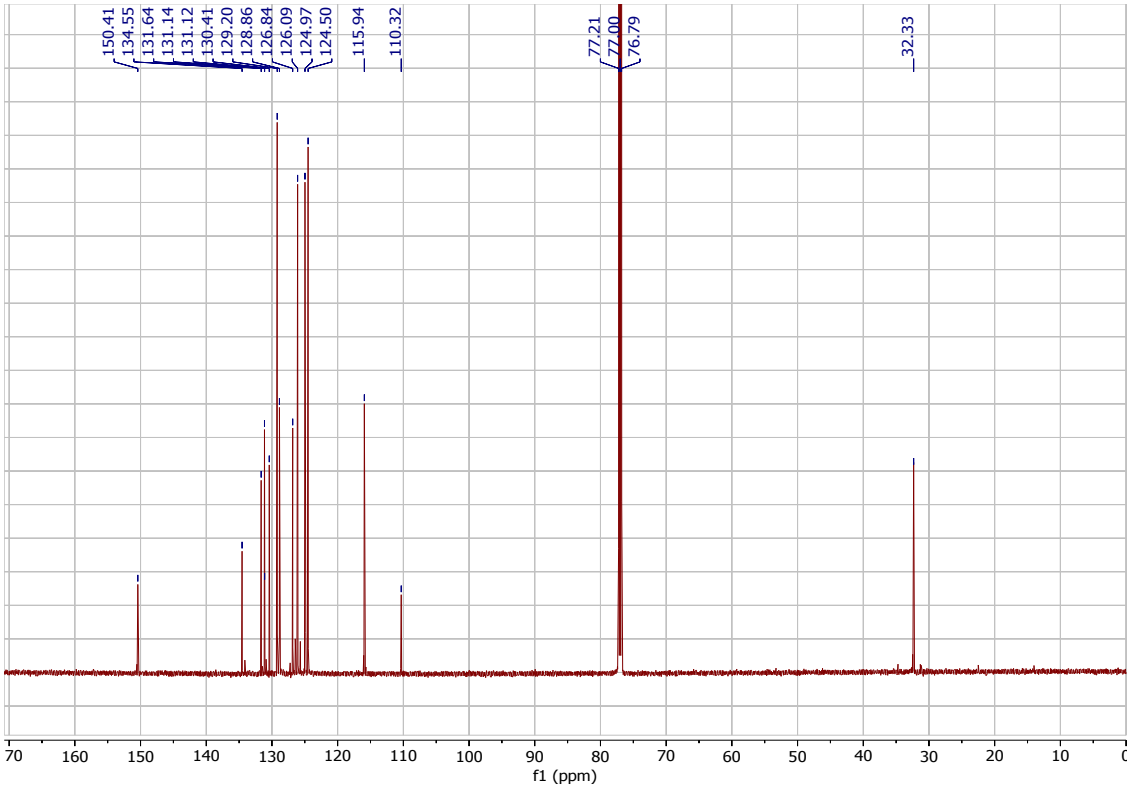

Figure S6. ^{13}C-NMR $CDCl_3$ 4-(anthracen-9-ylmethyl)-2-bromophenol (**11**).

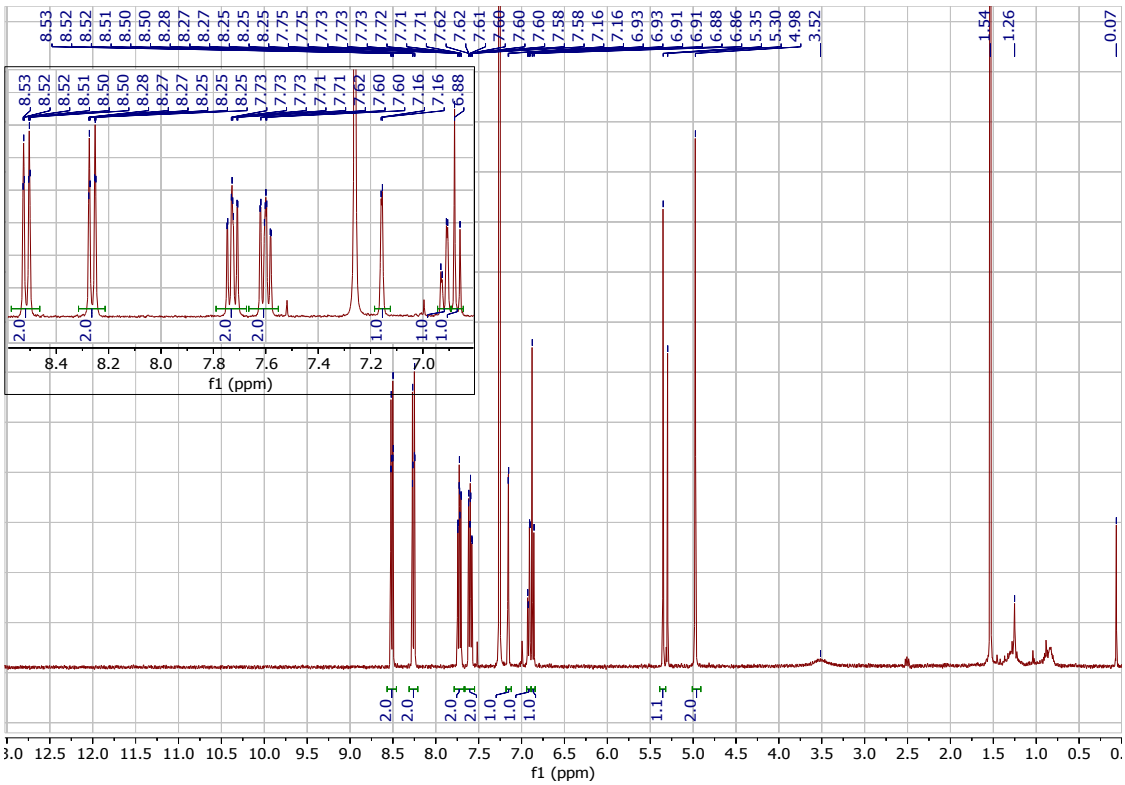

Figure S7. ^{1}H-NMR $CDCl_3$ 10-(3-bromo-4-hydroxybenzyl)anthracene-9-carbonitrile (**12**).

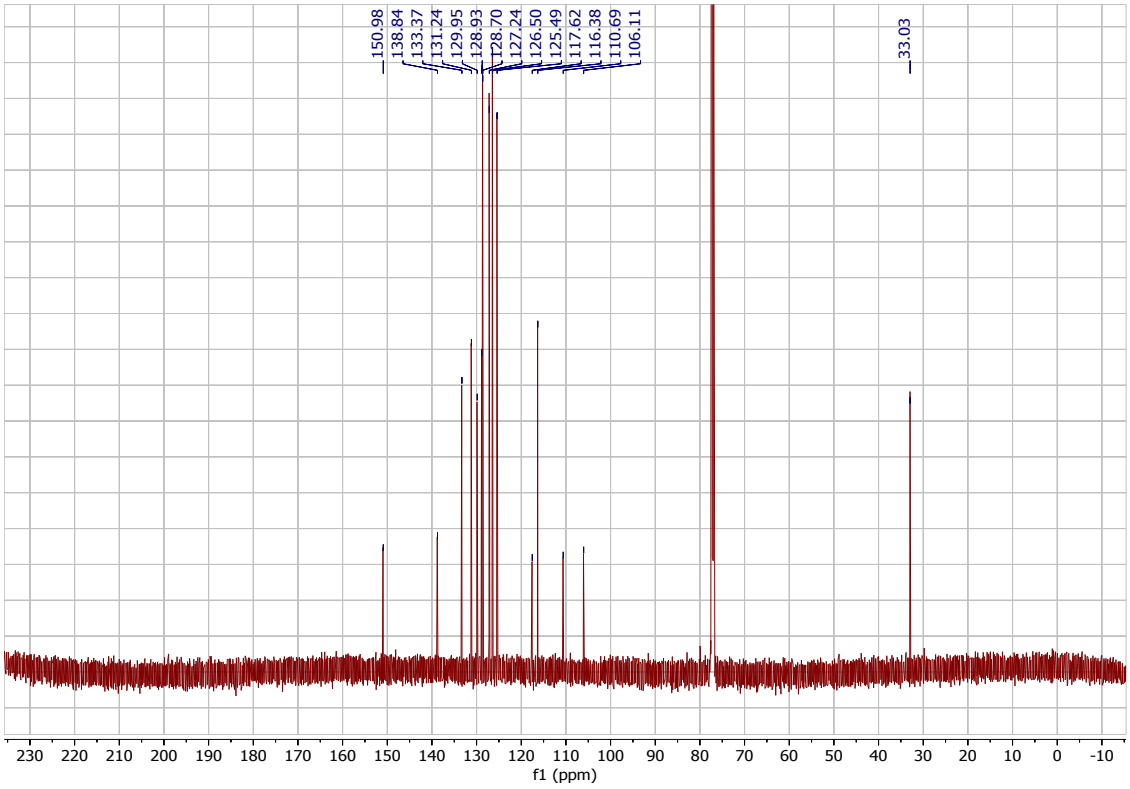

Figure S8. ^{13}C-NMR $CDCl_3$ 10-(3-bromo-4-hydroxybenzyl)anthracene-9-carbonitrile (**12**).

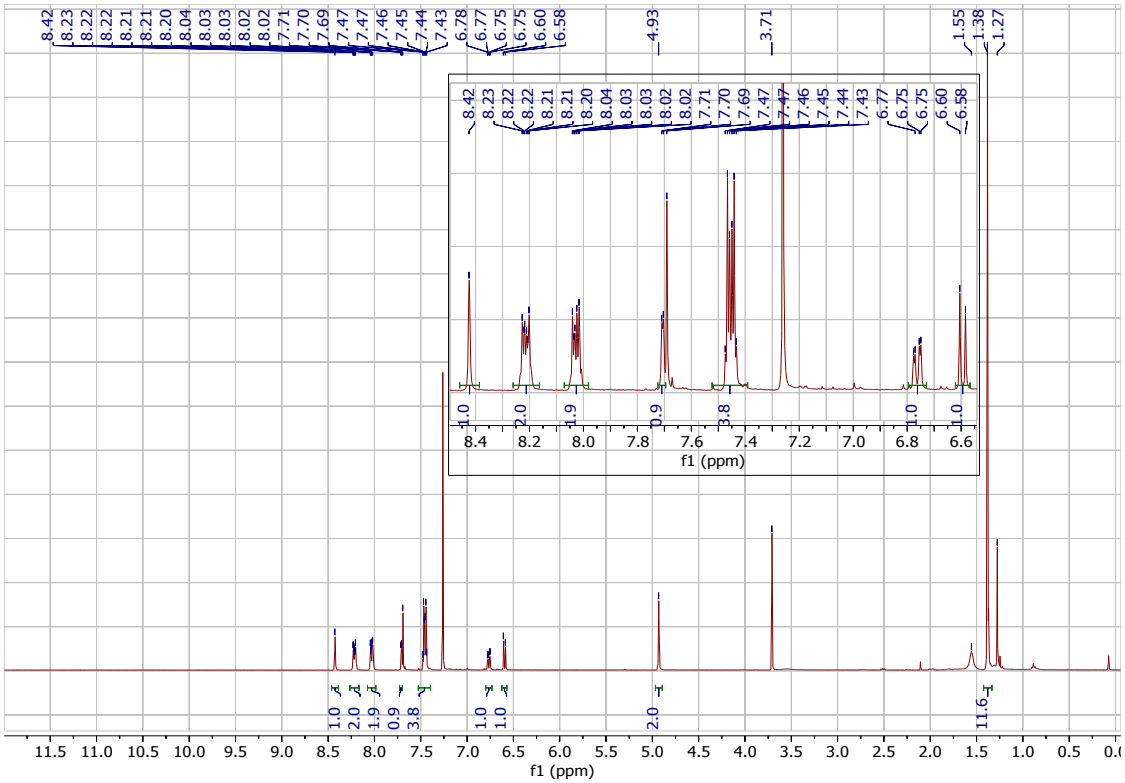

Figure S9. ^{1}H-NMR $CDCl_3$ 4-(anthracen-9-ylmethyl)-2-(4,4,5,5-tetramethyl-1,3,2-dioxaborolan-2-yl)phenol (**13**).

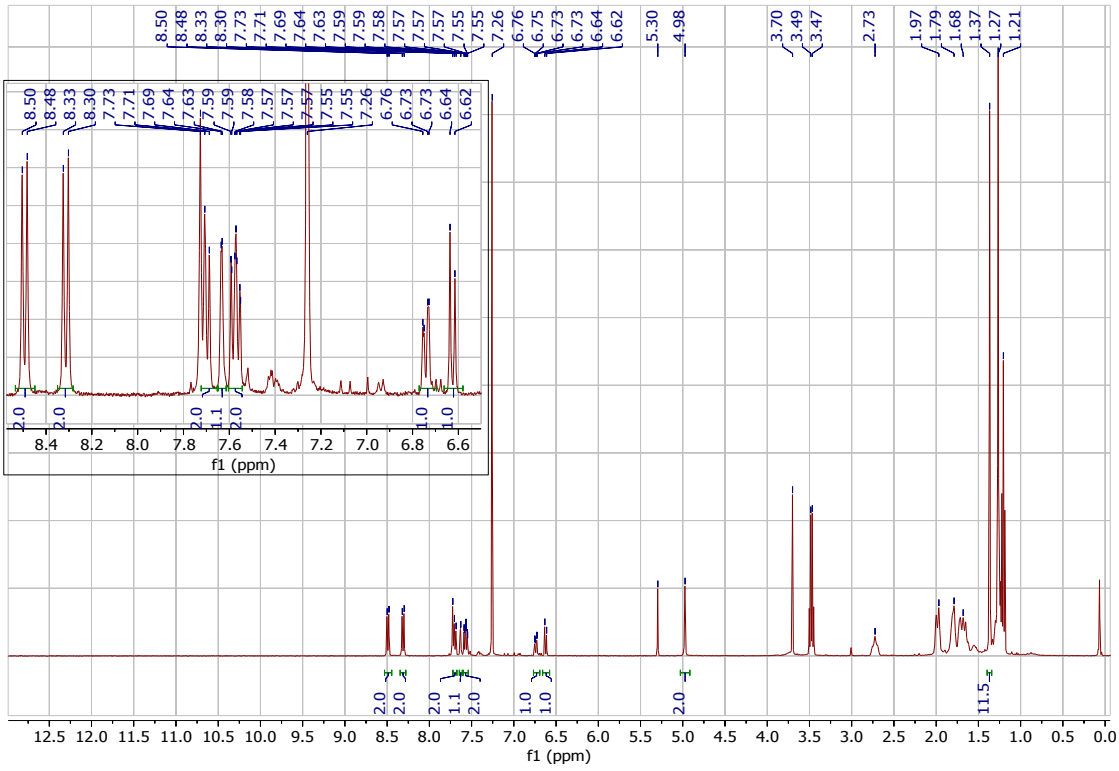

Figure S10. ^{1}H-NMR $CDCl_3$ 10-(4-hydroxy-3-(4,4,5,5-tetramethyl-1,3,2-dioxaborolan-2-yl)benzyl)anthracene-9-carbonitrile (**14**).

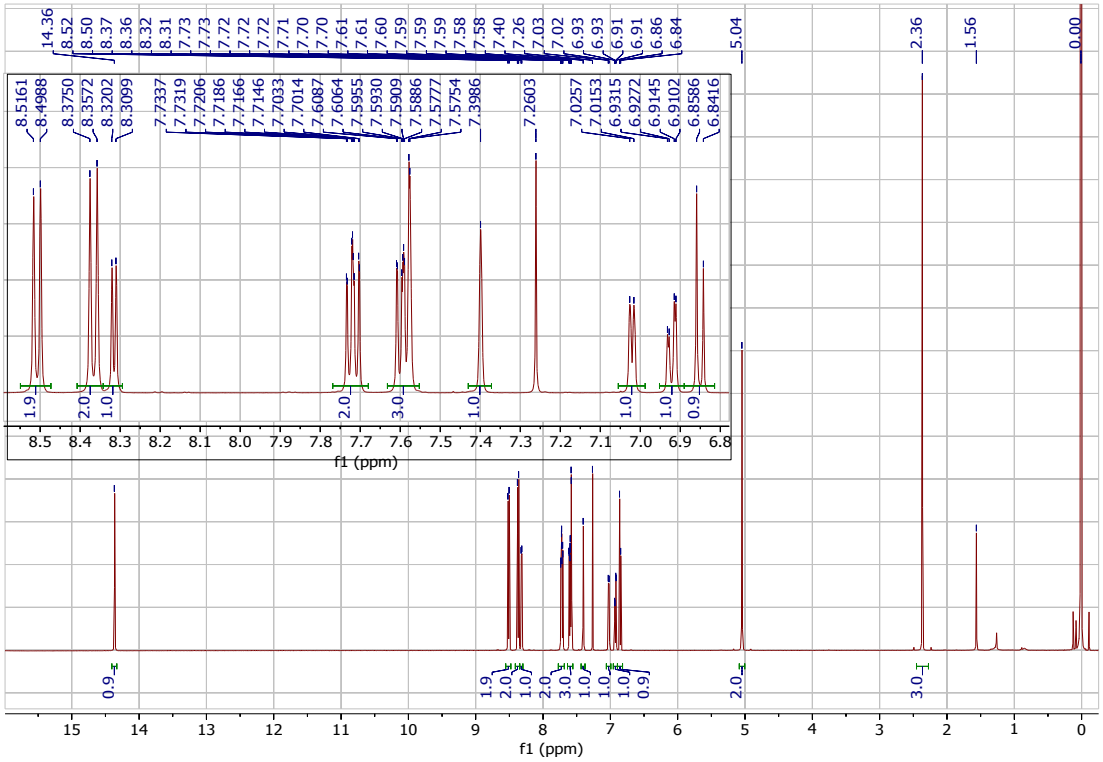

Figure S11. ^{1}H-NMR $CDCl_3$ 10-(4-hydroxy-3-(4-methylpyridin-2-yl)benzyl)anthracene-9-carbonitrile (**1**).

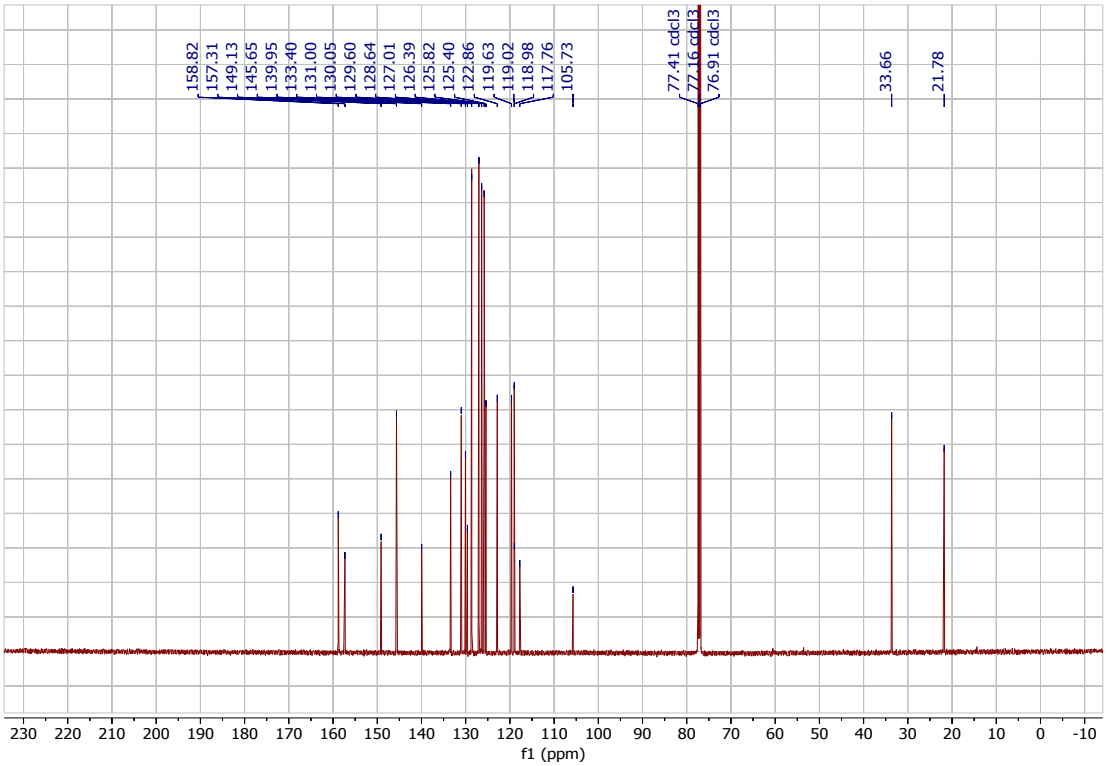

Figure S12. ^{13}C-NMR $CDCl_3$ 10-(4-hydroxy-3-(4-methylpyridin-2-yl)benzyl)anthracene-9-carbonitrile (**1**).

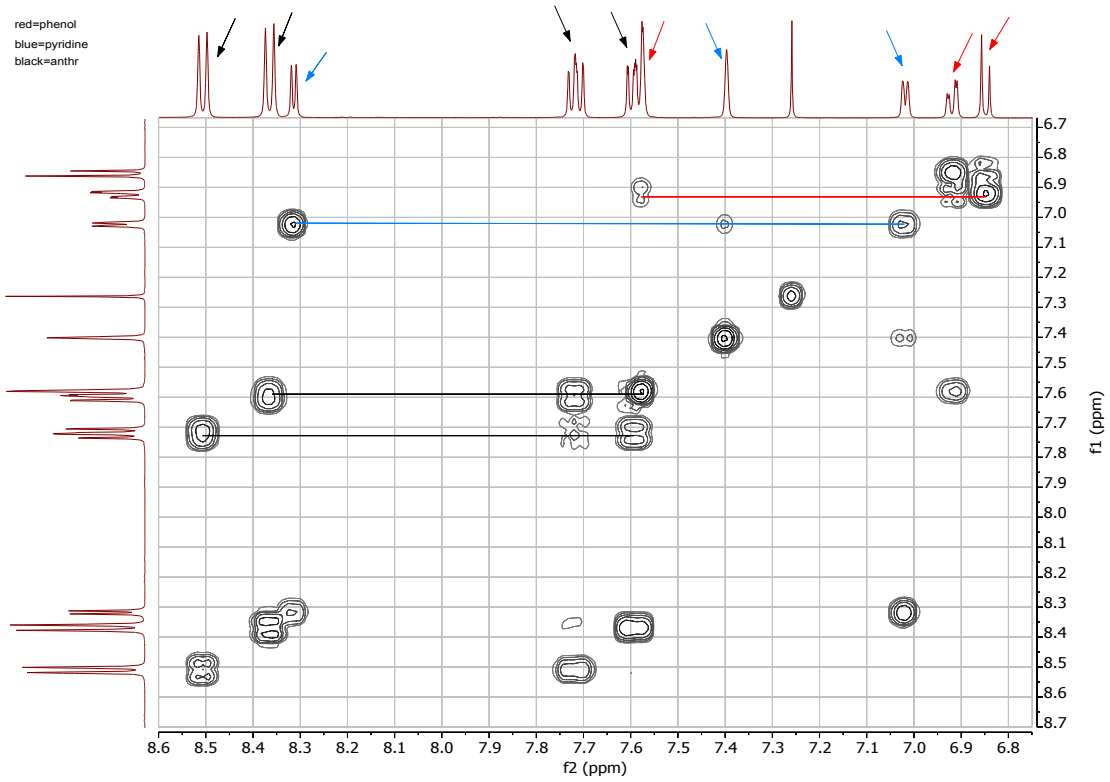

Figure S13. COSY ^{1}H-^{1}H-NMR $CDCl_3$ 10-(4-hydroxy-3-(4-methylpyridin-2-yl)benzyl)anthracene-9-carbonitrile (**1**).

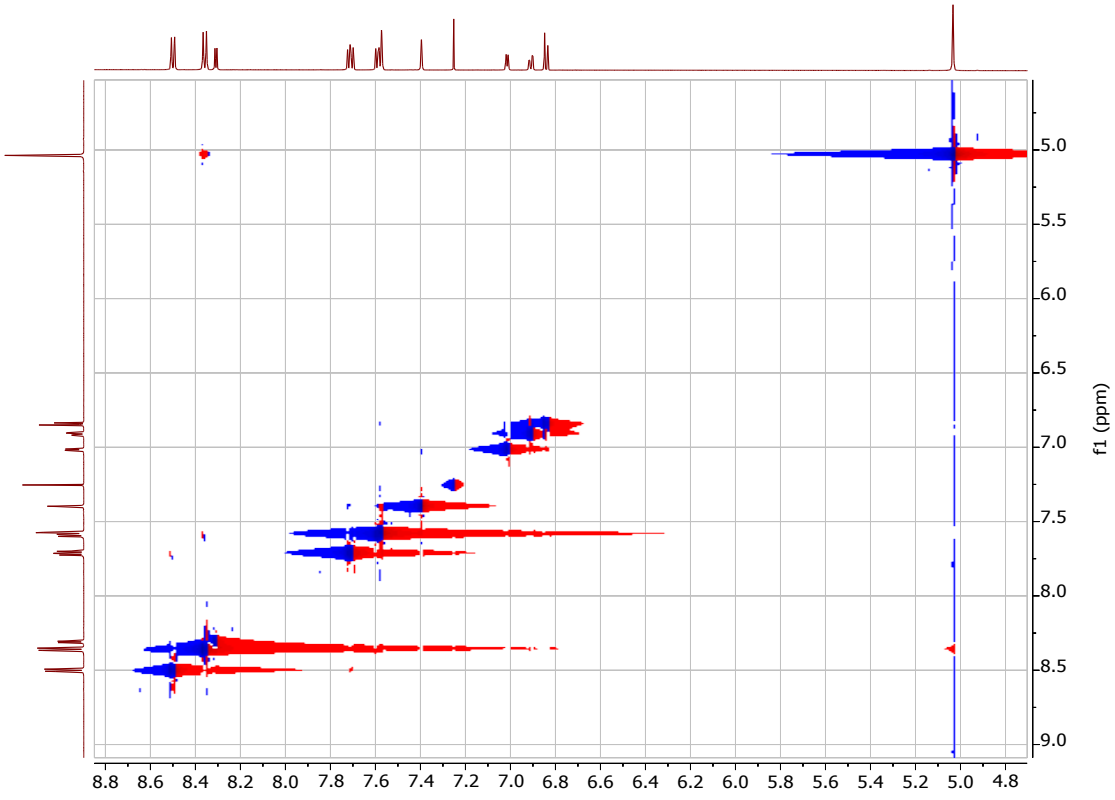

Figure S14. NOESY NMR $CDCl_3$ 10-(4-hydroxy-3-(4-methylpyridin-2-yl)benzyl)anthracene-9-carbonitrile (**1**).

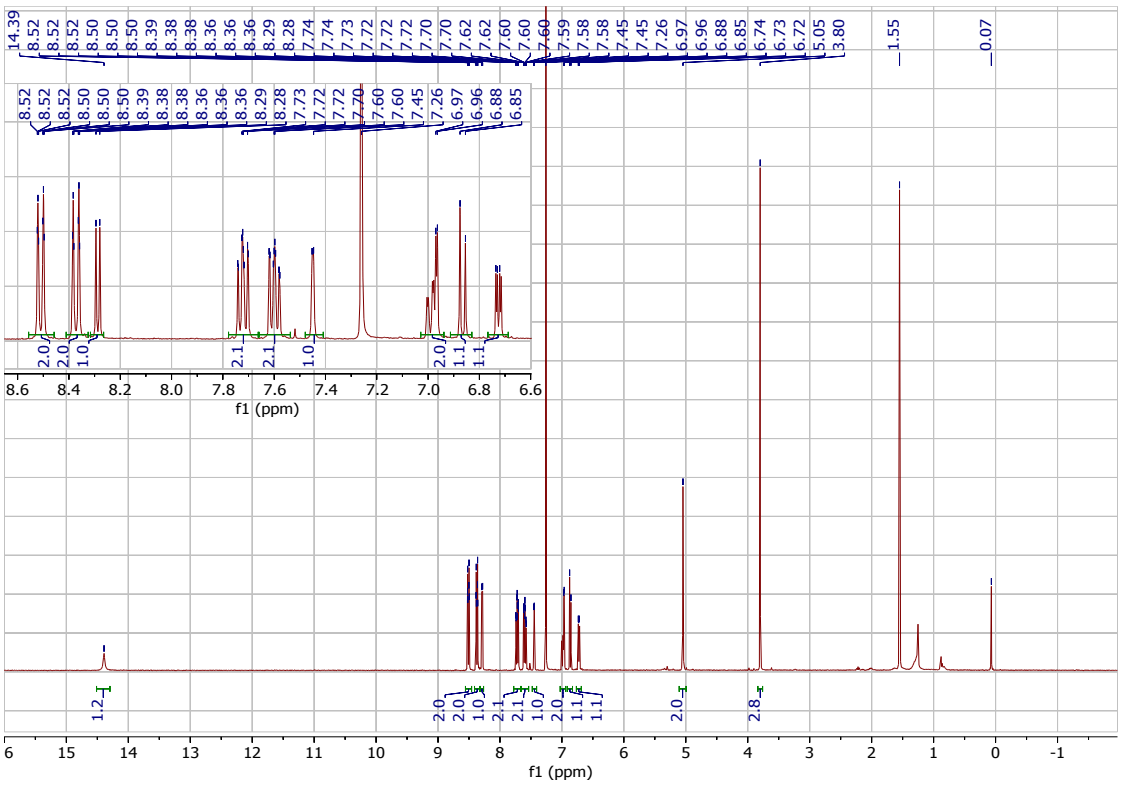

Figure S15. ^{1}H-NMR $CDCl_3$ 10-(4-hydroxy-3-(4-methoxypyridin-2-yl)benzyl)anthracene-9-carbonitrile (**2**).

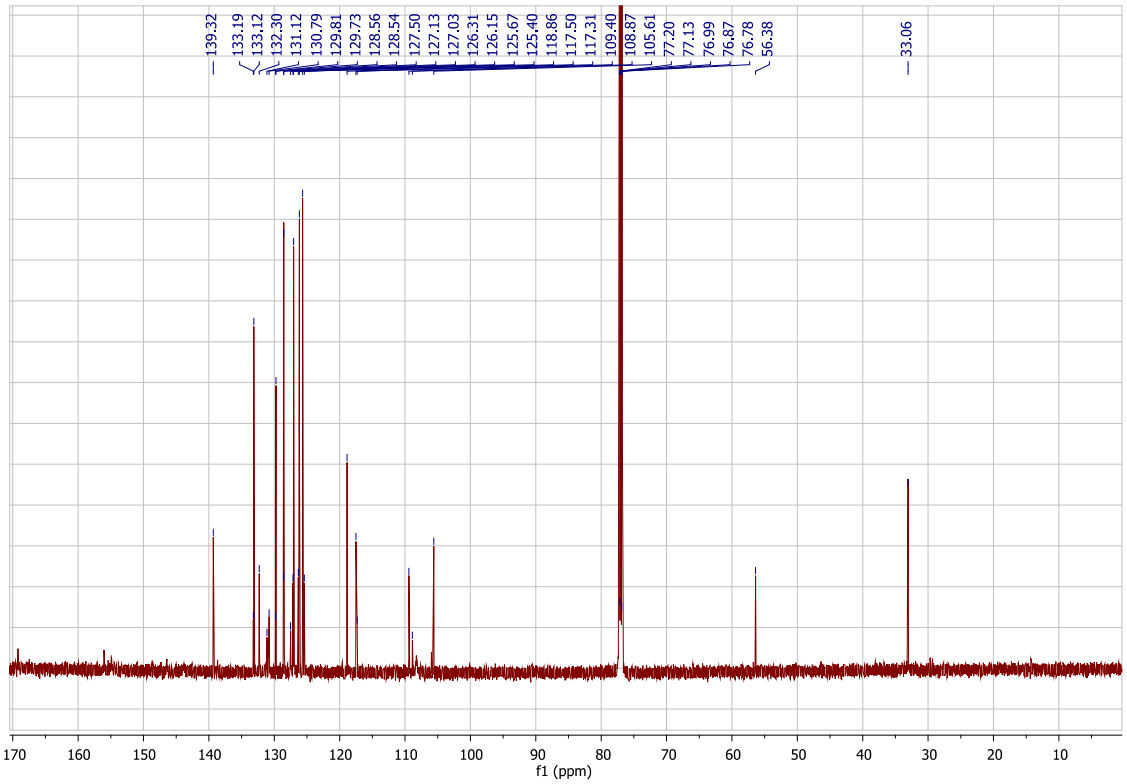

Figure S16. ^{13}C-NMR $CDCl_3$ ^{1}H-NMR $CDCl_3$ 10-(4-hydroxy-3-(4-methoxypyridin-2-yl)benzyl)anthracene-9-carbonitrile (**2**).

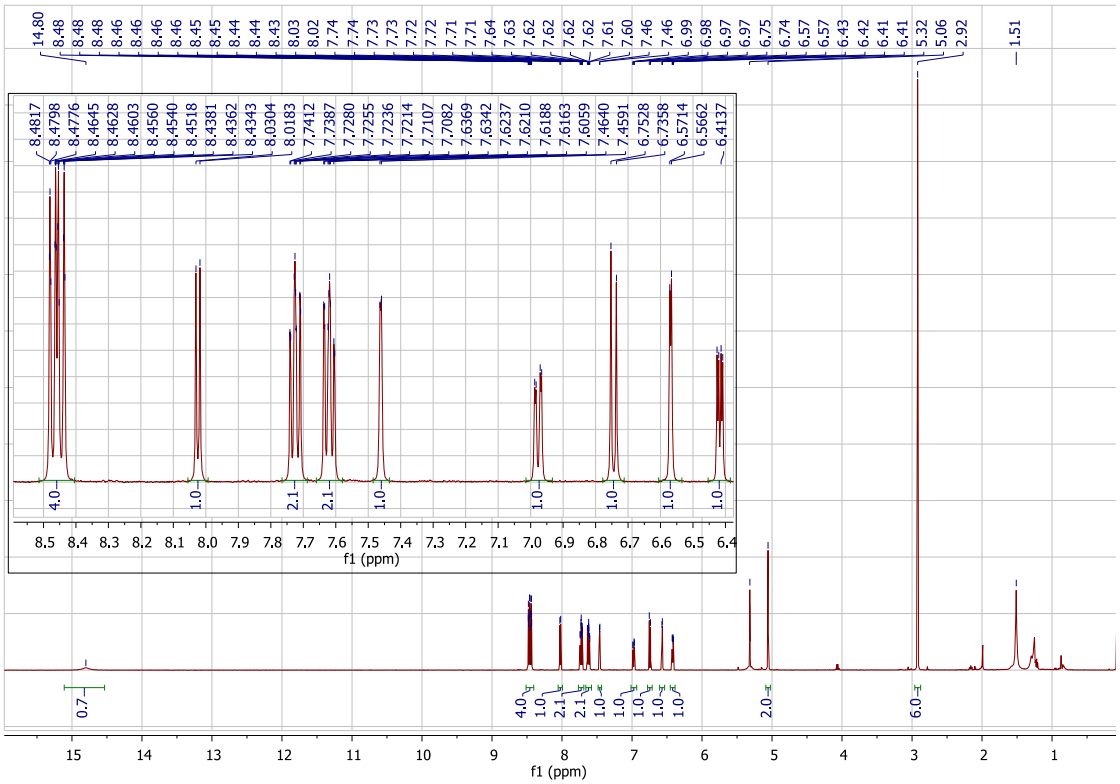

Figure S17. ^{1}H-NMR CD_2Cl_2 10-(3-(4-(dimethylamino)pyridin-2-yl)-4-hydroxybenzyl)anthracene-9-carbonitrile (**3**).

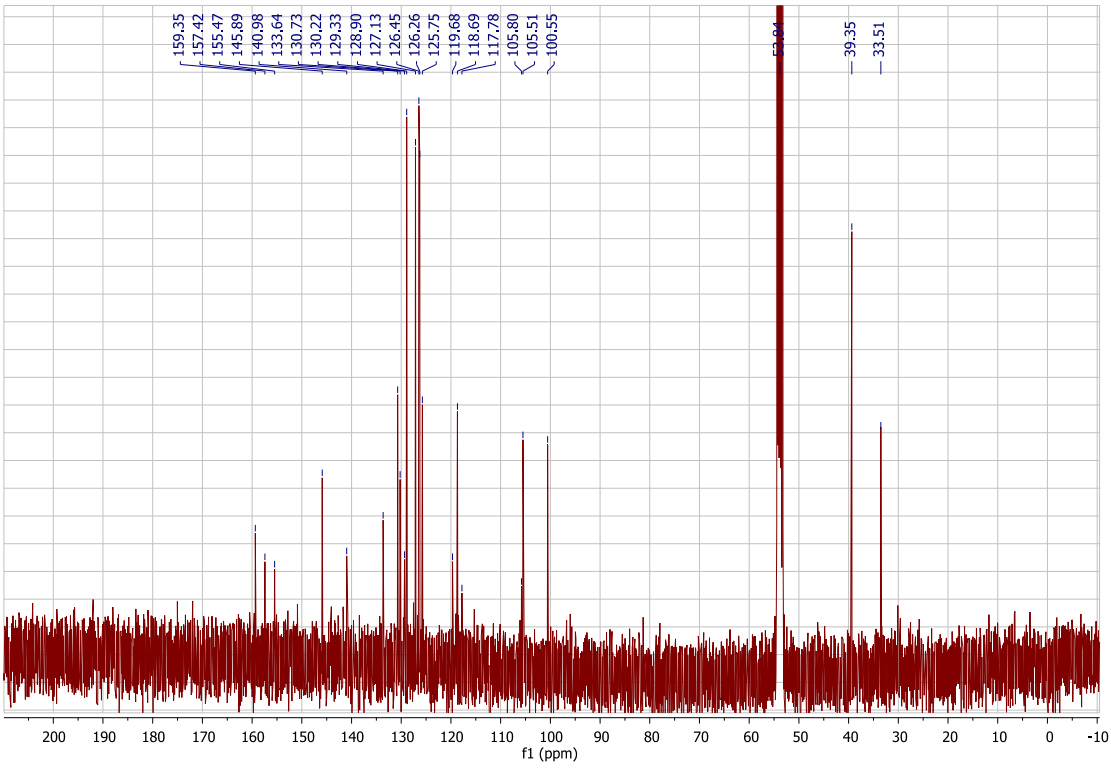

Figure S18 ^{13}C-NMR CD_2Cl_2 10-(3-(4-(dimethylamino)pyridin-2-yl)-4-hydroxybenzyl)anthracene-9-carbonitrile (**3**).

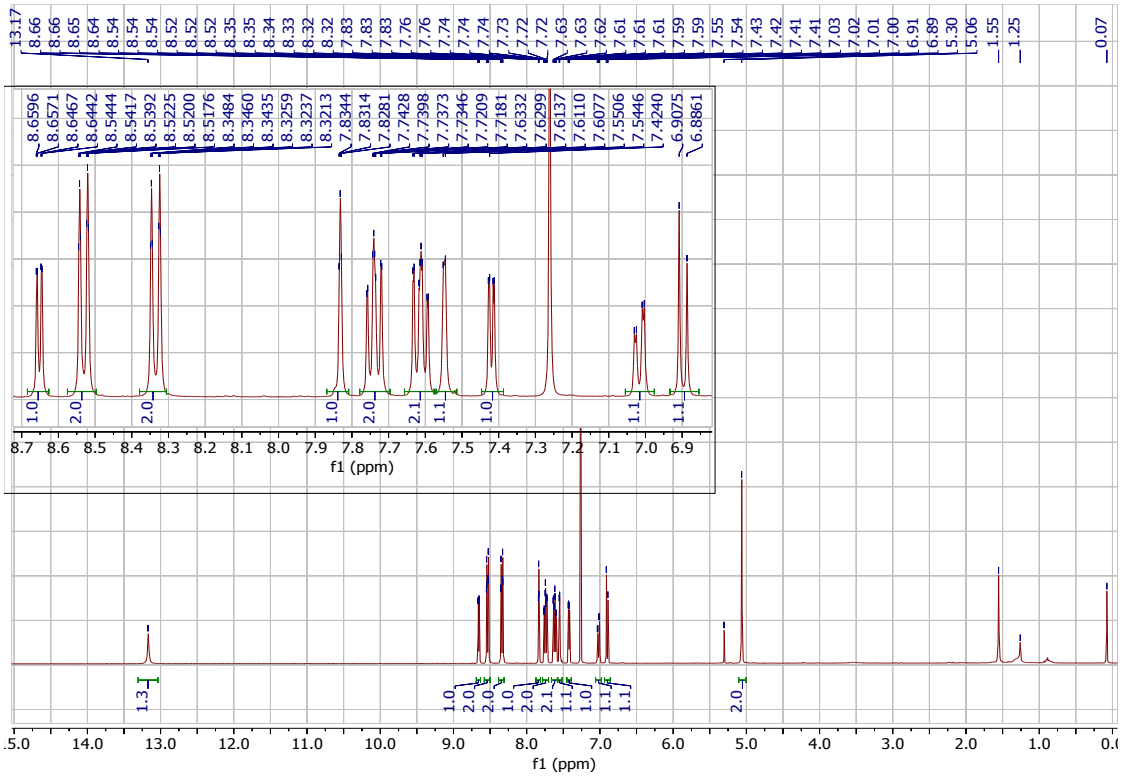

Figure S19. ^{1}H-NMR $CDCl_3$ 2-(5-((10-cyanoanthracen-9-yl)methyl)-2-hydroxyphenyl)isonicotinonitrile (**4**).

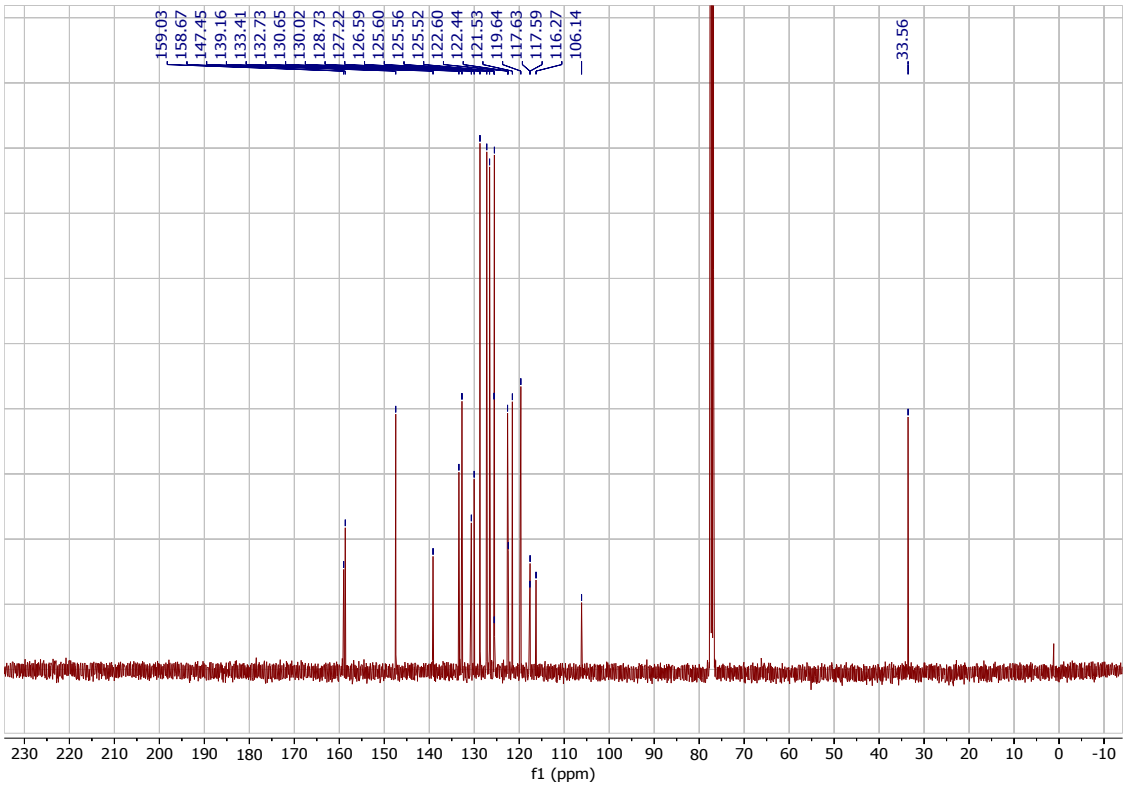

Figure S20. ^{13}C-NMR $CDCl_3$ 2-(5-((10-cyanoanthracen-9-yl)methyl)-2-hydroxyphenyl)isonicotinonitrile (**4**).

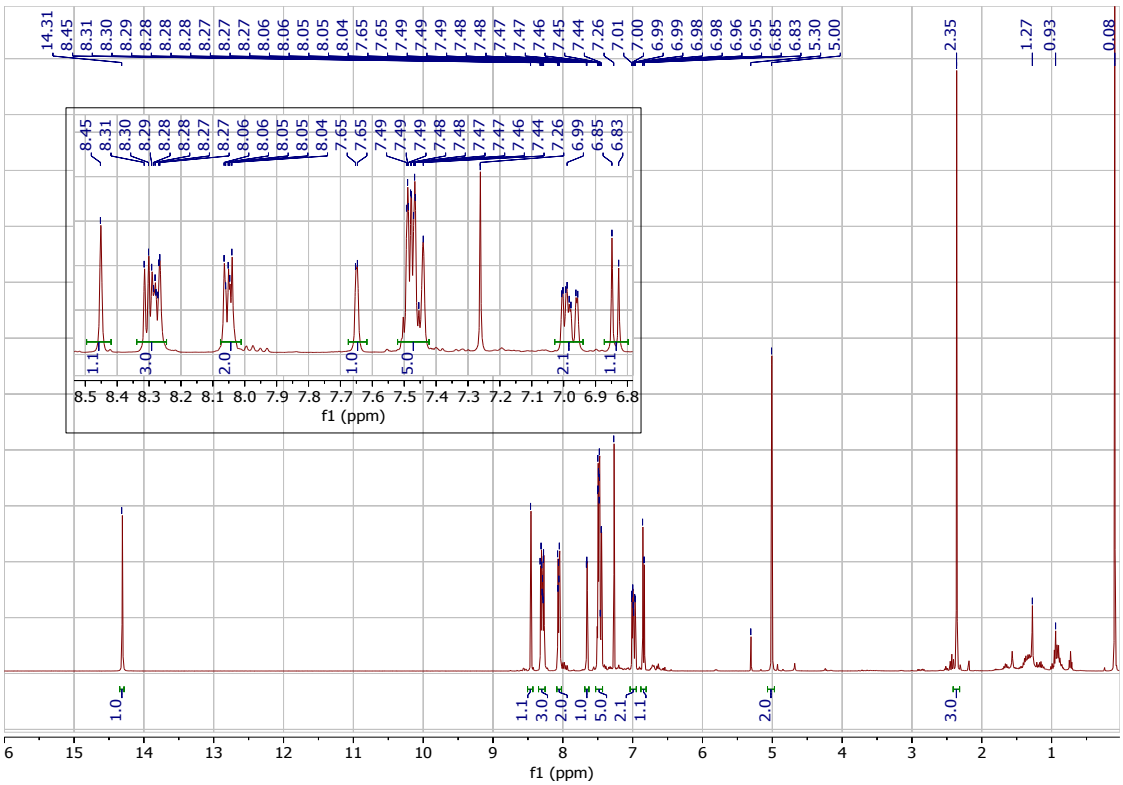

Figure S21. ^{1}H-NMR $CDCl_3$ 4-(anthracen-9-ylmethyl)-2-(4-methylpyridin-2-yl)phenol (**5**).

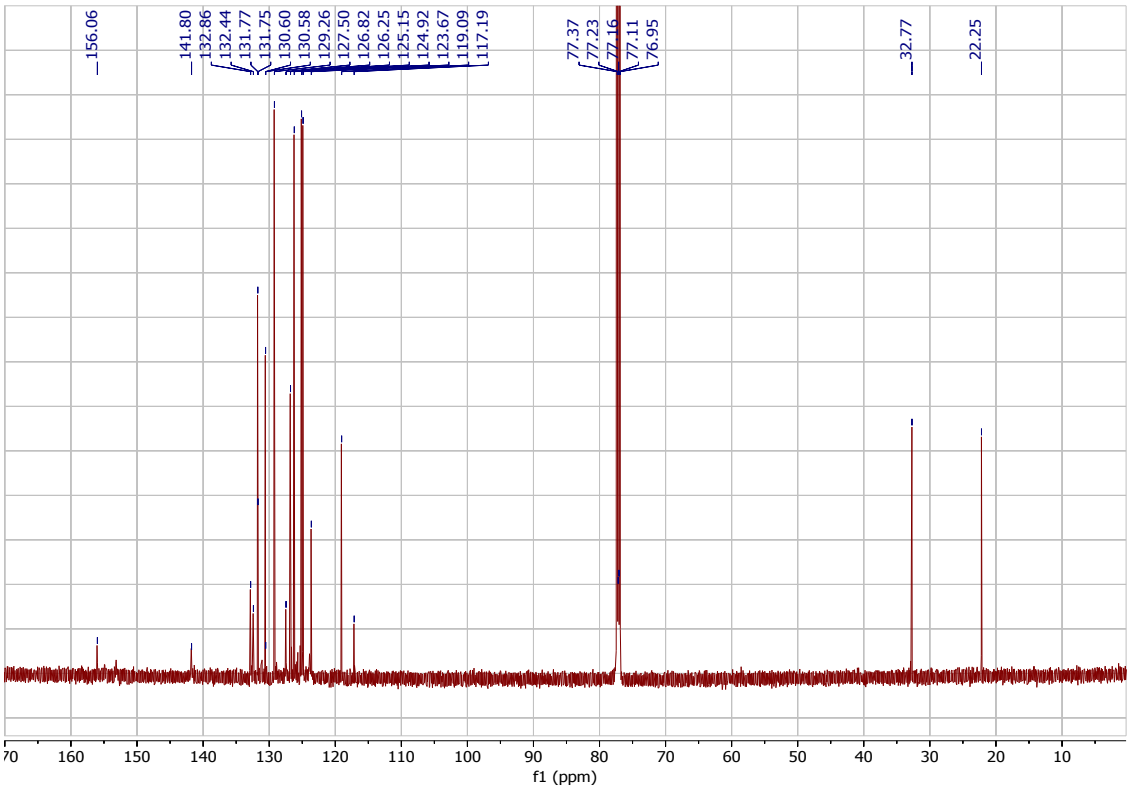

Figure S22. ^{13}C-NMR $CDCl_3$ 4-(anthracen-9-ylmethyl)-2-(4-methylpyridin-2-yl)phenol (**5**).

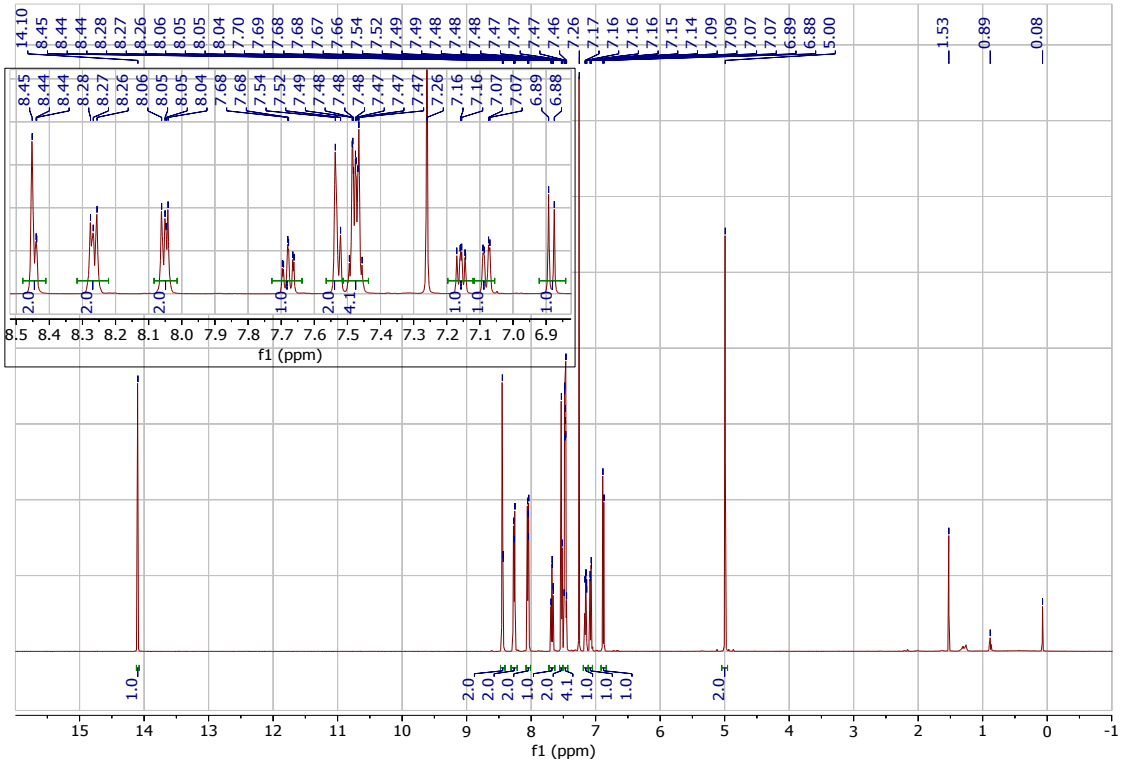

Figure S23. ^{1}H-NMR $CDCl_3$ 4-(anthracen-9-ylmethyl)-2-(pyridin-2-yl)phenol (**6**).

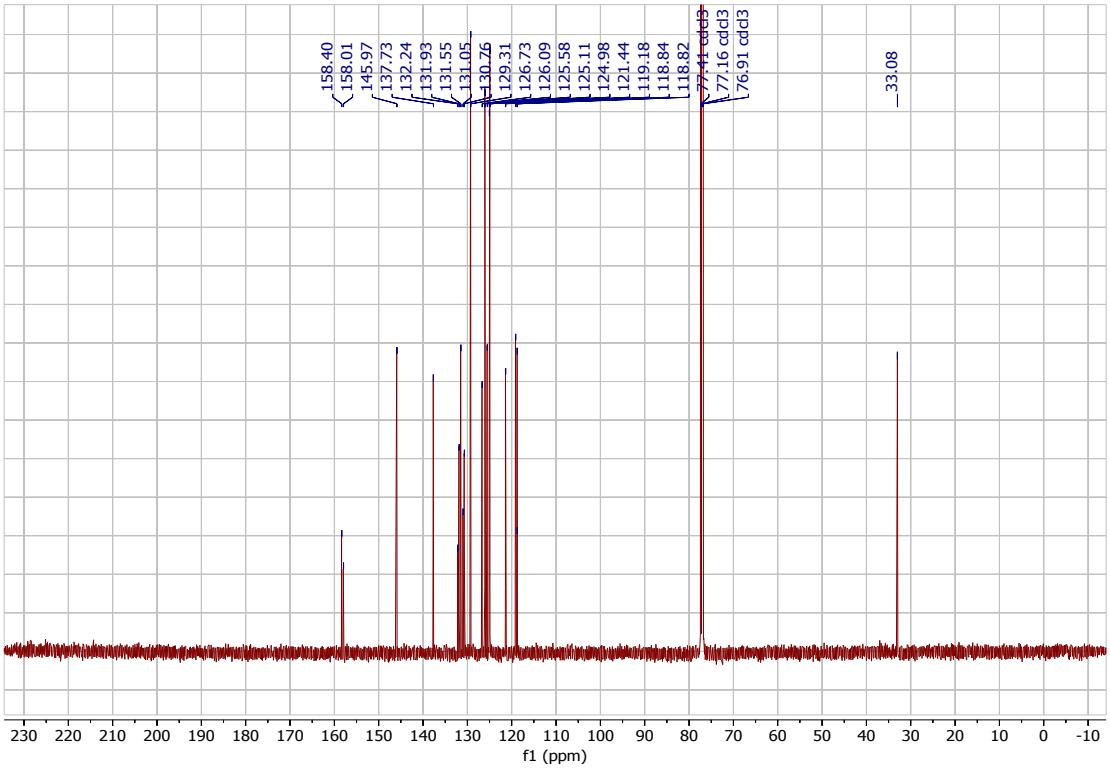

Figure S24. ^{13}C-NMR $CDCl_3$ 4-(anthracen-9-ylmethyl)-2-(pyridin-2-yl)phenol (**6**).

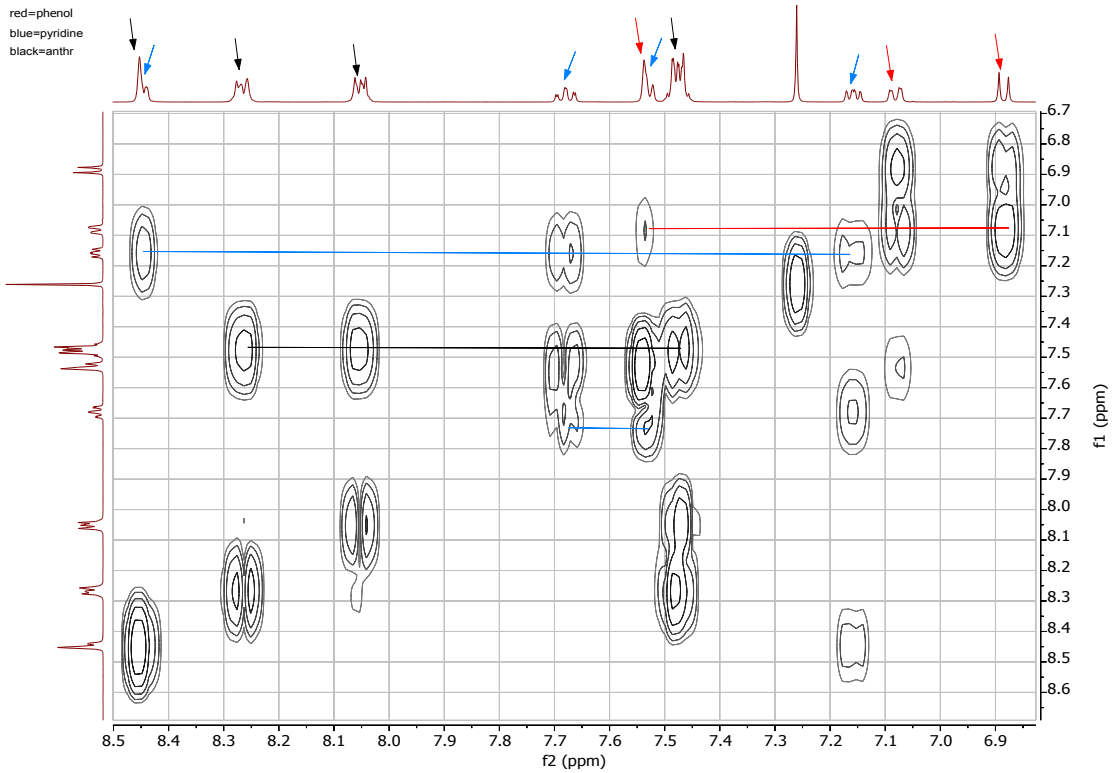

Figure S25. COSY ^{1}H-^{1}H-NMR $CDCl_3$ 4-(anthracen-9-ylmethyl)-2-(pyridin-2-yl)phenol (**6**).

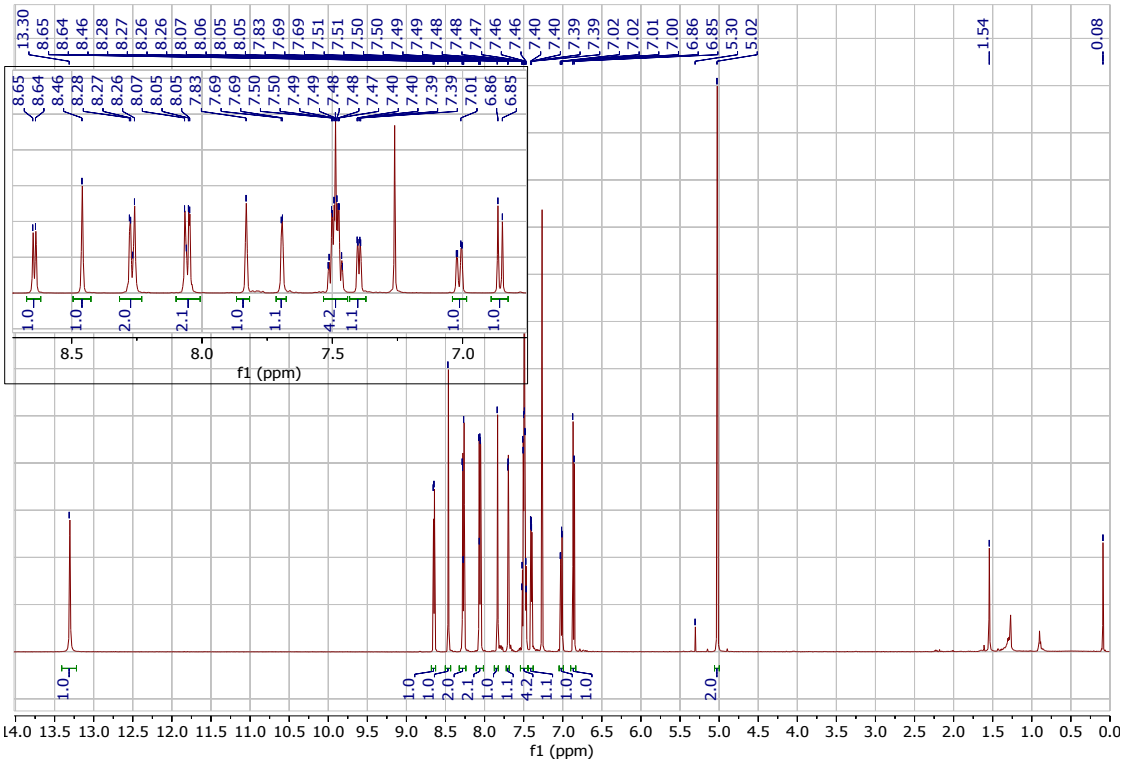

Figure S26. ^{1}H-NMR $CDCl_3$ 4-(anthracen-9-ylmethyl)-2-(4-(trifluoromethyl)pyridin-2-yl)phenol (**7**).

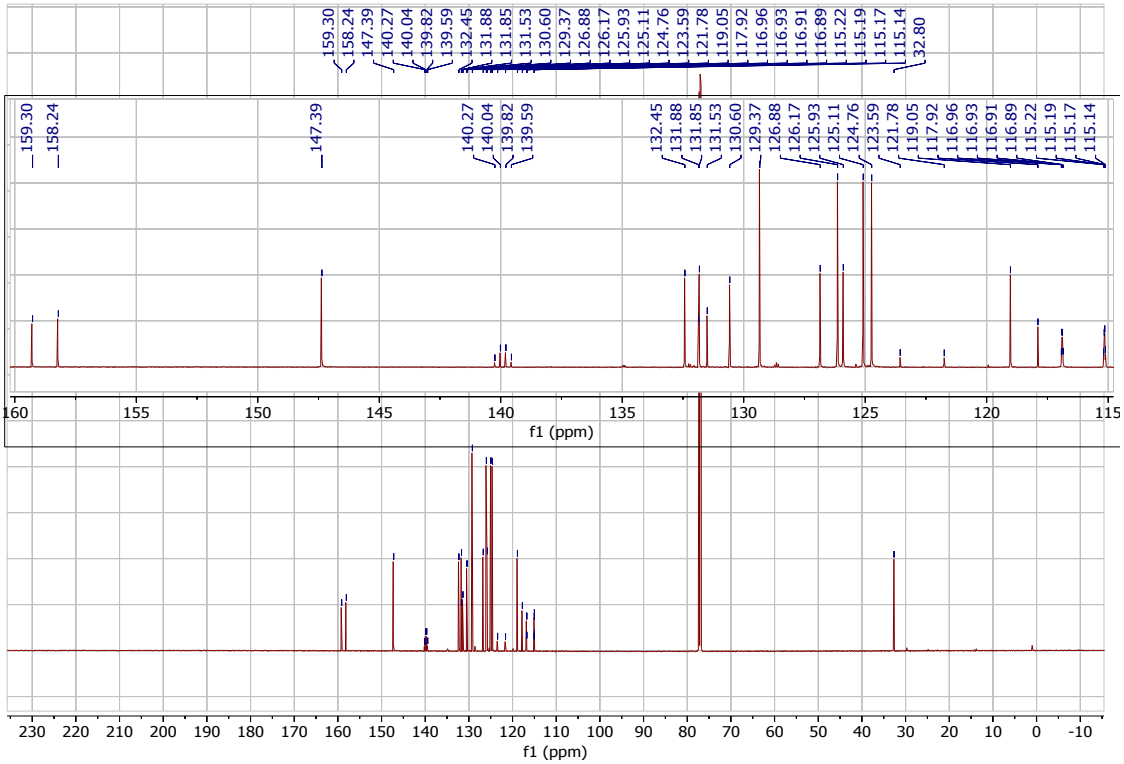

Figure S27. ^{13}C-NMR $CDCl_3$ 4-(anthracen-9-ylmethyl)-2-(4-(trifluoromethyl)pyridin-2-yl)phenol (**7**).

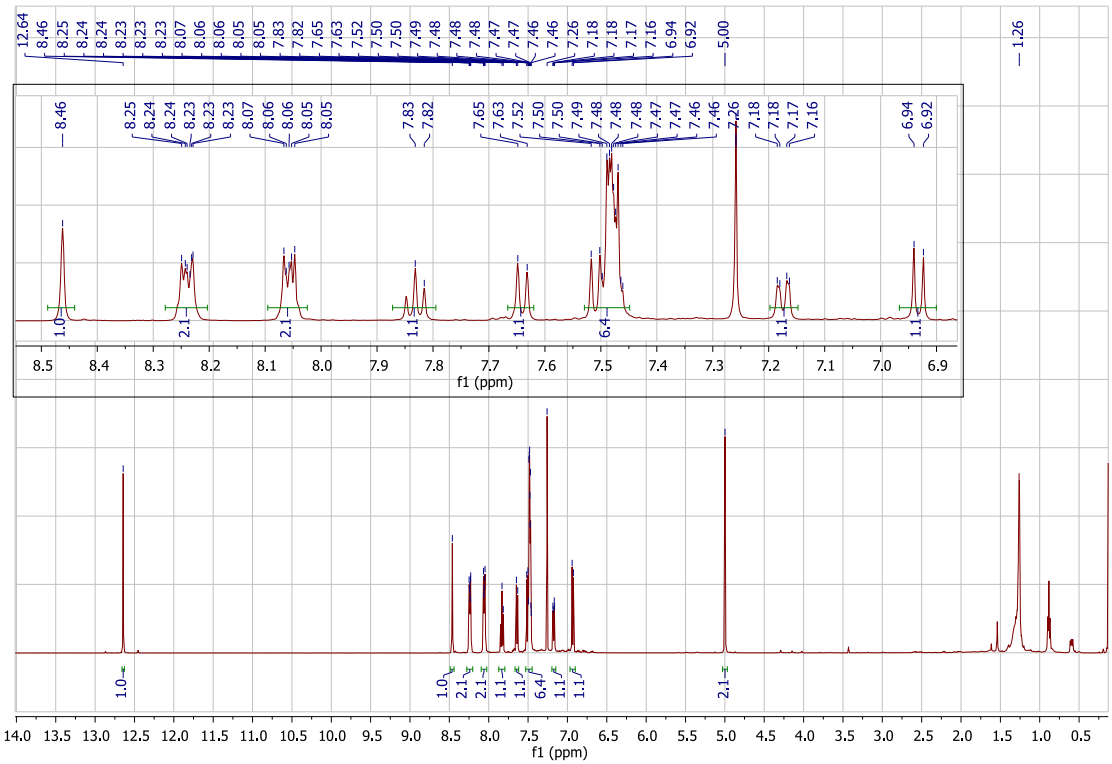

Figure S28. ^{1}H-NMR $CDCl_3$ 4-(anthracen-9-ylmethyl)-2-(6-(trifluoromethyl)pyridin-2-yl)phenol (**8**).

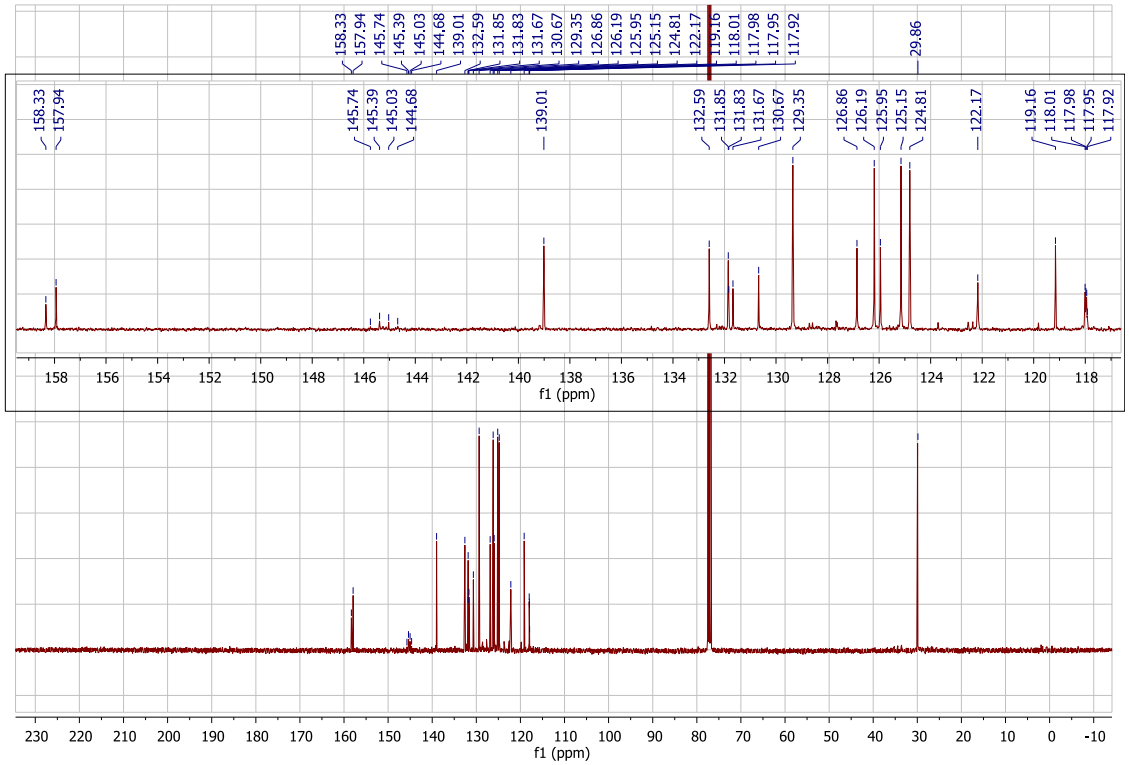

Figure S29. ^{13}C-NMR $CDCl_3$ 4-(anthracen-9-ylmethyl)-2-(6-(trifluoromethyl)pyridin-2-yl)phenol (**8**).

3. Femtosecond transient spectroscopy.

The probing in the UV-VIS and mid-IR was performed using two different laser systems present at Uppsala University. The differences between these systems will be separated with "/" in the otherwise general procedure. The samples of **1-8** were prepared in quartz cuvettes (1 mm pathlength × 1 cm), which were sealed with Teflon caps and parafilm. When possible, the concentration was adjusted in order to give an absorbance of 0.6 at 400 nm for **1-4** and 365 nm for **5-8**. The solutions were measured at ambient temperature. **1-4** were selectively photoexcited in the anthracene's lowest vibronic band (400-440 nm, cf. figure S49 below) at 400 nm for probing in the visible and at 410 nm for probing in the mid-IR. **5-8** were selectively photoexcited in the anthracene's second lowest vibronic band (355-375 nm, cf. figure S50 below) at 365 nm. Photoexcitation of **5-8** in their lowest vibronic band would require 375-400 nm excitation wavelengths, which are technically difficult to obtain in our setup.

The output from a Coherent Legend/Libra Ti:sapphire amplifier (1 mJ/1.5 mJ, 1 kHz/3 kHz, 800 nm, fwhm 100 fs/45 fs) was split into a pump and a probe. The pump beam was directed into the optical parametric amplifiers, TOPAS-White/TOPAS-Prime, (Light Conversion), and TOPAS SHS/TOPAS NirUVis (Light Conversion) to obtain the 365 nm excitation wavelength, which was then separated from the remaining visible light with dichroic mirrors. For the 400 nm excitation light, the fundamental 800 nm was frequency doubled. The output was passed through a mechanical chopper, blocking every second pulse, and was later focused in the sample cell. The pump intensity was attenuated to 300 μW.

The white-light supercontinuum probe was obtained by focusing part of the 800 nm light on a moving 3 mm thick CaF_2 crystal for roughly 380-750 nm probe light (home built/Newport TAS). The probe spectrum was recorded on a silicon diode array (home built/Newport custom made). The relative angle between the pump and probe polarization was kept at 54.7 degrees to avoid anisotropic effects. The instrumental response time depends on pump and probe wavelengths but is typically around 100 fs. The transient absorption spectra at different times were recorded for the sample by scanning the delay of the probe beam relative to the pump from -15 ps to 5 ns/8 ns with the help of an optical delay line. The samples were kept in constant motion during the measurement and 5 scans were collected and averaged for each sample.

Probing in the mid-IR: Samples of **1-4** and reference compound 9-cyano-10-methyl anthracene were kept in a home-built IR cell with CaF_2 windows using a Teflon spacer with a path length of 50 μm. The 1.5 mJ, 45 fs output of a 3 kHz Ti:sapphire amplifier (Libra, Coherent) was split into two separate commercial optical parametric amplifiers (TOPAS-Prime, Light Conversion), one generating the mid-IR probe (1850−2200 cm^{-1}). To generate the visible 410 nm light, the output beam of the mentioned TOPAS is centered onto a TOPAS-NirUVis (Coherent). Prior to reaching the sample, the probe beam was split into probe and reference beams using a wedged ZnSe window, where only the probe beam interacts with the sample. All beams are focused with a single f = 10 cm off axis parabolic mirror to a ~70 μm spot size in the sample. The pump intensity was attenuated to 650 μW. The probe and reference beams were dispersed by a commercial monochromator (Triax 190, HORIBA Jobin Yvon) equipped with a 75 groove/mm grating and detected on a dual array, 2 × 64 pixel mercury cadmium telluride detector (InfraRed Associated, Inc.). The instrument response function for the experiments was approximately 300 fs.

Global analysis of the time-resolved full spectra (*30*) was performed by least-squares fitting performed with the R package TIMP and its GUI Glotaran (*31,32*). The fitting uses a sequential

irreversible decay scheme with increasing lifetimes (A→B, B→C, C→D), and assumes that the time dependent spectra are a linear combination of difference absorption of various species with their respective population. The sequential irreversible decay scheme used three component exponential decays $\Delta A(\lambda,t) = \varepsilon_1(\lambda)c_1e^{-k_1t} + \varepsilon_2(\lambda)c_2e^{-k_2t} + \varepsilon_3(\lambda)c_3e^{-k_3t}$ where ε, c and k are the absorptivity coefficient, concentration and decay time constant of the species. The instrument response function was convoluted with a Gaussian function to account for coherent artifacts and a third-order polynomial function for the wavelength dispersion. The Gaussian FWHM was a free fit parameter that typically resulted in FWHM ranging from 120 to 200 ps for the visible data, and ranging from 250 to 350 ps for the mid-IR data. No sub-picosecond components are observed in the data and therefore the fitted time constants are insensitive to the instrument response function. The third-order polynomial function used time zero at the wavelength of maximum ΔAbs as the initial parameter; the appropriateness of the polynomial function was checked after analysis by visually comparing the time zero across the spectra versus the onset of the signals. A thermal artifact in the TA mid-IR spectra was seen as a flat, positive baseline signal that decayed on a 1 ps time scale. The spectra were thus corrected by subtracting the signal at a wavenumber where there is no molecular signal (2180 cm^{-1}) from all data.

Triads **1-3** show a non-monotonic decay of the LES due to accumulation of the CSSs, whereas triads **4-8** show monotonic decay of the LES. A long-lived component is included in the all the fits. In the case of **1-3** in CH_2Cl_2, the long lived-component features a band at 425 nm. This component could correspond to a minor fraction of decays of the CSS by ET to the CH_2Cl_2, with the feature at 425 nm arising from the phenoxyl radical portion of the originally formed CSS. Or, it could result from intersystem crossing of the CSS to the anthracene triplet state, which also has a feature at ca. 425 nm (*33*). The long-lived component is absent in all other solvents studied, such as MeCN, DMF and n-butyronitrile. These results, together with the observed monotonic decay of the CSS in **1-3** probed by mid-IR transient absorption indicate that the primary decay pathway of the CSS in **1-3** is to the GS considering that the mid-IR data allows simultaneous monitoring of the kinetics of both, the CSS and GS.

As described in the main text, triads **4-8** show monotonic decay of the LES, without observation of a CSS. This is likely due to decay of the CSS being faster than forward CPET charge separation. Triads **4-8** have the slowest and least negative free energy for charge separation reactions (Figure 3). This implies that they have the most negative driving forces for recombination: according to Table S3, spanning from -2.92 eV for **4** to -3.44 eV for **8**. In this regime of extremely negative driving forces other mechanistic deactivation paths of the CSS could be at play including stepwise PCET pathways or ET to the solvent.

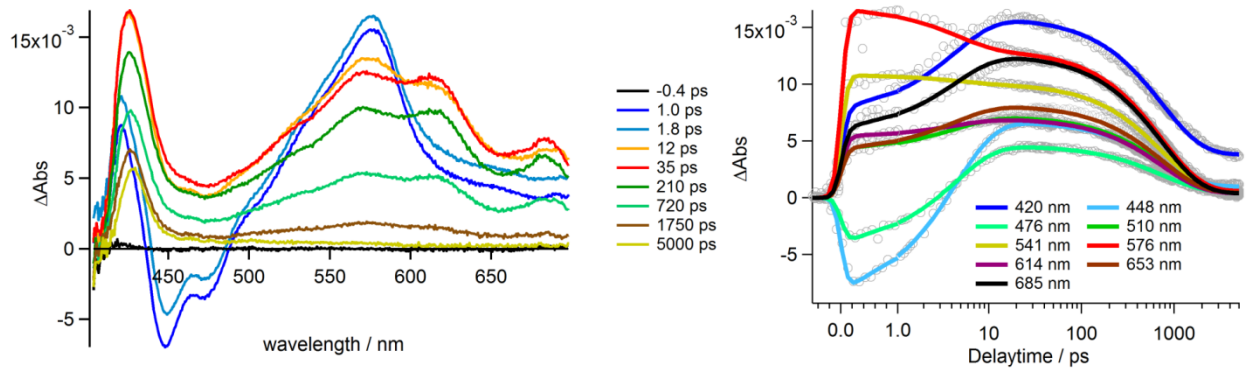

Figure S30. **1** in CH_2Cl_2. Right: Visible transient absorption spectra at various delay times. Left: time traces at various probe wavelengths (the delay time scale is logarithmic above 1 ps). Data fitted to τ_1=4.42 (decay of the LES and formation of the CSS), τ_2=754.77 (decay of the CSS) and τ_3>1000 ps (long-lived component).

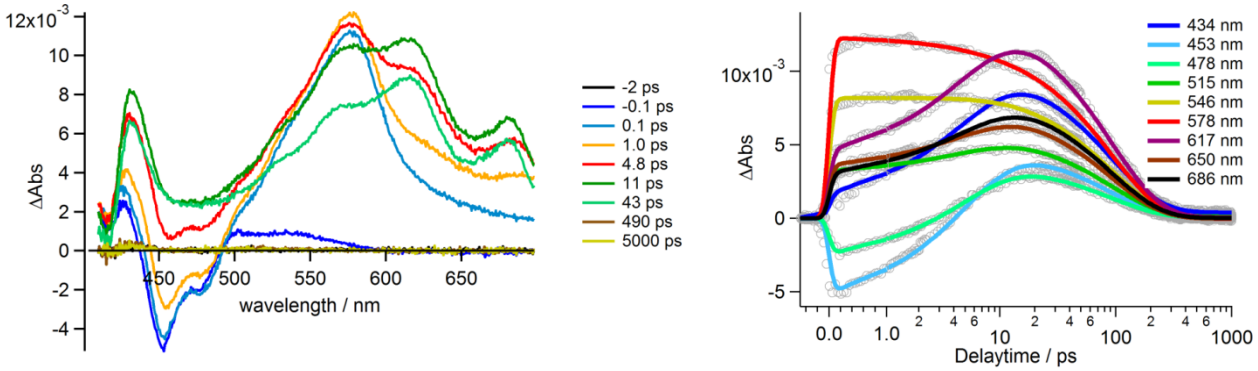

Figure S31. **1** in n-BuCN. Left: Visible transient absorption spectra at various delay times. Right: time traces at various probe wavelengths (the delay time scale is logarithmic above 1 ps). Data fitted to τ_1=5.21 (decay of the LES and formation of the LES), τ_2=91.77 (decay of the CSS) and τ3>1000 ps (long-lived component).

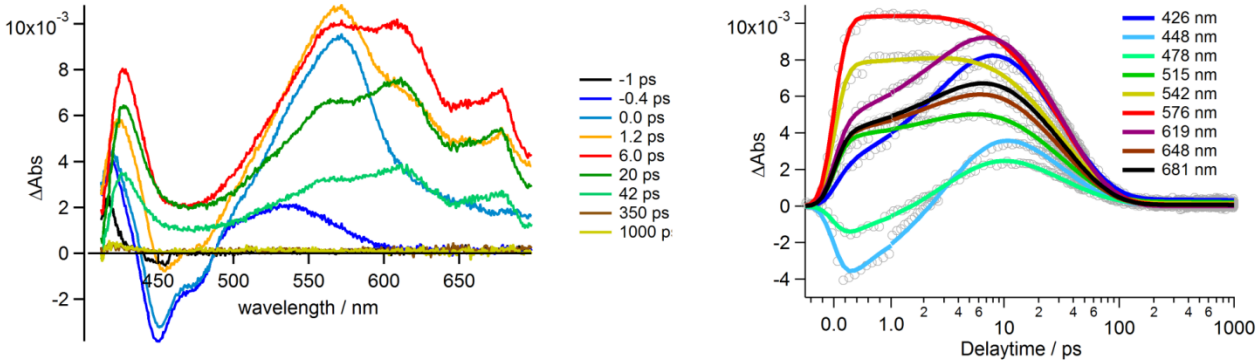

Figure S32. **1** in MeCN. Left: Visible transient absorption spectra at various delay times. Right: time traces at various probe wavelengths (the delay time scale is logarithmic above 1 ps). Data fitted to τ_1=3.31 (decay of the LES and formation of the CSS), τ_2=32.26 (decay of the CSS) and τ3>1000 ps (long-lived component).

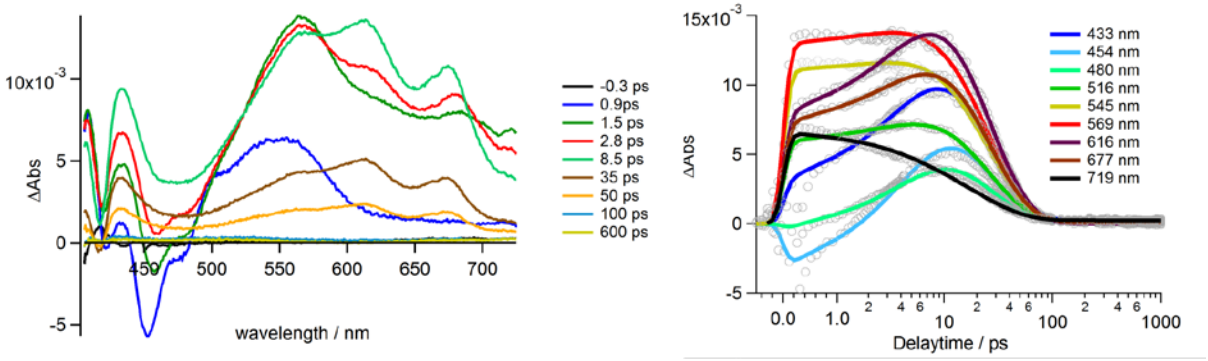

Figure S33. **1** in DMF. Left: Visible transient absorption spectra at various delay times. Right: time traces at various probe wavelengths (the delay time scale is logarithmic above 1 ps). Data fitted to

τ_1=5.12 (decay of the LES and formation of the CSS), τ_2=21.60 (decay of the CSS) and τ3>1000 ps (long-lived component).

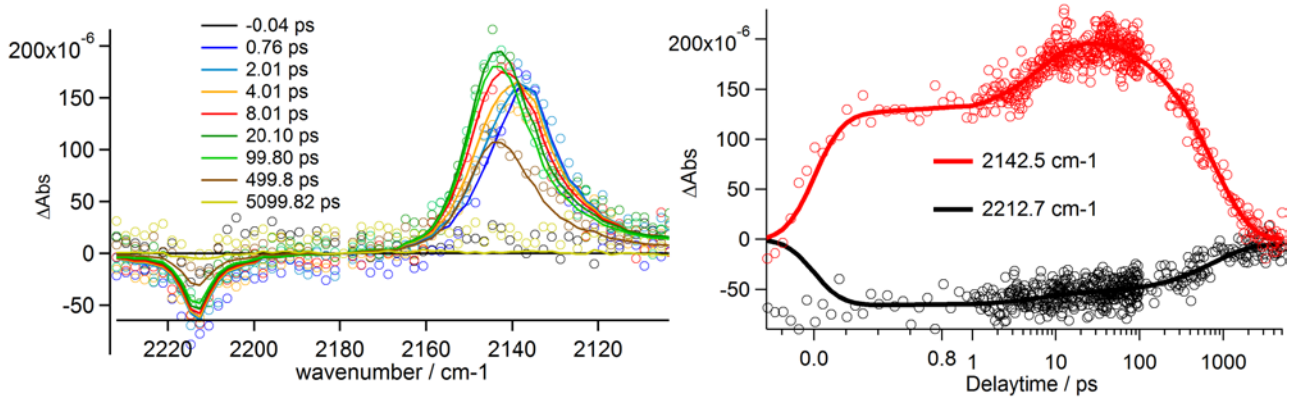

Figure S34. Left: **1** in CH_2Cl_2. mid-IR transient absorption spectra at various delay times. Right: time traces at various probe wavelengths (the delay time scale is logarithmic above 1 ps). Data fitted to τ_1=7.0 ps (decay of the LES and formation of the CSS), τ_2=764 ps (decay of the CSS) and τ3>1000 ps (long-lived component).

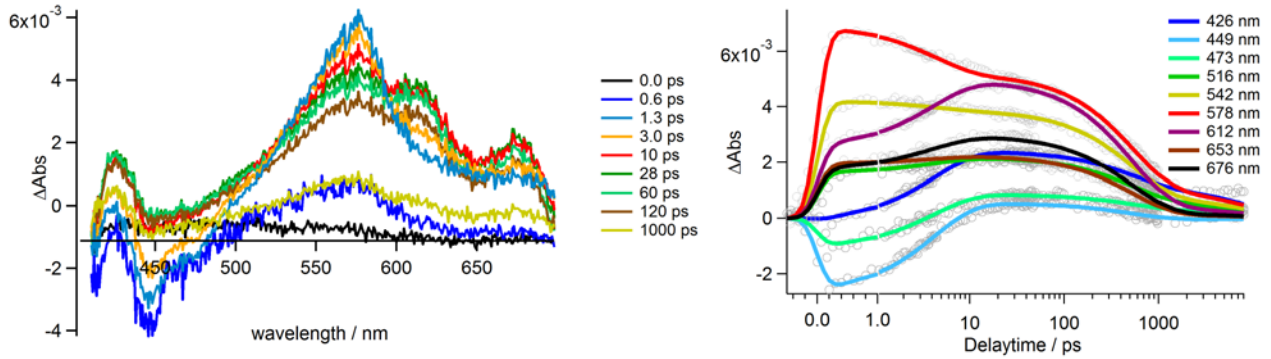

Figure S35. **2** in CH_2Cl_2. Left: Visible transient absorption spectra at various delay times. Right: time traces at various probe wavelengths (the delay time scale is logarithmic above 1 ps). Data fitted to τ_1=7.48 (decay of the LES and formation of the CSS), τ_2=578.01 (decay of the CSS) and τ3>1000 ps (long-lived component).

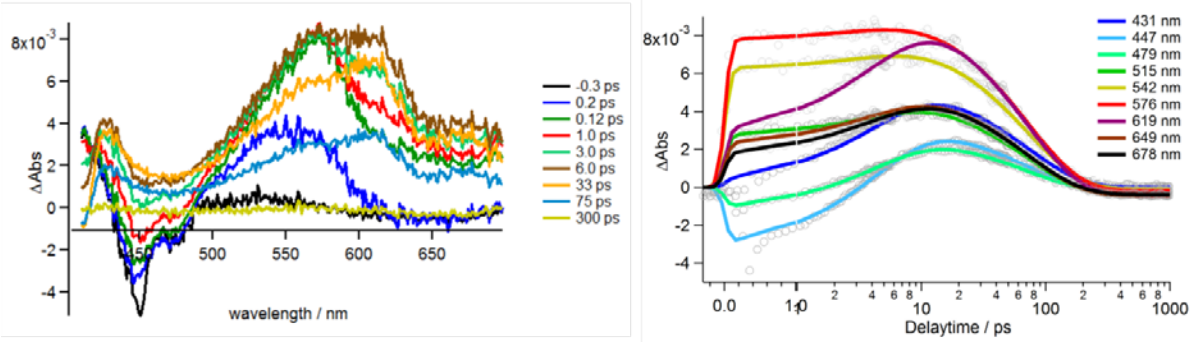

Figure S36. **2** in n-BuCN. Left: Visible transient absorption spectra at various delay times. Right: time traces at various probe wavelengths (the delay time scale is logarithmic above 1 ps). Data fitted to τ_1=4.62 (decay of the LES and formation of the CSS), τ_2=71.71(decay of the CSS) and τ3>1000 ps (long-lived component).

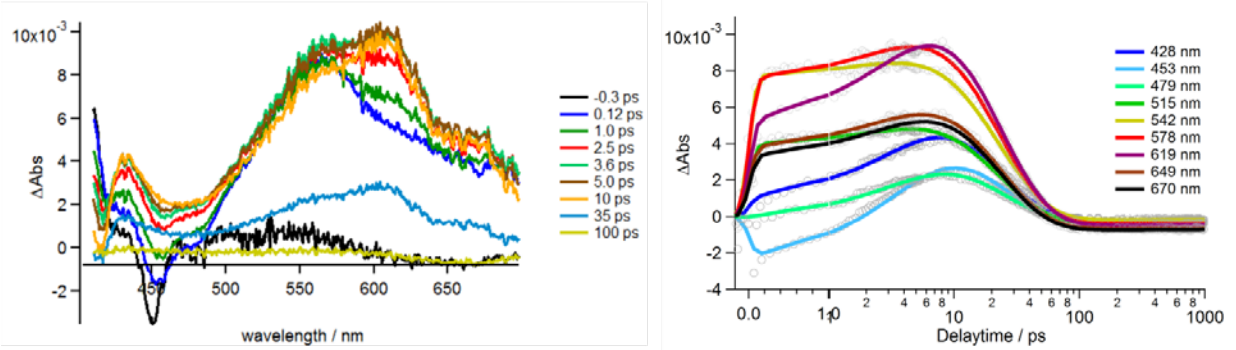

Figure S37. **2** in DMF. Left: Visible transient absorption spectra at various delay times. Right: time traces at various probe wavelengths (the delay time scale is logarithmic above 1 ps). Data fitted to τ_1=4.38 (decay of the LES and formation of the CSS), τ_2=20.22 (decay of the CSS) and τ3>1000 ps (long-lived component).

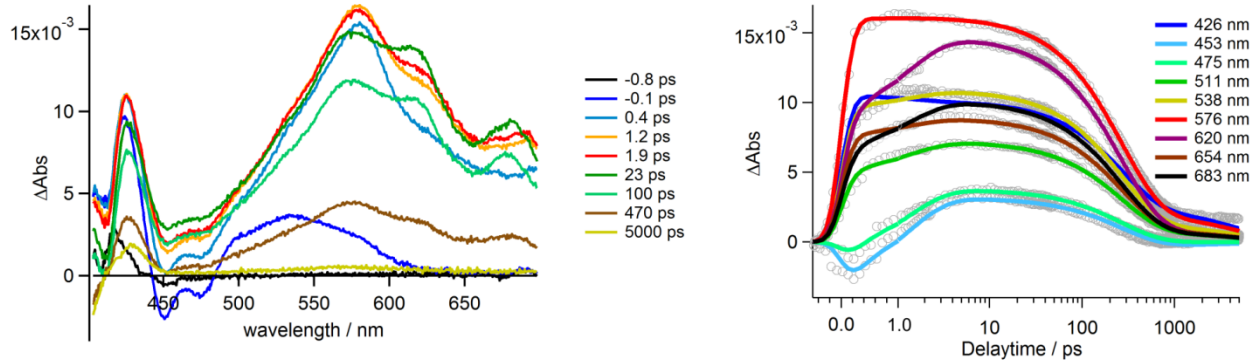

Figure S38. **3** **i**n CH_2Cl_2. Left: Visible transient absorption spectra at various delay times. Right: time traces at various probe wavelengths (the delay time scale is logarithmic above 1 ps). Data is fitted to τ_1=1.32 (decay of the LES and formation of the CSS), τ_2=268.44 (decay of the CSS) and τ3>1000 ps (long-lived component).

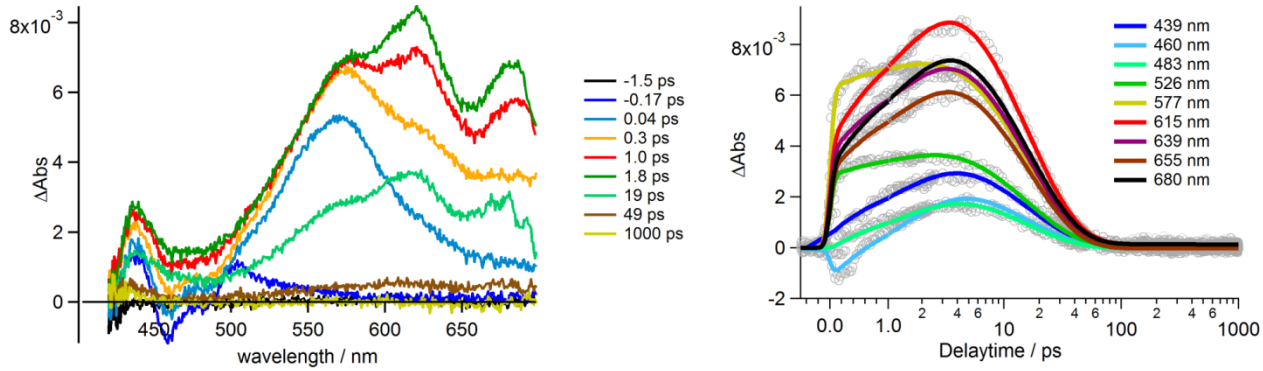

Figure S39. **3** in DMF. Left: Visible transient absorption spectra at various delay times. Right: time traces at various probe wavelengths (the delay time scale is logarithmic above 1 ps). Data fitted to τ_1=1.62 (decay of the LES and formation of the CSS), τ_2=16.06 (decay of the CSS) and τ3>1000 ps (long-lived component).

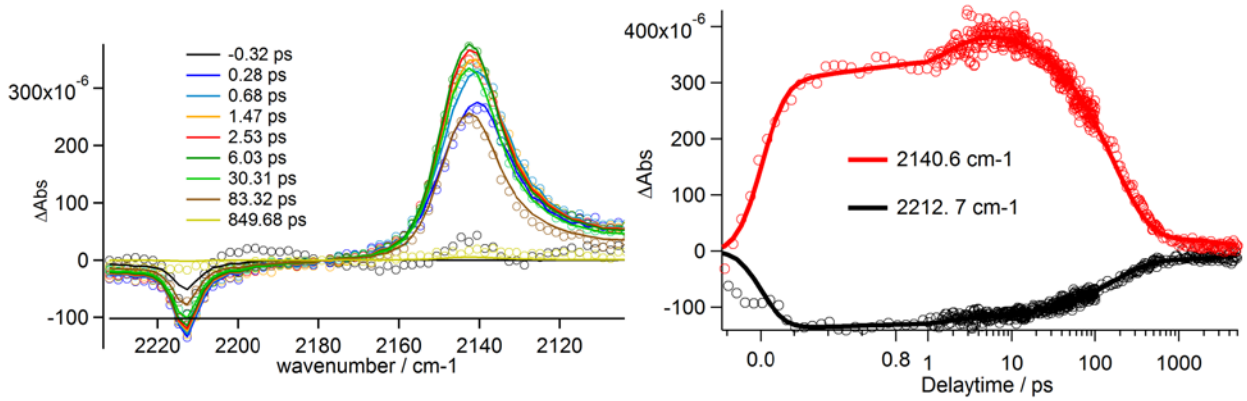

Figure S40. **3** in CH_2Cl_2. Left: mid-IR transient absorption spectra at various delay times. Right: time traces at various probe wavelengths (the delay time scale is logarithmic above 1 ps). Data is fitted to τ_1=1.40 (decay of the LES and formation of the CSS), τ_2=230.4 (decay of the CSS) and τ3>1000 ps (long-lived component).

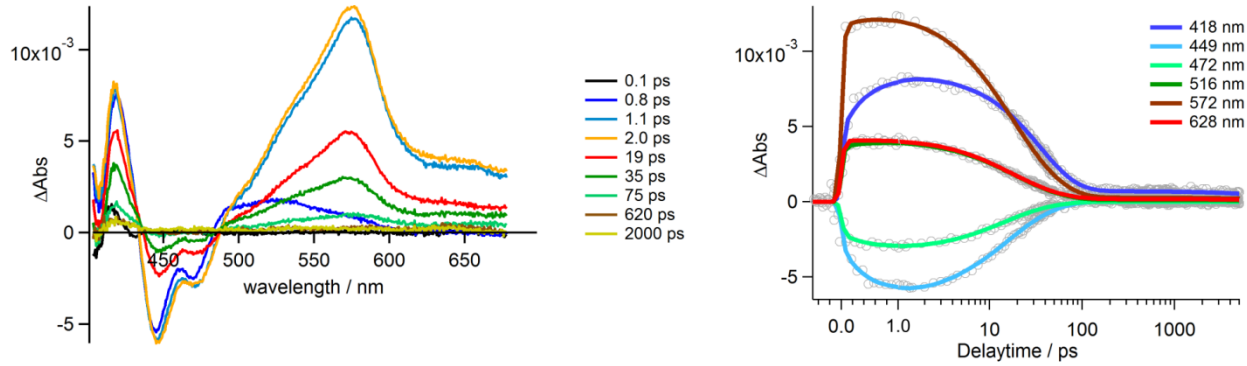

Figure S41. **4** in CH_2Cl_2. Left: Visible transient absorption spectra at various delay times. Right: time traces at various probe wavelengths (the delay time scale is logarithmic above 1 ps). Data is fitted to τ_1=11.78 (vibrational relaxation), τ_2=30.96 (decay of the LES) and τ3>1000 ps (long-lived component).

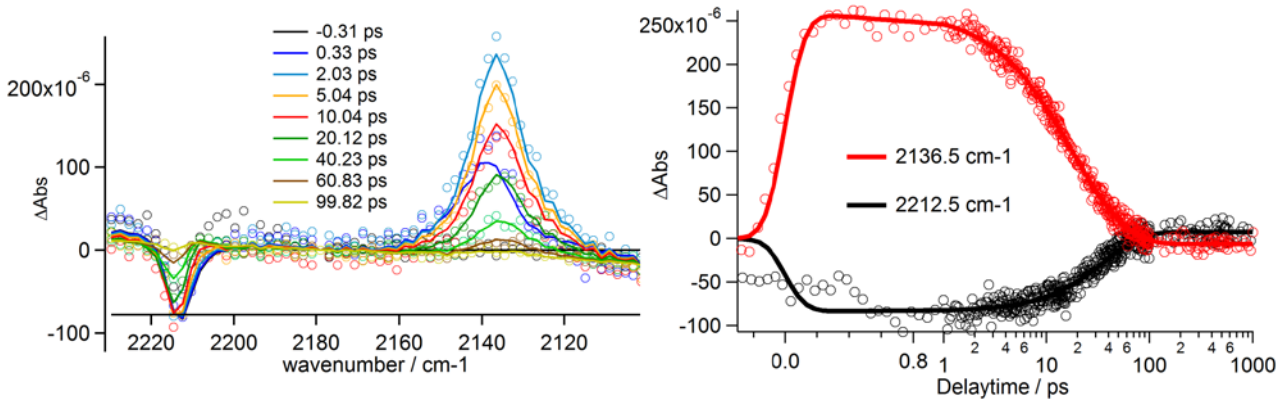

Figure S42. **4** in CH_2Cl_2. Left: mid-IR transient absorption spectra at various delay times. Right: time traces at various probe wavelengths (the delay time scale is logarithmic above 1 ps). Data is fitted to τ_1=12.07 (vibrational relaxation), τ_2=29.44 (decay of the LES) and τ_3>1000 ps (long-lived component).

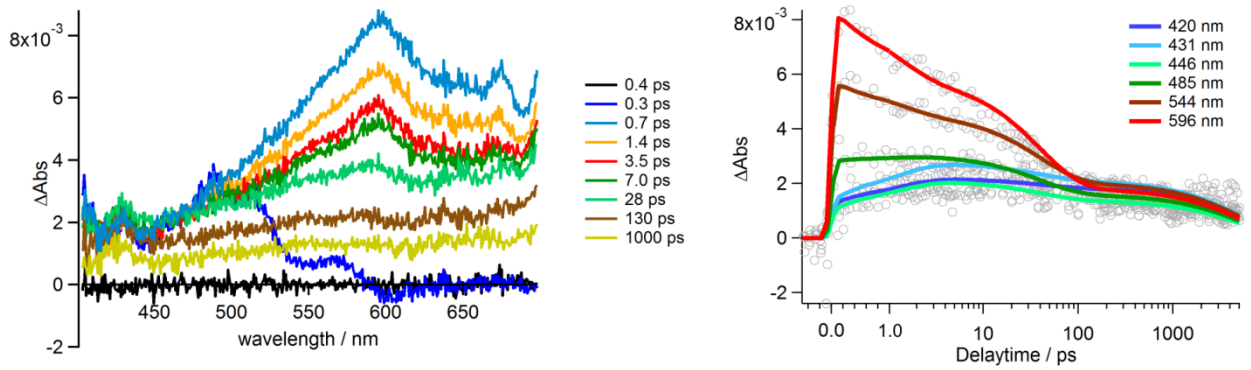

Figure S43. **5** in CH_2Cl_2. Left: Visible transient absorption spectra at various delay times. Right: time traces at various probe wavelengths (the delay time scale is logarithmic above 1 ps). Data fitted to τ_1=1.70, τ_2=39.53 (decay of the LES) and τ3>1000 ps (long-lived component).

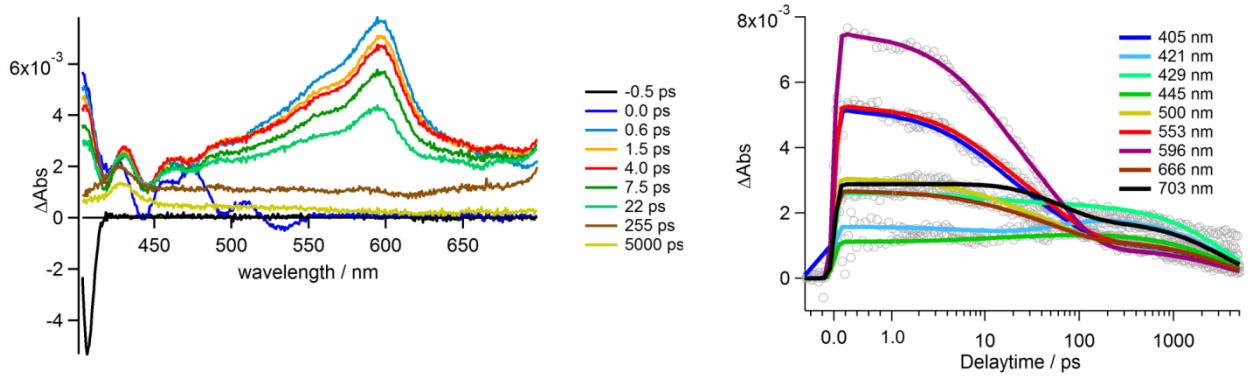

Figure S44. **6** in CH_2Cl_2 Left: Visible transient absorption spectra at various delay times. Right: time traces at various probe wavelengths (the delay time scale is logarithmic above 1 ps). Data fitted to τ_1=9.32 (vibrational relaxation), τ_2=59.95 (decay of the LES) and τ3>1000 ps (long-lived component).

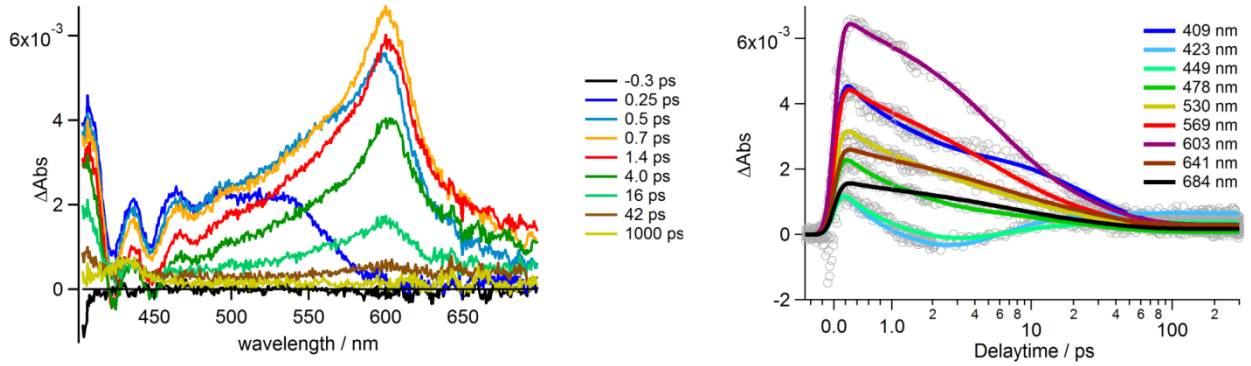

Figure S45. **7** in CH_2Cl_2. Left: Visible transient absorption spectra at various delay times. Right: time traces at various probe wavelengths (the delay time scale is logarithmic above 1 ps). Data fitted to τ_1=5.17 (vibrational relaxation), τ_2=25.20 (decay of the LES) and τ3>1000 ps (long-lived component).

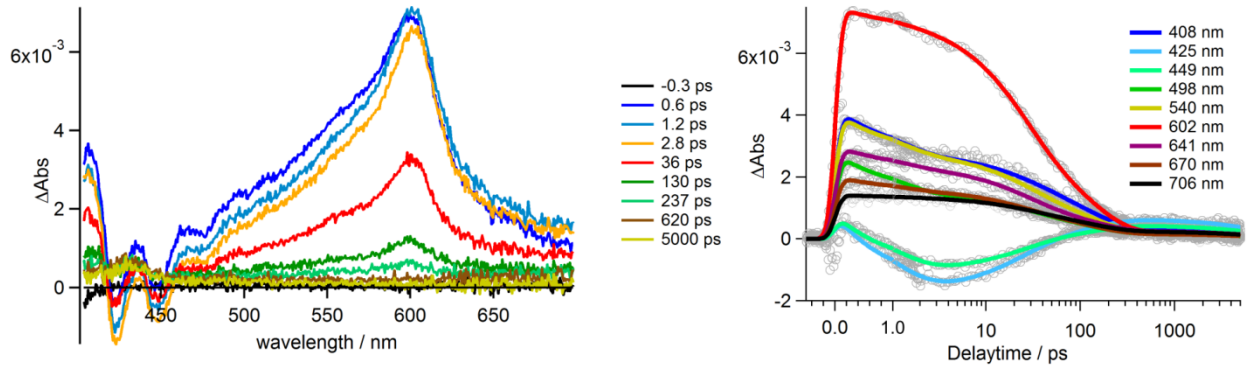

Figure S46. **8** in CH_2Cl_2. Left: Visible transient absorption spectra at various delay times. Right: time traces at various probe wavelengths (the delay time scale is logarithmic above 1 ps). Data fitted to τ_1=1.02, τ_2=22.98 (vibrational relaxation), τ_3=120.16 (decay of the LES) and τ_4> 1000ps (long-lived component).

The mid-IR transient absorption spectra of 9-cyano-10-methyl-anthracene shows natural decay of the LES and recovery of the GS with a time constants longer than it can be properly measured in a 5 ns time window. In addition, no upshift of the initially formed excited state absorption feature is observed, in contrast to triads **1**-**3**.

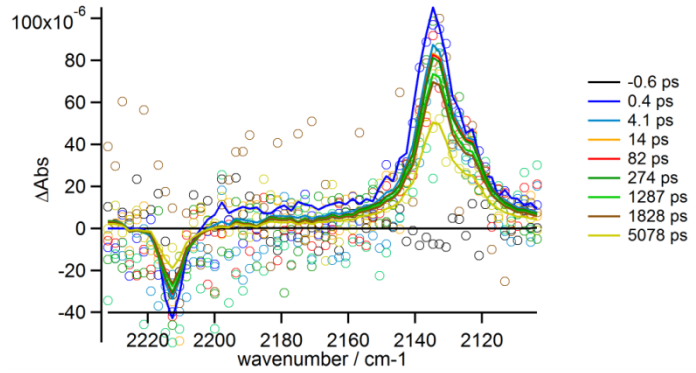

Figure S47. **9-cyano-10-methyl-anthracene** in CH_2Cl_2: mid-IR transient absorption spectra at various delay times.

Table S1. Summary of the CEPT rate constants for charge separation (CS) and recombination (CR). n.o. = not observed, n.d.= not determined.

		determined by UV-Vis TA		determined by mid-IR TA	
Triad	Solvent	$k_{(CPET-CS)}$ / s^{-1}	$k_{(CPET-CR)}$ / s^{-1}	$k_{(CPET-CS)}$ / s^{-1}	$k_{(CPET-CR)}$ / s^{-1}
1	CH_2Cl_2	$2.3(2) \times 10^{11}$	$1.3(1) \times 10^{9}$	$1.4(1) \times 10^{11}$	$1.3(2) \times 10^{9}$
	n-BuCN	$1.9(1) \times 10^{11}$	$1.1(1) \times 10^{10}$	n.d.	n.d.
	MeCN	$3.0(1) \times 10^{11}$	$3.1(1) \times 10^{10}$	n.d.	n.d.
	DMF	$2.0(1) \times 10^{11}$	$4.6(1) \times 10^{10}$	n.d.	n.d.
2	CH_2Cl_2	$1.3(3) \times 10^{11}$	$1.7(2) \times 10^{9}$	n.d.	n.d.
	n-BuCN	$2.2(1) \times 10^{11}$	$1.4(1) \times 10^{10}$	n.d.	n.d.
	DMF	$2.3(1) \times 10^{11}$	$5.0(1) \times 10^{10}$	n.d.	n.d.
3	CH_2Cl_2	$7.6(5) \times 10^{11}$	$3.7(3) \times 10^{9}$	$7.1(1) \times 10^{11}$	$4.3(2) \times 10^{9}$
	DMF	$6.2(2) \times 10^{11}$	$6.2(1) \times 10^{10}$	n.d.	n.d.
4	CH_2Cl_2	$3.2(3) \times 10^{10}$	n.o.	$3.4(1) \times 10^{10}$	n.o.
5	CH_2Cl_2	$2.5(1) \times 10^{10}$	n.o.	n.d.	n.d.
6	CH_2Cl_2	$1.7(1) \times 10^{10}$	n.o.	n.d.	n.d.
7	CH_2Cl_2	$4.0(1) \times 10^{10}$	n.o.	n.d.	n.d.
8	CH_2Cl_2	$8.3(2) \times 10^{10}$	n.o.	n.d.	n.d.

4. Kinetic isotope effect (KIE).

H/D isotopic exchanges were performed in the glove box dissolving **1**-**3** in CH_2Cl_2 with excess MeOD (typically ~ 10 % of the total volume) and evaporating under *vacuum*. This procedure was repeated 5 times. Afterward, KIEs were measured in samples of **1**-**3** re-dissolved in CH_2Cl_2 with excess MeOD (~ 1 % of the total volume, to ensure high enrichment) and measuring the visible transient absorption as described above. Control samples prepared with the same procedure using MeOH were used to measure k_H, with rate constants being within the uncertainty of measurements in pure CH_2Cl_2. **1** was additionally measured in MeCN by the same procedure. The KIEs were measured in 4 to 6 independent replicates.

Table S2. Summary of KIE for charge separation (CS) and recombination (CR) for **1** and **3**.

Triad	Solvent	KIE_{CS}	KIE_{CR}
1	CH_2Cl_2	1.8 ± 0.1	1.0 ± 0.1
1	MeCN	1.7 ± 0.1	1.1 ± 0.1
2	CH_2Cl_2	1.6 ± 0.1	1.0 ± 0.1
3	CH_2Cl_2	1.7 ± 0.1	0.9 ± 0.1

5. Spectro-electrochemistry.

Spectro-electrochemistry of 9-cyano-10-methyl-anthracene 0.4 mM in MeCN with $TBAPF_6$ 0.1 M was performed in a 1 mm length path cuvette with a Pt mesh working electrode, Pt rod counter electrode and Ag^+/Ag pseudo-reference electrode. The electrolysis potential was set at -2.0 V for 5 minutes (this is 0.4 V more negative than the cathodic peak potential of 9-cyano-10-methyl-anthracene *versus* the Ag^+/Ag pseudo-reference electrode used). UV-vis spectra were collected every 30 seconds. The spectra of the 9-CN-10-Me-AN radical anion shows a sharp band at 325 nm and a broad band in the visible with peaks at 550, 600 and 662 nm. The spectra did not change after 2 minutes. After 5 minutes the potential was set at -1.0 V for 5 more minutes, after which time the spectra returned completely to that of neutral 9-cyano-10-methyl-anthracene.

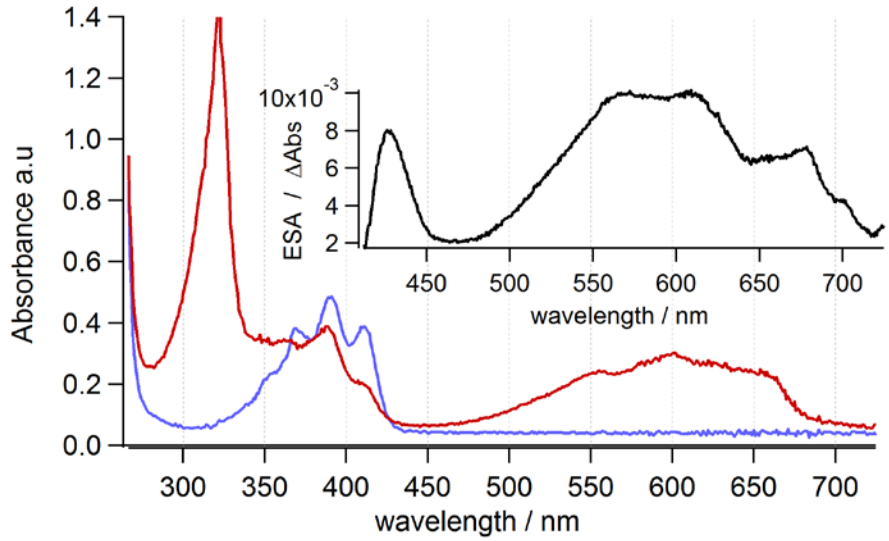

Figure S48. Blue: UV-vis spectrum of 9-cyano-10-methyl-anthracene in MeCN before electrolysis. Red: Spectrum of the 9-cyano-10-methyl-anthracene radical anion produced by electrolysis. Insert: Visible transient absorption spectrum of **1** at 6 ps delay time in MeCN (See also Figure S32 above); the absorbance at ~425 nm is assigned to the phenoxyl radical in the CSS of **1** (not expected for reference compound 9-cyano-10-methyl-anthracene).

The broad band in the visible of the 9-cyano-10-methyl-anthracene radical anion obtained by spectro-electrochemistry is in excellent agreement with the band in the same region observed in the transient absorption spectra for **1-3** upon CPET-CS. Therefore, the latter is assigned to the anthracene radical anion portion of the CSS in the triads.

6. Calculation of CPET free-energies by the Weller approximation.

The calculation of the free energies for CPET charge separation (CS) and recombination (CR) requires calculating the free-energies of the transient LESs relative to the GSs, and the free-energies of the transient CSSs relative to the GSs. The free energies of CS and CR were calculated using two different approaches: (1) using the Weller approximation for electron transfer processes (*34*), and (2) using constrained density functional theory methods (see section S7 below). In the Weller approximation, the CS process is viewed as an electron transfer from the phenol-pyridine unit to the excited anthracene. The proton-transfer portion of the CPET is included in the electrochemical potential for oxidation of the phenol-pyridine unit, which occurs by CPET (*18*).

$$\Delta G^{o\prime}_{\text{CPET-CS}} = E^{o}(T^{\bullet+}/T) - E^{o}(T/T^{\bullet-}) - E_{\text{O-O}} - \frac{e^2}{4\pi\varepsilon_o Dr_{12}} \qquad \text{(S1)}$$

In equation (S1), $E°(T^{\bullet+}/T)$ and $E°(T/T^{\bullet-})$ are, respectively, the reduction potential for the (AN–PhO$^{\bullet}$–pyH^{+}/An–PhOH–py) couple (coupled to proton transfer) and reduction potential for the (AN–PhOH–py/An$^{\bullet-}$–PhOH–py) couple according to:

$$\text{AN–PhO}^{\bullet}\text{–pyH}^{+} + e^{-} \rightarrow \text{An–PhOH–py} \qquad E°(T^{\bullet+}/T) \qquad \text{(S2)}$$

$$\text{AN–PhOH–py} + e^{-} \rightarrow \text{An}^{\bullet-}\text{–PhOH–py} \qquad E°(T/T^{\bullet-}) \qquad \text{(S3)}$$

$E_{0\text{-}0}$ in eq. (S1) is the energy of the vibrational relaxed local excited state of the anthracenes portion of the triads. $E_{0\text{-}0}$ approximates the free-energies of the transient LESs relative to the GSs. The band of 0→0 transitions for anthracene ground state excitation and local excited state emission overlap significantly in the absorption and emission spectra and the $E_{0\text{-}0}$ can be estimated at the interception of the spectra. Figure S49 and S50 show representative absorption and emission spectra of triads with 9-cyano-10-methylantharacene fragments (**1**-**4**) and 9-methylanthracene fragments (**5**-**8**). $E_{0\text{-}0}$ was estimated to be ca. 2.97 eV for **1**-**4** and ca. 3.20 eV for **5**-**8** (Figs. S49-50).

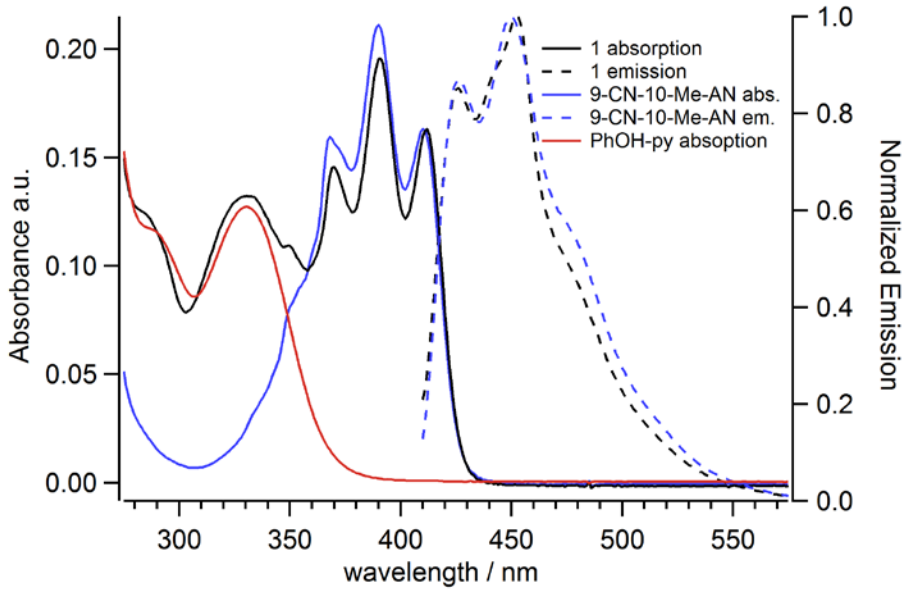

Figure S49. Absorption and emission spectra of **1**, reference compound 9-cyano-10-methylanthracene (9-CN-10-Me-AN), and reference compound 2,4-di-tertbutyl-6-(pyridin-2-yl)phenol (PhOH-py, ref (*18*)).

Black solid line: UV-vis spectrum of **1** (0.020 ± 0.005 mM) in MeCN. Black dotted line: steady state emission spectrum of **1** (0.020 ± 0.005 mM) in MeCN. Blue solid line: UV-vis spectrum of 9-CN-10-Me-AN (0.022 ± 0.05 mM) in MeCN. Blue dotted line: steady state emission spectrum of 9-CN-10-Me-AN (0.022 ± 0.005 mM) in MeCN. Red solid line: UV-vis spectrum of PhOH-py (0.015 ± 0.006 mM) in MeCN. Steady state emission spectra of **1** and 9-CN-10-Me-AN with excitation at 400 nm with excitation and detection monochromators slits at 5 nm for **1** and 1 nm for 9-CN-10-Me-AN (under these conditions the (9-CN-10-Me-AN/**1**) emission intensity ratio is ca. 24).

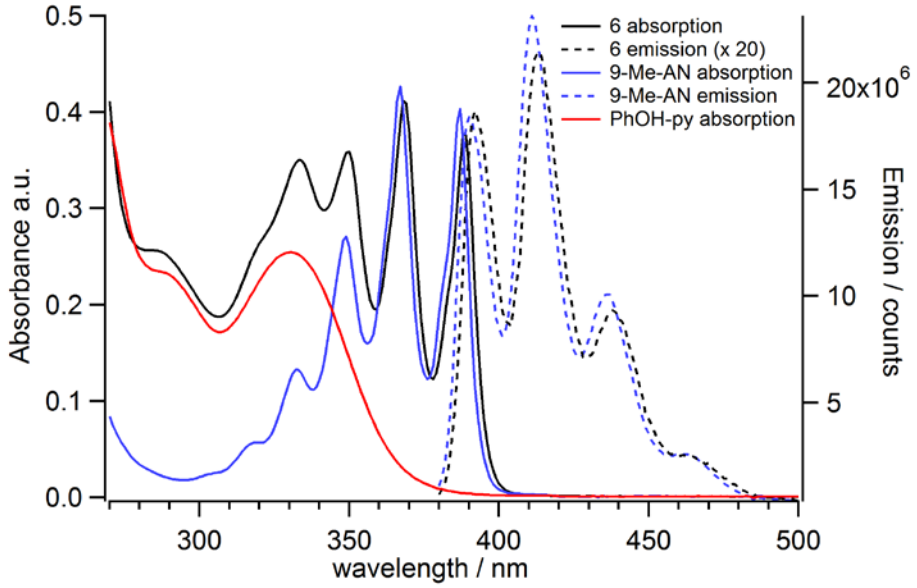

Figure S50. Absorption and emission spectra of **6**, reference compound 9-methylanthracene (9-Me-AN), and reference compound PhOH-py.

Black solid line: UV-vis spectrum of 6 (0.044 ± 0.010 mM) in MeCN. Black dotted line: steady state emission spectrum of 6 (0.044 ± 0.010 mM) in MeCN, increased by a factor of 20 to fit the scale. Blue solid line: UV-vis spectrum of 9-Me-AN (0.057 ± 0.010 mM) in MeCN. Blue dotted line: steady state emission spectrum of 9-Me-anth (0.057 ± 0.010 mM) in MeCN. Red solid line: UV-vis spectrum of PhOH-py (0.033 ± 0.011 mM) in MeCN. Steady state emission spectra of **6** and 9-Me-AN 365 nm with excitation wavelength with slits at 1 nm for both excitation and detection monochromators.

Figures S49 and 50 show negligible spectral overlap between the anthracene emission and the phenol−pyridine absorption, indicating that Förster and Dexter energy transfer would be energetically uphill. Therefore, energy transfer are unlikely quenching mechanisms of the LES.

The term $e^2/4\pi\varepsilon_o Dr_{12}$ in eq. (S1) estimates the Columbic stabilization of the charge-separated state. ε_o is the permittivity of vacuum, *e* is the electron charge, D is the static solvent dielectric constant, and r_{12} is the distance between charges. The latter was estimated as the distance between the centroids of the phenol ring and anthracene central ring. r_{12} is 4.89±0.07 Å using atomic coordinates from X-ray crystallography of **1**,**3**, **5** and **6** and 5.055±0.006Å using atomic coordinates from optimized DFT structures for **1**-**8** (DFT details below). Calculations of the Columbic term used r_{12} from optimized DFT structures considering that distance packing effects could be at play in the structure from X-ray crystallography.

Electrochemical determination of reduction potentials $E°$ ($T^{\bullet+}/T$) and $E°$ ($T/T^{\bullet-}$) according to eqs. S2 and S3 was pursued. We observed reversible one electron reductions of the anthracene portion of the triads. The phenol oxidation was, however, irreversible even at fast scan rates. This is likely due to fast dimerization of the phenoxyl radical cation as described for phenols with un-substituted *para*- and *ortho*-positions (*35*). Considering such an EC mechanism for the phenol-base one-electron oxidation followed by dimerization, we performed scan rate dependence cyclic voltammetry at low triad concentrations in MeCN in order to obtain formal reduction potentials for eq. 2 following the analysis developed by Savéant and co-workers (*35*). In this analysis, the peak

potential (E_p) varies with the scan rate according to:

$$E_p = E^o + 0.903\frac{RT}{F} - (\ln 10\frac{RT}{3F})\log(\frac{4RTk_{dim}C^o}{3F\upsilon}) \quad \text{(S4)}$$

where $E°$, k_{dim}, C° and υ are respectively the standard reduction potential, the rate constant for dimerization, substrate concentration and scan rate, while R, F and T are the gas constant, Faraday constant and temperature. Taking k_{dim} = 2.0x10^9 M^{-1}s^{-1}, C°=0.1 mM and T=298 K (*35*), equation S4 leads to E_p=$E°$-0.0918V+0.0197V log(υ). E_p *versus* log(υ) was evaluated between 0.05 and 0.5 V/s. where we observed a linear dependence with slope ca. 20 mV. Scan rates higher than 0.5 V/s led to increasing peak potential separation of the anthracene waves indicative of competing interfacial ET kinetics at play. Therefore, we limit the analysis to scan rates lower than 0.5 V/s. The reduction potential for the **1**$^{\bullet+}$/**1** and **1**/**1**$^{\bullet-}$ couples are +0.75 and -1.83V *versus* ferrocene (Figure S51).

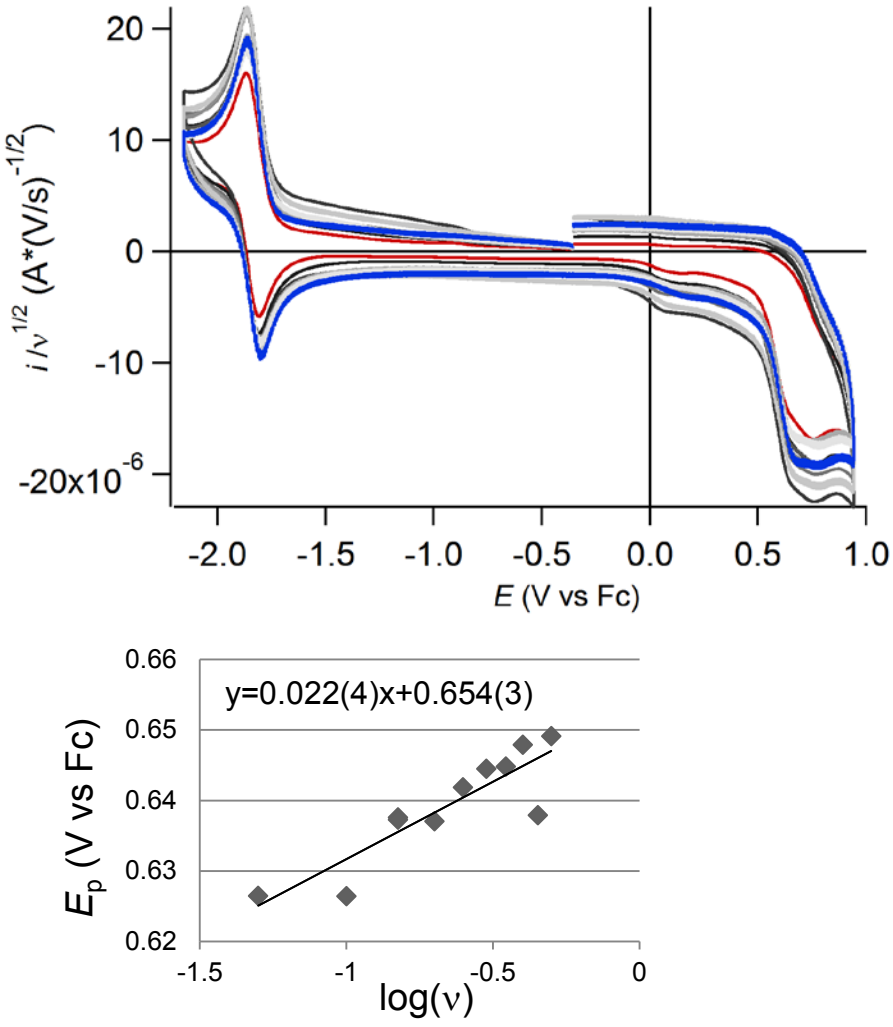

Figure S51. Cyclic voltammetry of 0.13 mM **1** in MeCN with 0.1 M $TBAPF_6$ as a function of scan rate. Top) -2.2 V to 1.0 V window including reduction and oxidation of **1** (each scan is done in a freshly polished electrode). Bottom) Plot of E_p *versus* log(υ).

The above analysis yields a good linear dependence of E_p versus log(υ) in MeCN. However, a similar treatment did not afford satisfactory linear correlations in other solvents relevant for the study, particularly in CH_2Cl_2. In order to circumvent this limitation we used density functional theory (DFT) to calculate the standard reduction potentials for eq. (S2) and (S3) from the calculated free energy $\Delta G^{\circ,red}_{solv}$ of the reductions according to $E^{\circ} = -\Delta G^{\circ,red}_{solv}/F$ in the different solvents used for transient absorption spectroscopy studies. $\Delta G^{\circ,red}_{solv}$ was calculated using quantum chemistry methods with structures optimized in solution (*36*). The free energies were calculated from Gibbs free energies $G_{(solv)}$ for the species in eqs. S2 and S3; namely, the one-electron oxidized (AN-PhO$^{\bullet}$-pyH^{+}), neutral (AN-PhOH-py), and one-electron reduced (AN$^{\bullet-}$-PhOH-py) triads.

$$\Delta G^{\circ,red}_{solv\ (AN\text{-}PhO\bullet\text{-}pyH+/AN\text{-}PhOH\text{-}py)} = G_{(solv,AN\text{-}PhO\bullet\text{-}pyH+)} - G_{(solv,AN\text{-}PhOH\text{-}py)} \quad \text{(S5)}$$

$$\Delta G^{\circ,red}_{solv\ (AN\text{-}PhOH\text{-}py/AN\bullet\text{-}\text{-}PhOH\text{-}py)} = G_{(solv,AN\text{-}PhOH\text{-}py)} - G_{(solv,AN\bullet\text{-}\ \text{-}PhOH\text{-}py)} \quad \text{(S6)}$$

Computations of the experimentally relevant standard reduction potential require consideration of a reference electrode. In the calculation of $\Delta G^{\circ\prime}_{CPET\text{-}CR}$ using eq. S1, the experimental value of the reduction potential for the $\mathbf{1}^{\bullet+}/\mathbf{1}$ (+0.75 V) and $\mathbf{1}/\mathbf{1}^{\bullet-}$ (-1.83 V) couples *versus* ferrocene were used to reference all other calculated reduction potentials for the (AN–PhO$^{\bullet}$–pyH^{+}/An–PhOH–py) and (AN–PhOH–py/An$^{\bullet-}$–PhOH–py) couples of **1**-**8**, such that calculated values for **1** agree with experimental values by construction. First, the calculated and experimental reduction potentials for **1**, and other phenol-bases and anthracenes previously reported in MeCN were compared in order to evaluate the accuracy of the method to reproduce changes in reduction potential due to substituent effects (Fig. S52 and Table S3).

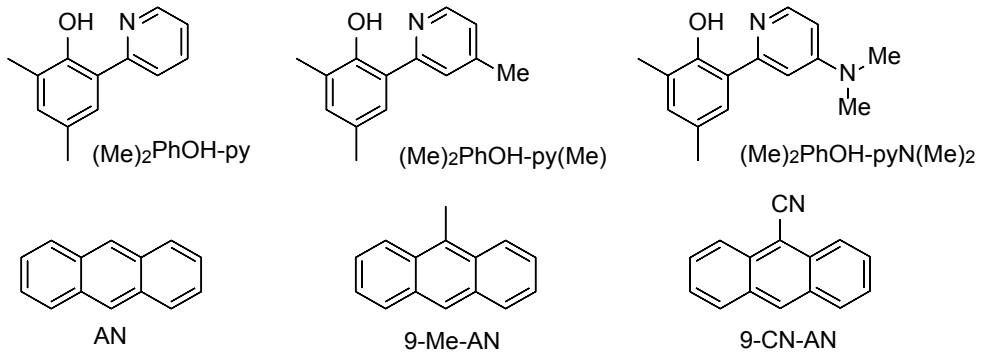

Figure S52. Phenol-bases and anthracenes used for reduction potential benchmarking.

All computations to obtain reduction potentials were performed using Gaussian09 (*37*). Gibbs free energies $G_{(solv)}$ for oxidized and reduced species were calculated using DFT. The geometries were optimized using the B3LYP (*38,39*) functional, the 6-31++G** basis set (*40-42*), and the conductor-like polarizable continuum model (C-PCM) (*43*) for the solvent.

Table S3. Experimental and computed reduction potentials for phenol-bases and anthracenes.

	E^o vs Fc in MeCN / V		
Compound	experimental	calculated*	ΔE^o / V
$1^{\bullet+}/1$	0.75	0.48	0.27
$1/1^{\bullet-}$	-1.83	-1.84	0.01
$(Me)_2PhO^{\bullet}$-$pyH^+/(Me)_2PhOH$-py	0.58†	0.27	0.31
$(Me)_2PhO^{\bullet}$-pyH^+(Me)/$(Me)_2PhOH$-py(Me)	0.53†	0.21	0.32
$(Me)_2PhO^{\bullet}$-$pyH^+(NMe_2)$/ $(Me)_2PhOH$-py(NMe_2)	0.32†	0.03	0.29
AN/ $AN^{\bullet-}$	-2.43‡	-2.52	0.09
9-Me-AN/9-Me-$AN^{\bullet-}$	-2.45‡	-2.54	0.09
9-CN-AN/9-CN-$AN^{\bullet-}$	-1.96‡	-1.94	0.02

* Computed *versus* the free energy of the ferrocenium/ferrocene couple from ref. (*44*). † Data from ref. (*21*). ‡ Data from ref. (*45*).

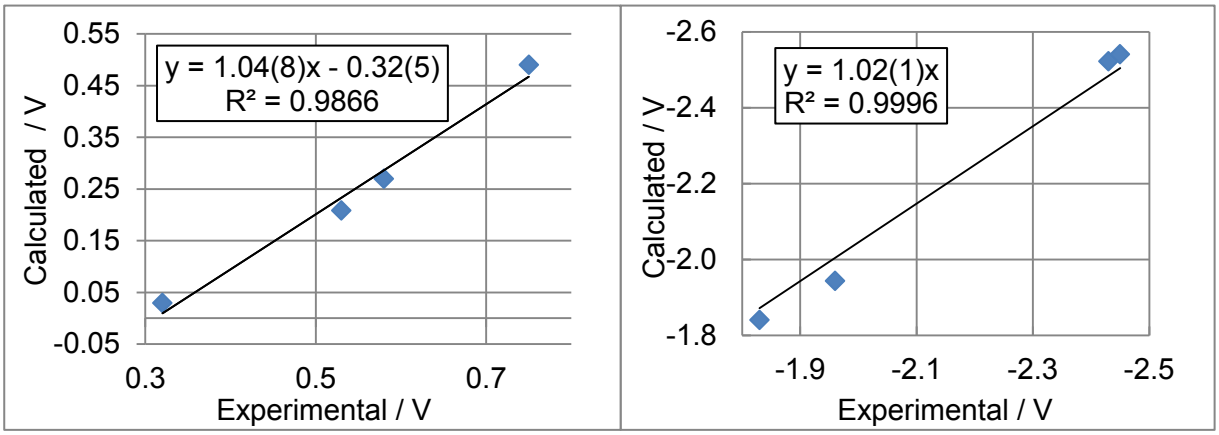

Figure S53. Experimental *versus* computed reduction potentials for phenol-bases (right) and anthracenes (left).

Plots of computed *versus* experimental reduction potentials for **1** and related phenol-bases and anthracenes show linear correlations with slope close to unity (Fig. S53). This shows that the computed and experimental reduction potentials fulfill the idealized relationship $E°_{calc} = E°_{exp} - E°_{ref}$ (*46*), and therefore the computed values accurately reproduce the changes in reduction potentials due to substituent effects. The intercept in the plot for one-electron oxidation of phenol-bases reflects systematically underestimated computed reduction potentials (Table S3, and Figure S53 left). This is accounted for by referencing all computed reduction potentials to the experimental reduction potential of the $\mathbf{1}^{\bullet+}$ / **1** couple. The computed reduction potentials for anthracenes are in excellent agreement with experimental values. After accounting for systematic deviations of the

computed reduction potentials by referencing to the experimental reduction potentials of the $\mathbf{1}^{\bullet+}$ / **1** (+0.75 V) and **1** / $\mathbf{1}^{\bullet-}$ (-1.83 V) couples *versus* ferrocene, the RMSD between computed and experimental reduction potentials is ±0.05 V.

Considering that the CPET reactions studied are photo-initiated CPET charge *separation* and *recombination* to the GS (thereby closing a photochemical cycle), the CPET-CR free-energy can be estimated as $\Delta G^{\circ\prime}_{\text{CPET-CR}} = -(\Delta G^{\circ\prime}_{\text{CPET-CS}} + E_{0\text{-}0})$.

Table S4. CEPT free-energies for charge separation (CS) and recombination (CR). Reduction potentials computed from thermochemical data obtained by DFT. Benchmarking *versus* electrochemical data.

Triad	Solvent	E° ($T^{\bullet+}$/T) /eV	E° (T/$T^{\bullet-}$) /eV	$E_{0\text{-}0}$ / eV	ω / eV*	$\Delta G^{o\prime}_{\text{(CPET-CS)}}$ /eV †	$\Delta G^{o\prime}_{\text{(CPET-CR)}}$ / eV†
1	CH_2Cl_2	0.89	-2.01	2.97	0.32	-0.39	-2.58
	n-BuCN	0.62	-1.89	2.97	0.14	-0.59	-2.38
	DMF	0.62	-1.83	2.97	0.08	-0.59	-2.38
	MeCN	0.75	-1.83	2.97	0.08	-0.47	-2.50
2	CH_2Cl_2	0.74	-2.02	2.97	0.32	-0.53	-2.44
	n-BuCN	0.62	-2.01	2.97	0.14	-0.47	-2.50
	DMF	0.60	-1.99	2.97	0.08	-0.46	-2.51
3	CH_2Cl_2	0.57	-2.04	2.97	0.32	-0.67	-2.30
	DMF	0.45	-1.91	2.97	0.08	-0.69	-2.28
4	CH_2Cl_2	1.23	-2.00	2.97	0.32	-0.05	-2.92
5	CH_2Cl_2	0.77	-2.62	3.20	0.32	-0.13	-3.07
6	CH_2Cl_2	0.82	-2.61	3.20	0.32	-0.08	-3.12
7	CH_2Cl_2	0.99	-2.44	3.20	0.32	-0.09	-3.11
8	CH_2Cl_2	1.15	-2.61	3.20	0.32	0.24	-3.44

*ω is the Coulombic term with D(CH_2Cl_2)=8.9, D(n-BuCN)=20.7, D(DMF)=36.7, D(MeCN)=37.5. † Estimated error ±0.05V.

CPET free energies above calculated by the Weller approximation using reduction potentials from DFT calculation in general reproduce the expected trend due to substituent effect and solvent polarity. However, some outliers within the expected trends are observed. Therefore, alternative DFT methods, including constrained DFT, were also used to calculate CPET free-energies (see Section S7 below).

Optimized Cartesian coordinates for calculating driving forces by the Weller approximation:

Table S5. Cartesian coordinates for optimized geometries for **1**.

1 in CH_2Cl_2 / -1263.524957 Ha				**1** rad. anion CH_2Cl_2 / -1263.634002 Ha				**1** rad. cation CH_2Cl_2 / -1263.318667 Ha			
O	4.855735	-1.88731	0.210479	O	4.978873	-1.6844	0.126513	O	-4.91402	-1.72771	0.00021
H	5.073708	-0.96675	-0.14529	H	5.146032	-0.69831	-0.00727	N	-4.55139	0.846762	0.000144
N	4.596385	0.527334	-0.55704	N	4.575014	0.816696	-0.18352	C	0.669998	-2.61378	0.00129
C	-0.70253	-2.10957	1.489959	C	-0.66283	-2.56341	0.449159	H	0.888608	-3.25474	0.863987
H	-1.04759	-3.12579	1.278647	H	-0.90515	-3.35155	-0.27405	H	0.888829	-3.25568	-0.86066
H	-0.79061	-2.01315	2.575689	H	-0.85664	-3.02353	1.425984	C	1.603888	-1.4166	0.000736
C	-1.63883	-1.12243	0.817903	C	-1.59911	-1.39147	0.250566	C	2.046417	-0.86703	-1.23155
C	-2.01172	0.077641	1.475286	C	-2.01613	-0.61354	1.378902	C	1.581061	-1.34931	-2.50256
C	-1.47935	0.451235	2.755304	C	-1.50558	-0.83251	2.692622	H	0.85254	-2.1489	-2.53811
H	-0.75259	-0.18892	3.239296	H	-0.75082	-1.59552	2.847934	C	2.02758	-0.80777	-3.68437
C	-1.85312	1.61405	3.38014	C	-1.92999	-0.08886	3.789361	H	1.657338	-1.18975	-4.62944
H	-1.42849	1.870103	4.345776	H	-1.51265	-0.29196	4.772226	C	2.974708	0.255681	-3.67851
C	-2.7929	2.489324	2.768304	C	-2.88839	0.924083	3.620976	H	3.322606	0.67046	-4.61816
H	-3.0866	3.404318	3.273347	H	-3.22791	1.509451	4.471256	C	3.44297	0.756398	-2.48771
C	-3.32334	2.182156	1.541095	C	-3.39878	1.181774	2.350457	H	4.16008	1.569733	-2.48331
H	-4.03528	2.854328	1.073396	H	-4.13468	1.970761	2.220991	C	2.996169	0.225194	-1.23669
C	-2.95043	0.984918	0.855411	C	-2.98572	0.445484	1.214764	C	3.459113	0.742159	-0.00031
C	-3.47445	0.663679	-0.41946	C	-3.50071	0.715321	-0.10405	C	2.996139	0.22641	1.23657
C	-3.0864	-0.51303	-1.10527	C	-3.04294	-0.02191	-1.25489	C	3.442907	0.758858	2.487074
C	-3.59748	-0.83331	-2.40052	C	-3.51336	0.251408	-2.56123	H	4.159996	1.572206	2.481885
H	-4.30779	-0.15819	-2.86648	H	-4.24997	1.038803	-2.69619	C	2.974641	0.2593	3.678358
C	-3.19988	-1.97165	-3.05546	C	-3.05771	-0.45674	-3.67116	H	3.322502	0.675013	4.617608
H	-3.5969	-2.19806	-4.04018	H	-3.44021	-0.22	-4.66039	C	2.027548	-0.80419	3.685247
C	-2.26488	-2.85586	-2.44969	C	-2.09855	-1.46857	-3.50067	H	1.657324	-1.18525	4.630688
H	-1.94835	-3.74927	-2.97886	H	-1.72362	-2.01999	-4.35906	C	1.581053	-1.34689	2.503967
C	-1.7603	-2.58361	-1.20278	C	-1.61905	-1.76343	-2.2282	H	0.852575	-2.14648	2.540291
H	-1.04057	-3.26625	-0.769	H	-0.86535	-2.53647	-2.12725	C	2.0464	-0.86583	1.232485
C	-2.14919	-1.41061	-0.47432	C	-2.07237	-1.07525	-1.06423	C	-1.33543	-1.01236	0.000696
C	1.338026	-0.84688	0.586368	C	1.350837	-1.00355	0.166789	H	-0.6217	-0.19979	0.000882
H	0.692722	0.008477	0.426373	H	0.639009	-0.19062	0.084841	C	-0.82067	-2.32621	0.000917
C	0.771694	-2.0095	1.101772	C	0.838518	-2.28335	0.351776	C	-1.72308	-3.4276	0.00077
C	1.612415	-3.12011	1.301097	C	1.75618	-3.34594	0.456785	H	-1.32679	-4.43717	0.000922
H	1.200177	-4.04531	1.696523	H	1.390073	-4.36036	0.600463	C	-3.07939	-3.21574	0.000473
C	2.96517	-3.05335	0.999253	C	3.124335	-3.12247	0.37906	H	-3.78874	-4.03444	0.0004
H	3.614609	-3.90991	1.151228	H	3.831554	-3.94272	0.45893	C	-3.62948	-1.88184	0.000292
C	3.530518	-1.8755	0.482702	C	3.631308	-1.8256	0.193165	C	-2.70254	-0.74424	0.000299
C	2.707796	-0.73664	0.261912	C	2.734603	-0.72863	0.082265	C	-3.19653	0.643457	-0.00012
C	3.267796	0.52083	-0.29193	C	3.231021	0.654466	-0.11555	C	-2.38098	1.782919	-0.0008
C	2.49385	1.670794	-0.5439	C	2.380704	1.772708	-0.23195	H	-1.30624	1.67622	-0.0011
H	1.430786	1.675403	-0.33701	H	1.305932	1.652178	-0.17861	C	-2.92894	3.074827	-0.00115
C	3.080299	2.824346	-1.06487	C	2.905119	3.051313	-0.41779	C	-4.33417	3.206533	-0.00072
C	4.461268	2.795236	-1.32698	C	4.303846	3.182105	-0.48365	H	-4.7994	4.183538	-0.00086
H	4.9728	3.662462	-1.73246	H	4.769664	4.152062	-0.62719	C	-5.12474	2.07229	-0.00013
C	5.16862	1.631996	-1.05856	C	5.087609	2.043628	-0.36178	H	-6.20509	2.100145	0.000172
H	6.236917	1.570882	-1.24856	H	6.171908	2.104565	-0.40755	C	4.402316	1.813415	-0.00083
C	-4.40971	1.552399	-1.0335	C	-4.45806	1.732356	-0.2744	N	5.177853	2.697712	-0.00126
N	-5.17294	2.278027	-1.53498	N	-5.25924	2.582261	-0.41694	C	-2.04718	4.292316	-0.00228
C	2.266227	4.062071	-1.34315	C	2.008656	4.256762	-0.54401	H	-2.24533	4.909377	-0.88633
H	2.662999	4.919942	-0.78936	H	2.218711	4.980486	0.251407	H	-0.98844	4.025988	0.001876
H	1.219326	3.925443	-1.06207	H	0.953355	3.979998	-0.48581	H	-2.25099	4.915464	0.876126
H	2.30566	4.319418	-2.40746	H	2.178577	4.767981	-1.49801	H	-5.12147	-0.018	0.000403
1 in nBuCN / -1263.526358 Ha				**1** rad. anion nBuCN / -1263.639628 Ha				**1** rad. cation nBuCN / -1263.330101 Ha			
O	4.850434	-1.89506	0.207911	O	4.976277	-1.69176	0.135226	O	4.866235	-1.75645	0.186438
H	5.068524	-0.9746	-0.15083	H	5.145122	-0.70566	-0.00523	N	4.538176	0.773168	-0.31047
N	4.596735	0.516776	-0.56326	N	4.580968	0.805512	-0.19003	C	-0.67759	-2.47486	0.812225
C	-0.70522	-2.09767	1.504801	C	-0.6665	-2.55464	0.47622	H	-0.946	-3.37636	0.251697
H	-1.05233	-3.11517	1.303549	H	-0.91073	-3.35137	-0.23672	H	-0.83162	-2.76736	1.856752
H	-0.79016	-1.99136	2.589732	H	-0.85916	-3.0028	1.458709	C	-1.61401	-1.34091	0.442434

C	-1.64109	-1.11493	0.825733	C	-1.60242	-1.3846	0.264834	C	-2.04794	-0.42417	1.432316
C	-2.01307	0.090401	1.474062	C	-2.02014	-0.59438	1.38456	C	-1.58469	-0.47638	2.790005
C	-1.48159	0.472522	2.751956	C	-1.5096	-0.79903	2.700672	H	-0.86594	-1.23025	3.0854
H	-0.75685	-0.1653	3.241948	H	-0.75469	-1.56009	2.864266	C	-2.02047	0.419385	3.733577
C	-1.85423	1.640509	3.367833	C	-1.93485	-0.0443	3.78944	H	-1.64937	0.355161	4.751524
H	-1.43043	1.902975	4.332078	H	-1.51773	-0.23673	4.774467	C	-2.95527	1.433586	3.38651
C	-2.79182	2.512749	2.748404	C	-2.8941	0.966055	3.610233	H	-3.29708	2.133733	4.142219
H	-3.08438	3.432033	3.24622	H	-3.23418	1.560061	4.454201	C	-3.42163	1.529994	2.100013
C	-3.32158	2.197221	1.522946	C	-3.40441	1.209815	2.33683	H	-4.13118	2.307364	1.836567
H	-4.0318	2.867403	1.049807	H	-4.14082	1.997023	2.199394	C	-2.98467	0.62092	1.088139
C	-2.95002	0.994341	0.846617	C	-2.9906	0.461878	1.209118	C	-3.44203	0.717034	-0.24761
C	-3.47348	0.664004	-0.42632	C	-3.50611	0.716808	-0.11303	C	-2.99481	-0.17265	-1.25352
C	-3.0869	-0.51864	-1.103	C	-3.04677	-0.03232	-1.25618	C	-3.44133	-0.06592	-2.60643
C	-3.59745	-0.84833	-2.39605	C	-3.51645	0.226568	-2.56566	H	-4.1488	0.71464	-2.86601
H	-4.30609	-0.17587	-2.86836	H	-4.25318	1.012201	-2.71024	C	-2.98646	-0.92914	-3.57081
C	-3.20151	-1.99272	-3.04161	C	-3.06	-0.49357	-3.66766	H	-3.33521	-0.83293	-4.59419
H	-3.59817	-2.22626	-4.02479	H	-3.44186	-0.26777	-4.65962	C	-2.05591	-1.95086	-3.23431
C	-2.26898	-2.87404	-2.42789	C	-2.10085	-1.50344	-3.48545	H	-1.69595	-2.6256	-4.00451
H	-1.95437	-3.77265	-2.94929	H	-1.72575	-2.06443	-4.33745	C	-1.61106	-2.08787	-1.94349
C	-1.76475	-2.59252	-1.18283	C	-1.62201	-1.78411	-2.20956	H	-0.89774	-2.87162	-1.72141
H	-1.04765	-3.2737	-0.74253	H	-0.86892	-2.55646	-2.09952	C	-2.06014	-1.21415	-0.89741
C	-2.1516	-1.4127	-0.46437	C	-2.07571	-1.0828	-1.05352	C	1.330941	-0.96233	0.317093
C	1.336807	-0.8433	0.592809	C	1.350473	-1.00036	0.178001	H	0.627752	-0.14697	0.204225
H	0.694025	0.01399	0.432981	H	0.641485	-0.18528	0.091989	C	0.80529	-2.23347	0.621729
C	0.768152	-2.00336	1.111952	C	0.835002	-2.27768	0.37287	C	1.69386	-3.33513	0.776035
C	1.605715	-3.11629	1.310991	C	1.749606	-3.34242	0.483212	H	1.287597	-4.31465	1.01005
H	1.191655	-4.03941	1.709182	H	1.380954	-4.35473	0.63448	C	3.042941	-3.16671	0.630554
C	2.958028	-3.05437	1.00505	C	3.118188	-3.1233	0.40125	H	3.739367	-3.99087	0.741597
H	3.604638	-3.91316	1.156897	H	3.822824	-3.94536	0.485354	C	3.615335	-1.8714	0.316271
C	3.525387	-1.87938	0.484706	C	3.628397	-1.8291	0.20552	C	2.692362	-0.7315	0.159876
C	2.705991	-0.73814	0.26436	C	2.734924	-0.73009	0.088694	C	3.195698	0.616447	-0.1542
C	3.269062	0.516655	-0.29302	C	3.23632	0.650086	-0.11991	C	2.3972	1.756263	-0.30356
C	2.499301	1.669623	-0.54293	C	2.391151	1.770986	-0.24406	H	1.324734	1.68199	-0.18759
H	1.437156	1.679427	-0.33157	H	1.31579	1.656034	-0.18933	C	2.958919	3.002658	-0.60224
C	3.089046	2.8201	-1.06744	C	2.92159	3.046006	-0.43971	C	4.356495	3.086818	-0.75093
C	4.468847	2.784407	-1.33498	C	4.32078	3.169691	-0.50733	H	4.83889	4.028888	-0.98327
H	4.982672	3.648888	-1.7433	H	4.790975	4.13632	-0.65826	C	5.123886	1.950184	-0.59807
C	5.17223	1.618416	-1.06818	C	5.099599	2.028654	-0.37768	H	6.201866	1.937632	-0.69674
H	6.239456	1.552447	-1.26224	H	6.184024	2.084232	-0.42465	C	-4.37358	1.745342	-0.59219
C	-4.40707	1.548983	-1.04763	C	-4.46525	1.7292	-0.29416	N	-5.13336	2.583947	-0.87346
N	-5.16952	2.271408	-1.55519	N	-5.26912	2.575491	-0.44568	C	2.100389	4.225037	-0.75921
C	2.279673	4.061247	-1.34352	C	2.031196	4.254821	-0.57461	H	2.366995	4.972364	-0.00398
H	2.68206	4.917248	-0.79095	H	2.247364	4.984526	0.213574	H	1.039641	3.99003	-0.65762
H	1.233028	3.929152	-1.05948	H	0.974562	3.984218	-0.51154	H	2.267543	4.683532	-1.7394
H	2.317713	4.318317	-2.40792	H	2.201993	4.756524	-1.53344	H	5.090576	-0.09431	-0.18603
1 in MeCN / -1263.526629 Ha				**1** rad.anion MeCN / -1263.642259 Ha				**1** rad.cation MeCN / -1263.325569 Ha			
O	4.849287	-1.89677	0.207327	O	4.934511	-1.77177	0.281661	O	-4.91602	-1.73279	0.000157
H	5.067436	-0.97636	-0.15206	H	5.122364	-0.84331	-0.07013	N	-4.55681	0.844813	0.000709
N	4.596793	0.514509	-0.56466	N	4.595655	0.627673	-0.50709	C	0.669285	-2.60934	0.001223
C	-0.70577	-2.09509	1.507981	C	-0.68215	-2.26472	1.234309	H	0.888158	-3.25017	0.863831
H	-1.05333	-3.11285	1.308892	H	-0.9831	-3.25164	0.862723	H	0.888316	-3.25116	-0.86061
H	-0.79004	-1.98666	2.59273	H	-0.81437	-2.33276	2.321067	C	1.603718	-1.41255	0.000592
C	-1.64156	-1.11331	0.827415	C	-1.61577	-1.21076	0.678967	C	2.047015	-0.86339	-1.23167
C	-2.01332	0.093153	1.473784	C	-1.99169	-0.08773	1.484993	C	1.578267	-1.3436	-2.50215
C	-1.48201	0.47713	2.751194	C	-1.43786	0.149757	2.778195	H	0.84631	-2.13997	-2.53677
H	-0.75768	-0.16017	3.242461	H	-0.68109	-0.52484	3.163138	C	2.024772	-0.80286	-3.68436
C	-1.85438	1.64623	3.365125	C	-1.82244	1.230124	3.565849	H	1.651141	-1.18241	-4.62902
H	-1.43074	1.91009	4.329051	H	-1.37271	1.369934	4.545365	C	2.975564	0.257287	-3.67903
C	-2.79151	2.517799	2.744076	C	-2.78304	2.137913	3.090092	H	3.323038	0.671988	-4.6189
H	-3.08382	3.438006	3.240326	H	-3.09174	2.983918	3.698134	C	3.447352	0.755712	-2.48852
C	-3.32117	2.200456	1.519021	C	-3.33493	1.952036	1.824281	H	4.166676	1.567126	-2.48508
H	-4.03102	2.870187	1.04471	H	-4.07209	2.660061	1.455183	C	3.000368	0.225564	-1.23723
C	-2.94991	0.99636	0.844721	C	-2.96267	0.865661	0.997567	C	3.466495	0.739994	-0.00074
C	-3.47328	0.664055	-0.42777	C	-3.52092	0.675799	-0.31822	C	3.001269	0.226323	1.236368

C	-3.08703	-0.51986	-1.10248	C	-3.10244	-0.41626	-1.16176	C	3.449231	0.757192	2.487023
C	-3.59751	-0.85159	-2.39503	C	-3.6132	-0.59882	-2.46872	H	4.168591	1.56857	2.48254
H	-4.30581	-0.17971	-2.86867	H	-4.35009	0.105874	-2.84464	C	2.978349	0.259489	3.678174
C	-3.20194	-1.99727	-3.03856	C	-3.19636	-1.65075	-3.28194	H	3.32657	0.674705	4.617548
H	-3.59855	-2.23236	-4.02138	H	-3.60881	-1.76042	-4.28125	C	2.027509	-0.80063	3.684862
C	-2.2699	-2.87793	-2.42316	C	-2.23781	-2.55855	-2.80247	H	1.654601	-1.17959	4.630049
H	-1.9557	-3.77765	-2.94289	H	-1.89415	-3.37651	-3.43025	C	1.58008	-1.34205	2.503331
C	-1.76571	-2.59442	-1.17852	C	-1.71973	-2.4081	-1.51978	H	0.848142	-2.13839	2.538985
H	-1.04913	-3.27524	-0.73684	H	-0.96851	-3.11246	-1.18038	C	2.047874	-0.86262	1.23218
C	-2.15212	-1.41314	-0.46221	C	-2.1311	-1.3551	-0.65051	C	-1.33848	-1.0101	0.001066
C	1.336565	-0.84253	0.594185	C	1.351132	-0.90562	0.469119	H	-0.62701	-0.19565	0.001632
H	0.694321	0.015168	0.434393	H	0.664961	-0.09015	0.272506	C	-0.82156	-2.32272	0.000828
C	0.767413	-2.00203	1.114133	C	0.811628	-2.09459	0.950706	C	-1.7217	-3.42607	0.000227
C	1.604297	-3.11546	1.313109	C	1.69598	-3.16159	1.197442	H	-1.32334	-4.43475	0.000033
H	1.189848	-4.03814	1.7119	H	1.307592	-4.10705	1.569907	C	-3.07815	-3.21666	-5.8E-05
C	2.956505	-3.05459	1.006277	C	3.05942	-3.03052	0.968604	H	-3.78556	-4.03701	-0.00045
H	3.602513	-3.91385	1.158087	H	3.739983	-3.85615	1.154452	C	-3.63097	-1.88385	0.000205
C	3.5243	-1.88022	0.48511	C	3.59411	-1.82535	0.484474	C	-2.70625	-0.74449	0.00058
C	2.705617	-0.73847	0.26487	C	2.731315	-0.72594	0.224476	C	-3.20194	0.642557	0.000375
C	3.269335	0.515751	-0.29327	C	3.259999	0.562539	-0.2859	C	-2.38719	1.782372	-0.00017
C	2.500469	1.669373	-0.54269	C	2.449478	1.687477	-0.53771	H	-1.31246	1.676588	-0.00058
H	1.438536	1.68029	-0.33033	H	1.382113	1.645691	-0.35969	C	-2.9362	3.073836	-0.00024
C	3.090896	2.819192	-1.06797	C	3.005048	2.873806	-1.01686	C	-4.34121	3.204583	0.000238
C	4.470429	2.782092	-1.33672	C	4.393687	2.904629	-1.23628	H	-4.80728	4.181118	0.000282
H	4.984731	3.645989	-1.74566	H	4.882371	3.799989	-1.60729	C	-5.13106	2.06971	0.000646
C	5.172961	1.615504	-1.0703	C	5.138359	1.765094	-0.96749	H	-6.2113	2.096813	0.000959
H	6.239948	1.548494	-1.26528	H	6.213964	1.751196	-1.12277	C	4.415931	1.805304	-0.00143
C	-4.40653	1.548221	-1.05063	C	-4.48023	1.585764	-0.79663	N	5.198425	2.683747	-0.002
N	-5.16881	2.269952	-1.55949	N	-5.28389	2.346818	-1.19717	C	-2.05517	4.291819	-0.00113
C	2.282521	4.061075	-1.34354	C	2.151118	4.08412	-1.29624	H	-2.25402	4.908733	-0.88509
H	2.686173	4.91669	-0.7913	H	2.516763	4.954279	-0.74044	H	-0.99639	4.02574	0.002956
H	1.235962	3.929979	-1.05875	H	1.108172	3.911547	-1.02031	H	-2.25967	4.914436	0.877435
H	2.320141	4.318049	-2.40796	H	2.186241	4.343568	-2.36034	H	-5.12687	-0.01922	0.00076
1 in DMF / -1263.526652 Ha				**1** rad.anion DMF / -1263.642085 Ha				**1** rad.cation DMF / -1263.330393 Ha			
O	4.84929	-1.89677	0.20733	O	4.83725	-2.00111	0.24444	O	-4.91602	-1.73279	0.00016
H	5.06744	-0.97636	-0.15206	H	5.06934	-1.13807	-0.2157	N	-4.55681	0.84481	0.00071
N	4.59679	0.51451	-0.56466	N	4.60434	0.36491	-0.74843	C	0.66929	-2.60934	0.00122
C	-0.70577	-2.09509	1.50798	C	-0.70727	-1.94331	1.62424	H	0.88816	-3.25017	0.86383
H	-1.05333	-3.11285	1.30889	H	-1.07202	-2.97292	1.51791	H	0.88832	-3.25116	-0.86061
H	-0.79004	-1.98666	2.59273	H	-0.77339	-1.74198	2.70151	C	1.60372	-1.41255	0.00059
C	-1.64156	-1.11331	0.82742	C	-1.63438	-1.00273	0.88212	C	2.04702	-0.86339	-1.23167
C	-2.01332	0.09315	1.47378	C	-1.94074	0.28615	1.42585	C	1.57827	-1.3436	-2.50215
C	-1.48201	0.47713	2.75119	C	-1.3137	0.79645	2.59972	H	0.84631	-2.13997	-2.53676
H	-0.75768	-0.16017	3.24246	H	-0.54059	0.20896	3.08413	C	2.02477	-0.80286	-3.68436
C	-1.85438	1.64623	3.36512	C	-1.63792	2.03576	3.13741	H	1.65114	-1.18241	-4.62902
H	-1.43074	1.91009	4.32905	H	-1.13123	2.38313	4.03482	C	2.97556	0.25729	-3.67903
C	-2.79151	2.5178	2.74408	C	-2.60999	2.8353	2.51806	H	3.32304	0.67199	-4.6189
H	-3.08382	3.43801	3.24033	H	-2.87317	3.80547	2.9325	C	3.44735	0.75571	-2.48852
C	-3.32117	2.20046	1.51902	C	-3.23176	2.38322	1.35867	H	4.16668	1.56713	-2.48508
H	-4.03102	2.87019	1.04471	H	-3.9775	3.0071	0.87192	C	3.00037	0.22556	-1.23723
C	-2.94991	0.99636	0.84472	C	-2.92165	1.13028	0.7827	C	3.4665	0.73999	-0.00074
C	-3.47328	0.66406	-0.42777	C	-3.55368	0.66355	-0.42518	C	3.00127	0.22632	1.23637
C	-3.08703	-0.51986	-1.10248	C	-3.19636	-0.59963	-1.01979	C	3.44923	0.75719	2.48702
C	-3.59751	-0.85159	-2.39502	C	-3.77674	-1.05751	-2.22456	H	4.16859	1.56857	2.48254
H	-4.30581	-0.17971	-2.86867	H	-4.52107	-0.43274	-2.71235	C	2.97835	0.25949	3.67817
C	-3.20194	-1.99727	-3.03856	C	-3.4202	-2.27445	-2.79675	H	3.32657	0.67471	4.61755
H	-3.59855	-2.23236	-4.02138	H	-3.88691	-2.59498	-3.72508	C	2.02751	-0.80063	3.68486
C	-2.2699	-2.87793	-2.42316	C	-2.45214	-3.07511	-2.17289	H	1.6546	-1.17959	4.63005
H	-1.9557	-3.77765	-2.94289	H	-2.15347	-4.02196	-2.61679	C	1.58008	-1.34205	2.50333
C	-1.76571	-2.59442	-1.17852	C	-1.86585	-2.65506	-0.98501	H	0.84814	-2.13839	2.53899
H	-1.04913	-3.27524	-0.73684	H	-1.10181	-3.27921	-0.53356	C	2.04787	-0.86262	1.23218
C	-2.15212	-1.41314	-0.46221	C	-2.21488	-1.42526	-0.35779	C	-1.33848	-1.0101	0.00107
C	1.33657	-0.84253	0.59419	C	1.35958	-0.82292	0.61674	H	-0.62701	-0.19565	0.00163
H	0.69432	0.01517	0.43439	H	0.72011	0.02268	0.39162	C	-0.82156	-2.32272	0.00083

C	0.76741	-2.00203	1.11413	C	0.76858	-1.92664	1.22403	C	-1.7217	-3.42607	0.00023
C	1.6043	-3.11546	1.31311	C	1.58601	-3.03849	1.49281	H	-1.32334	-4.43475	0.00003
H	1.18985	-4.03813	1.7119	H	1.15596	-3.9205	1.96346	C	-3.07815	-3.21666	-0.00006
C	2.95651	-3.05459	1.00628	C	2.93257	-3.03488	1.15941	H	-3.78556	-4.03701	-0.00045
H	3.60251	-3.91385	1.15809	H	3.56273	-3.89772	1.35568	C	-3.63097	-1.88385	0.00021
C	3.5243	-1.88022	0.48511	C	3.52112	-1.91732	0.5458	C	-2.70625	-0.74449	0.00058
C	2.70562	-0.73847	0.26487	C	2.72629	-0.76989	0.26917	C	-3.20194	0.64256	0.00038
C	3.26933	0.51575	-0.29327	C	3.30845	0.4398	-0.36111	C	-2.38719	1.78237	-0.00017
C	2.50047	1.66937	-0.54269	C	2.58406	1.63148	-0.55857	H	-1.31246	1.67659	-0.00058
H	1.43854	1.68029	-0.33033	H	1.55398	1.70841	-0.23182	C	-2.9362	3.07384	-0.00024
C	3.0909	2.81919	-1.06797	C	3.17934	2.73645	-1.16438	C	-4.34121	3.20458	0.00024
C	4.47043	2.78209	-1.33672	C	4.52165	2.62051	-1.56076	H	-4.80728	4.18112	0.00028
H	4.98473	3.64599	-1.74566	H	5.03925	3.44861	-2.03539	C	-5.13106	2.06971	0.00065
C	5.17296	1.6155	-1.0703	C	5.18422	1.42504	-1.3273	H	-6.2113	2.09681	0.00096
H	6.23995	1.54849	-1.26528	H	6.2263	1.30032	-1.61211	C	4.41593	1.8053	-0.00143
C	-4.40653	1.54822	-1.05063	C	-4.52631	1.46777	-1.04882	N	5.19843	2.68375	-0.002
N	-5.16881	2.26995	-1.55949	N	-5.33944	2.13875	-1.56865	C	-2.05517	4.29182	-0.00113
C	2.28252	4.06107	-1.34354	C	2.41336	4.01514	-1.39031	H	-2.25402	4.90873	-0.88509
H	2.68617	4.91669	-0.7913	H	2.93884	4.86937	-0.94817	H	-0.99639	4.02574	0.00296
H	1.23596	3.92998	-1.05875	H	1.4107	3.96554	-0.95698	H	-2.25967	4.91444	0.87744
H	2.32014	4.31805	-2.40796	H	2.31154	4.22155	-2.46263	H	-5.12687	-0.01922	0.00076

Table S6. Cartesian coordinates for optimized geometries for **2**.

2 in CH_2Cl_2 / -1338.731972 Ha				**2** rad.anion CH_2Cl_2 / -1338.840762 Ha				**2** rad.cation CH_2Cl_2 / -1338.531229 Ha			
O	4.478858	-2.610585	0.096781	O	4.65701	-2.396181	0.067391	O	-4.549779	-2.430583	-0.000004
H	4.808803	-1.683244	-0.133651	H	4.932624	-1.429489	-0.022764	N	-4.481204	0.169232	0.000011
N	4.51478	-0.10569	-0.359435	N	4.535033	0.144581	-0.128484	C	1.06918	-2.710446	-0.000026
C	-1.109463	-2.362704	1.234636	C	-1.048635	-2.667852	0.347597	H	1.350246	-3.328247	0.859988
H	-1.556148	-3.298995	0.887418	H	-1.370316	-3.39723	-0.405721	H	1.350242	-3.328229	-0.860054
H	-1.222067	-2.395034	2.321941	H	-1.294105	-3.142068	1.306101	C	1.872318	-1.42417	-0.000013
C	-1.91008	-1.199686	0.678261	C	-1.857525	-1.39816	0.1958	C	2.250687	-0.829631	-1.229864
C	-2.174026	-0.059108	1.478665	C	-2.195995	-0.626734	1.354455	C	1.846224	-1.361322	-2.500152
C	-1.647121	0.088046	2.806074	C	-1.703665	-0.941315	2.65556	H	1.218081	-2.24232	-2.53941
H	-1.00824	-0.684005	3.215862	H	-1.021811	-1.775831	2.776824	C	2.225619	-0.772022	-3.679746
C	-1.91543	1.195857	3.569634	C	-2.053876	-0.203297	3.781961	H	1.901634	-1.196573	-4.624704
H	-1.497527	1.279081	4.568027	H	-1.653576	-0.480396	4.753781	C	3.041443	0.393111	-3.673421
C	-2.736438	2.239438	3.059284	C	-2.915827	0.898771	3.657652	H	3.340051	0.847645	-4.612764
H	-2.947607	3.109488	3.673281	H	-3.197335	1.480502	4.531299	C	3.447971	0.943289	-2.484433
C	-3.255868	2.150956	1.792762	C	-3.404057	1.250267	2.40096	H	4.066871	1.834414	-2.481343
H	-3.876118	2.951403	1.402923	H	-4.064242	2.10812	2.305814	C	3.065887	0.362958	-1.235967
C	-2.989885	1.017208	0.964304	C	-3.063548	0.522836	1.235815	C	3.462101	0.92669	0.00001
C	-3.502827	0.920321	-0.351227	C	-3.555131	0.888229	-0.068833	C	3.065886	0.362934	1.235976
C	-3.218659	-0.19433	-1.177251	C	-3.168085	0.157434	-1.249353	C	3.447969	0.94324	2.484453
C	-3.716306	-0.288466	-2.513285	C	-3.613301	0.522851	-2.541912	H	4.06687	1.834366	2.481381
H	-4.334454	0.514499	-2.901374	H	-4.274525	1.379226	-2.643056	C	3.041441	0.393039	3.67343
C	-3.419534	-1.370441	-3.303339	C	-3.226244	-0.180898	-3.680346	H	3.340048	0.847555	4.612782
H	-3.804328	-1.424166	-4.317061	H	-3.586647	0.127987	-4.657908	C	2.225617	-0.772095	3.679732
C	-2.604832	-2.421923	-2.799747	C	-2.363469	-1.281996	-3.553516	H	1.901631	-1.196663	4.624682
H	-2.366615	-3.269533	-3.434762	H	-2.041482	-1.831554	-4.434302	C	1.846223	-1.361371	2.500126
C	-2.117175	-2.368188	-1.518035	C	-1.911935	-1.668985	-2.295513	H	1.21808	-2.242371	2.539366
H	-1.488601	-3.174901	-1.162846	H	-1.232309	-2.511297	-2.227663	C	2.250686	-0.829655	1.22985
C	-2.404013	-1.262471	-0.650459	C	-2.298859	-0.987606	-1.103915	C	-1.093593	-1.335335	-0.000013
C	1.085435	-1.234783	0.538174	C	1.124268	-1.323848	0.137448	H	-0.472794	-0.448318	-0.000011
H	0.543592	-0.298499	0.47693	H	0.506698	-0.434338	0.091826	C	-0.440084	-2.582913	-0.000021
C	0.378726	-2.381264	0.890069	C	0.47425	-2.547045	0.261946	C	-1.218483	-3.775283	-0.000023
C	1.086082	-3.59567	0.960865	C	1.270102	-3.707211	0.318063	H	-0.714477	-4.737357	-0.000029
H	0.562259	-4.51065	1.226798	H	0.794627	-4.681077	0.414217	C	-2.584443	-3.714468	-0.000018
C	2.446949	-3.644283	0.694901	C	2.654592	-3.631196	0.251435	H	-3.198973	-4.60833	-0.00002
H	2.993544	-4.580756	0.747827	H	3.267583	-4.526651	0.293104	C	-3.286959	-2.445048	-0.00001
C	3.154701	-2.482243	0.343707	C	3.3016	-2.390214	0.126807	C	-2.477683	-1.212743	-0.000008
C	2.468529	-1.240106	0.255533	C	2.530159	-1.198498	0.067808	C	-3.114648	0.117068	0
C	3.179328	0.006875	-0.122992	C	3.175078	0.131166	-0.061018	C	-2.425232	1.322308	-0.000001

C	2.542586	1.24771	-0.239641	C	2.453559	1.33022	-0.1115	H	-1.345021	1.357562	-0.00001
H	1.482524	1.370188	-0.06093	H	1.373153	1.352539	-0.058211	C	-3.123239	2.545533	0.000009
C	3.283593	2.379517	-0.599799	C	3.132877	2.547592	-0.2324	C	-4.533294	2.540957	0.00002
C	4.660741	2.249186	-0.840301	C	4.535535	2.54685	-0.301347	H	-5.120151	3.448545	0.000027
H	5.287605	3.084606	-1.122141	H	5.118346	3.453506	-0.394796	C	-5.175193	1.320791	0.00002
C	5.214175	0.980638	-0.703885	C	5.174724	1.313038	-0.243806	H	-6.254078	1.229698	0.000028
H	6.275762	0.829221	-0.880479	H	6.259355	1.261066	-0.292824	C	4.2755	2.102818	0.000022
C	-4.319377	1.976136	-0.861204	C	-4.417704	1.992792	-0.194413	N	4.93783	3.062225	0.000032
N	-4.986336	2.837815	-1.277395	N	-5.140015	2.915906	-0.297538	O	-2.368223	3.642416	0.000006
O	2.593457	3.539114	-0.690018	O	2.36193	3.658874	-0.273564	H	-4.949952	-0.753177	0.00001
C	3.294032	4.73582	-1.060656	C	2.997702	4.939018	-0.394173	C	-2.99273	4.945013	0.000018
H	2.541622	5.523437	-1.066118	H	3.566204	5.006782	-1.327215	H	-2.167512	5.654125	0.000015
H	3.732586	4.637795	-2.058697	H	3.654378	5.131207	0.46036	H	-3.599088	5.07666	0.899836
H	4.07272	4.974726	-0.32951	H	2.18719	5.666771	-0.404899	H	-3.599101	5.076669	-0.89979
2 in n-BuCN / -1338.733496 Ha				**2** rad.anion n-BuCN* / -1338.842399 Ha				**2** rad.cation n-BuCN / -1338.537040 Ha			
O	4.472406	-2.617445	0.095708	O	4.652588	-2.401044	0.070521	O	-4.552204	-2.433557	-0.000025
H	4.802841	-1.689584	-0.136395	H	4.928843	-1.433548	-0.022561	N	-4.486056	0.169183	0.000032
N	4.514072	-0.11525	-0.362724	N	4.535791	0.136616	-0.131486	C	1.066899	-2.706503	-0.000126
C	-1.112849	-2.353845	1.248	C	-1.052467	-2.663879	0.365935	H	1.348027	-3.324302	0.859775
H	-1.561899	-3.291844	0.908765	H	-1.376611	-3.399139	-0.380424	H	1.347993	-3.324207	-0.860106
H	-1.222053	-2.37844	2.335748	H	-1.29589	-3.130266	1.328666	C	1.8711	-1.420817	-0.00007
C	-1.912686	-1.193282	0.685388	C	-1.860743	-1.394735	0.205885	C	2.251081	-0.826956	-1.229835
C	-2.174747	-0.047511	1.479087	C	-2.197177	-0.61413	1.359195	C	1.843095	-1.356738	-2.499715
C	-1.647928	0.10635	2.805782	C	-1.703848	-0.919963	2.662091	H	1.210551	-2.234524	-2.538174
H	-1.01124	-0.664727	3.220671	H	-1.023598	-1.754922	2.788817	C	2.223485	-0.768648	-3.679602
C	-1.914161	1.219176	3.562811	C	-2.051633	-0.173306	3.783483	H	1.895962	-1.191026	-4.624281
H	-1.496562	1.307358	4.560867	H	-1.650853	-0.443983	4.756828	C	3.044269	0.392972	-3.673592
C	-2.732847	2.261397	3.046031	C	-2.912254	0.929067	3.652206	H	3.343268	0.847001	-4.613083
H	-2.942297	3.135514	3.654787	H	-3.191854	1.517501	4.52189	C	3.454544	0.941057	-2.484788
C	-3.252324	2.16639	1.779904	C	-3.401537	1.271897	2.393425	H	4.076655	1.829965	-2.482522
H	-3.870825	2.966006	1.385608	H	-4.060653	2.130063	2.293331	C	3.071217	0.362138	-1.236143
C	-2.988596	1.027244	0.958259	C	-3.063457	0.535503	1.233278	C	3.470852	0.923491	0.000036
C	-3.501705	0.923144	-0.356816	C	-3.556471	0.891769	-0.073935	C	3.071233	0.362015	1.236165
C	-3.219971	-0.197218	-1.176187	C	-3.171018	0.151731	-1.24985	C	3.454576	0.940808	2.484863
C	-3.717885	-0.29886	-2.511527	C	-3.616802	0.507958	-2.544706	H	4.076687	1.829717	2.482679
H	-4.334296	0.502756	-2.90513	H	-4.277016	1.364373	-2.652344	C	3.044316	0.392605	3.673617
C	-3.4237	-1.386652	-3.294704	C	-3.231633	-0.204839	-3.678287	H	3.343327	0.846539	4.61315
H	-3.808751	-1.446042	-4.307995	H	-3.592394	0.097067	-4.657827	C	2.223532	-0.769017	3.679522
C	-2.611625	-2.436895	-2.784358	C	-2.370354	-1.306259	-3.543759	H	1.896021	-1.191489	4.624163
H	-2.376047	-3.289448	-3.413667	H	-2.050291	-1.863126	-4.420555	C	1.843127	-1.356988	2.49958
C	-2.123609	-2.375823	-1.503042	C	-1.918351	-1.684294	-2.283239	H	1.210585	-2.23478	2.537958
H	-1.497843	-3.18227	-1.142429	H	-1.24071	-2.527658	-2.209478	C	2.251097	-0.827079	1.229748
C	-2.407453	-1.263643	-0.642758	C	-2.303075	-0.993114	-1.096473	C	-1.09733	-1.333031	-0.000056
C	1.083307	-1.232769	0.544215	C	1.122093	-1.322998	0.145398	H	-0.478366	-0.444825	-0.00005
H	0.544099	-0.294931	0.483377	H	0.506663	-0.432013	0.098614	C	-0.44238	-2.579487	-0.000091
C	0.374289	-2.377083	0.899205	C	0.470278	-2.544886	0.275313	C	-1.218887	-3.773163	-0.000099
C	1.078337	-3.593346	0.969616	C	1.264007	-3.706476	0.333063	H	-0.713489	-4.734432	-0.000125
H	0.552649	-4.506533	1.23776	H	0.787226	-4.679203	0.433327	C	-2.584737	-3.714054	-0.000076
C	2.438633	-3.64589	0.700311	C	2.648473	-3.632885	0.26298	H	-3.197614	-4.60904	-0.000083
H	2.982272	-4.584151	0.753106	H	3.259551	-4.52959	0.306071	C	-3.289158	-2.445745	-0.00004
C	3.148415	-2.48621	0.346107	C	3.297268	-2.393299	0.133051	C	-2.481726	-1.212227	-0.000029
C	2.465651	-1.242263	0.258173	C	2.528015	-1.200293	0.07195	C	-3.119677	0.1171	0.00001
C	3.179511	0.002267	-0.12347	C	3.176027	0.127705	-0.06274	C	-2.430399	1.322377	0.000027
C	2.54668	1.244901	-0.240114	C	2.458043	1.328379	-0.117225	H	-1.350243	1.357612	0.000011
H	1.487408	1.370883	-0.059027	H	1.377702	1.353922	-0.063277	C	-3.128649	2.545344	0.000066
C	3.290891	2.373926	-0.603284	C	3.141009	2.543638	-0.243228	C	-4.538374	2.540784	0.000089
C	4.667108	2.238536	-0.846591	C	4.543555	2.538167	-0.313226	H	-5.125613	3.448062	0.00012
H	5.29622	3.071453	-1.130711	H	5.12918	3.442564	-0.41047	C	-5.180206	1.320534	0.000071
C	5.216672	0.968447	-0.709989	C	5.179282	1.302855	-0.251743	H	-6.258973	1.22937	0.000086
H	6.277304	0.813377	-0.888719	H	6.263591	1.247559	-0.301549	C	4.29211	2.093685	0.000089
C	-4.316261	1.977064	-0.873096	C	-4.418309	1.995083	-0.206523	N	4.962558	3.047707	0.000133
N	-4.982022	2.837282	-1.294557	N	-5.140883	2.917782	-0.315375	O	-2.373671	3.6428	0.000081
O	2.604777	3.535582	-0.69343	O	2.3735	3.656708	-0.287977	H	-4.955789	-0.751999	0.00002
C	3.309247	4.730055	-1.066857	C	3.013723	4.935499	-0.413609	C	-2.999838	4.944616	0.000123

H	2.559622	5.520249	-1.071134	H	3.581376	4.997565	-1.3473	H	-2.175558	5.65484	0.000121
H	3.744911	4.629165	-2.065723	H	3.67141	5.127831	0.43982	H	-3.606473	5.07544	0.899807
H	4.090304	4.966244	-0.33759	H	2.205404	5.665527	-0.426143	H	-3.606512	5.075481	-0.899527
2 in DMF / -1338.733820 Ha				**2** rad.anion DMF† / -1338.843628 Ha				**2** rad.cation DMF / -1338.538231 Ha			
O	4.470990	-2.618964	0.095469	O	4.651658	-2.402046	0.071181	O	-4.552695	-2.434198	0.000004
H	4.801544	-1.691007	-0.137025	H	4.928039	-1.43438	-0.022515	N	-4.487069	0.169144	0.000000
N	4.513911	-0.117351	-0.363501	N	4.535928	0.13497	-0.132105	C	1.066440	-2.705671	0.000020
C	-1.113575	-2.351887	1.250921	C	-1.053259	-2.663023	0.369966	H	1.347561	-3.323405	0.859950
H	-1.563147	-3.290251	0.913437	H	-1.377941	-3.39957	-0.374858	H	1.347567	-3.323420	-0.859898
H	-1.222034	-2.374788	2.338759	H	-1.296224	-3.127683	1.333621	C	1.870858	-1.420105	0.000011
C	-1.913245	-1.191868	0.686947	C	-1.861406	-1.394012	0.2081	C	2.251185	-0.826467	-1.229772
C	-2.174881	-0.044961	1.479169	C	-2.197414	-0.611405	1.360224	C	1.842482	-1.355937	-2.499534
C	-1.648062	0.110379	2.805694	C	-1.703884	-0.915314	2.663513	H	1.209031	-2.233059	-2.537774
H	-1.011843	-0.660474	3.221693	H	-1.023978	-1.750357	2.79145	C	2.223088	-0.768177	-3.679519
C	-1.913831	1.224302	3.561284	C	-2.051154	-0.166765	3.783788	H	1.894841	-1.190165	-4.624114
H	-1.496280	1.313576	4.559255	H	-1.65028	-0.436027	4.757469	C	3.044895	0.392713	-3.673644
C	-2.732017	2.266213	3.043102	C	-2.911483	0.935666	3.650966	H	3.343981	0.846576	-4.613194
H	-2.941083	3.141220	3.650706	H	-3.190677	1.525568	4.51977	C	3.455936	0.940442	-2.484910
C	-3.251520	2.169771	1.777075	C	-3.400982	1.27659	2.391729	H	4.078708	1.828892	-2.482870
H	-3.869646	2.969194	1.381800	H	-4.059864	2.134817	2.290532	C	3.072342	0.361900	-1.236194
C	-2.988298	1.029443	0.956930	C	-3.063417	0.538232	1.232695	C	3.472675	0.922840	-0.000005
C	-3.501463	0.923759	-0.358030	C	-3.556727	0.892493	-0.075076	C	3.072339	0.361919	1.236192
C	-3.220279	-0.197856	-1.175931	C	-3.1716	0.150439	-1.249964	C	3.455931	0.940480	2.484900
C	-3.718283	-0.301153	-2.511101	C	-3.617485	0.504654	-2.545322	H	4.078703	1.828930	2.482847
H	-4.334324	0.500163	-2.905897	H	-4.277479	1.36107	-2.654386	C	3.044888	0.392770	3.673641
C	-3.424682	-1.390216	-3.292764	C	-3.232704	-0.210114	-3.677824	H	3.343972	0.846647	4.613185
H	-3.809814	-1.450854	-4.305947	H	-3.593527	0.090264	-4.657798	C	2.223080	-0.768120	3.679533
C	-2.613166	-2.440173	-2.780950	C	-2.371751	-1.311593	-3.541596	H	1.894831	-1.190093	4.624133
H	-2.378176	-3.293806	-3.409005	H	-2.052088	-1.87005	-4.417507	C	1.842476	-1.355898	2.499556
C	-2.125043	-2.377487	-1.499740	C	-1.919666	-1.687666	-2.280527	H	1.209025	-2.233019	2.537809
H	-1.499873	-3.183859	-1.137949	H	-1.242449	-2.531246	-2.205459	C	2.251182	-0.826448	1.229787
C	-2.408216	-1.263896	-0.641058	C	-2.303936	-0.994352	-1.094836	C	-1.098101	-1.332552	0.000008
C	1.082852	-1.232327	0.545523	C	1.121636	-1.322811	0.147169	H	-0.479522	-0.444096	0.000009
H	0.544219	-0.294152	0.484760	H	0.506647	-0.431523	0.10016	C	-0.442842	-2.578771	0.000013
C	0.373330	-2.376158	0.901205	C	0.469451	-2.544422	0.278248	C	-1.218950	-3.772722	0.000013
C	1.076654	-3.592825	0.971551	C	1.262742	-3.706306	0.336323	H	-0.713257	-4.733820	0.000016
H	0.550558	-4.505615	1.240194	H	0.785694	-4.678793	0.437469	C	-2.584777	-3.713976	0.000009
C	2.436819	-3.646237	0.701512	C	2.647199	-3.633221	0.265474	H	-3.197305	-4.609198	0.000009
H	2.979814	-4.584883	0.754289	H	3.257881	-4.530185	0.308852	C	-3.289601	-2.445904	0.000005
C	3.147047	-2.487080	0.346630	C	3.296362	-2.393931	0.134405	C	-2.482560	-1.212128	0.000004
C	2.465030	-1.242738	0.258738	C	2.52756	-1.200658	0.072874	C	-3.120724	0.117092	-0.000002
C	3.179554	0.001250	-0.123595	C	3.176205	0.126987	-0.063088	C	-2.431489	1.322386	-0.000008
C	2.547584	1.244283	-0.240209	C	2.458948	1.327988	-0.118455	H	-1.351345	1.357630	-0.000011
H	1.488494	1.371040	-0.058568	H	1.37862	1.354196	-0.064377	C	-3.129805	2.545290	-0.000013
C	3.292487	2.372696	-0.604049	C	3.14266	2.542803	-0.245571	C	-4.539460	2.540719	-0.000011
C	4.668490	2.236196	-0.848008	C	4.545181	2.536358	-0.315788	H	-5.126789	3.447925	-0.000014
H	5.298087	3.068565	-1.132636	H	5.131384	3.440284	-0.413859	C	-5.181264	1.320444	-0.000004
C	5.217202	0.965767	-0.711389	C	5.180198	1.300744	-0.253437	H	-6.260006	1.229255	-0.000003
H	6.277619	0.809895	-0.890616	H	6.264439	1.244765	-0.303409	C	4.295557	2.091790	-0.000013
C	-4.315582	1.977260	-0.875690	C	-4.418414	1.995526	-0.209212	N	4.967681	3.044692	-0.000019
N	-4.981077	2.837155	-1.298305	N	-5.14105	2.918122	-0.319332	O	-2.374843	3.642875	-0.000019
O	2.607253	3.534805	-0.694150	O	2.375854	3.656233	-0.291114	H	-4.956991	-0.751794	0.000003
C	3.312563	4.728786	-1.068173	C	3.016987	4.934738	-0.417856	C	-3.001368	4.944520	-0.000021
H	2.563551	5.519546	-1.072161	H	3.584456	4.995582	-1.351685	H	-2.177292	5.654987	-0.000022
H	3.747578	4.627298	-2.067229	H	3.674891	5.127149	0.43533	H	-3.608087	5.075193	0.899614
H	4.094153	4.964367	-0.339328	H	2.209118	5.665229	-0.430794	H	-3.608087	5.075190	-0.899656

*Optimized structure for a shallow saddle point with -0.82 cm^{-1}. †Optimized structure for a shallow saddle point with -1.30 cm^{-1}.

Table S7. Cartesian coordinates for optimized geometries for **3**.

3 in CH_2Cl_2 / -1358.146873 Ha				**3** rad.anion CH_2Cl_2 / -1358.254814 Ha				**3** rad.cation CH_2Cl_2 / -1357.952281 Ha			
O	4.320422	-2.9268	0.053083	O	4.530158	-2.6735	0.090885	O	4.372829	-2.79603	0.090467
H	4.685394	-1.99537	-0.13417	H	4.823414	-1.71352	-0.05938	N	4.431078	-0.21472	-0.29679

N	4.469187	-0.42656	-0.29848	N	4.477587	-0.15542	-0.22202	C	-1.21729	-2.70024	0.72211
C	-1.2599	-2.4922	1.170524	C	-1.17475	-2.76743	0.489152	H	-1.61089	-3.53031	0.126204
H	-1.74286	-3.39766	0.7915	H	-1.53123	-3.52909	-0.21505	H	-1.42591	-3.00278	1.754303
H	-1.37997	-2.55443	2.255716	H	-1.42202	-3.17495	1.476991	C	-1.96992	-1.42632	0.38952
C	-2.00968	-1.28047	0.648633	C	-1.9405	-1.48095	0.26938	C	-2.2741	-0.49158	1.410494
C	-2.23453	-0.15739	1.485095	C	-2.25296	-0.6358	1.383039	C	-1.841	-0.66234	2.768392
C	-1.71273	-0.07566	2.820186	C	-1.78812	-0.90395	2.704668	H	-1.24616	-1.52566	3.039045
H	-1.10811	-0.88577	3.20789	H	-1.14826	-1.76219	2.87768	C	-2.15011	0.253094	3.742567
C	-1.94344	1.015591	3.619121	C	-2.11354	-0.09263	3.787218	H	-1.80635	0.096262	4.760092
H	-1.53084	1.04853	4.622635	H	-1.73585	-0.33719	4.776654	C	-2.91844	1.408121	3.428191
C	-2.71866	2.107375	3.138888	C	-2.92082	1.040682	3.59586	H	-3.16253	2.122446	4.208152
H	-2.90092	2.963736	3.780802	H	-3.18322	1.679491	4.434946	C	-3.34776	1.621202	2.14288
C	-3.23057	2.082261	1.866407	C	-3.37981	1.348455	2.316836	H	-3.93049	2.5047	1.903975
H	-3.81607	2.919093	1.499852	H	-3.99822	2.229856	2.169979	C	-3.03851	0.694751	1.099918
C	-3.00287	0.967225	1.001839	C	-3.06335	0.545998	1.194916	C	-3.45717	0.909174	-0.23463
C	-3.50773	0.935468	-0.32004	C	-3.52204	0.868206	-0.13293	C	-3.13654	-0.00061	-1.27026
C	-3.26213	-0.16195	-1.1809	C	-3.1659	0.055367	-1.26896	C	-3.54397	0.22273	-2.62136
C	-3.75225	-0.19145	-2.52269	C	-3.58247	0.373076	-2.58343	H	-4.12303	1.109959	-2.8553
H	-4.33422	0.648441	-2.88791	H	-4.19765	1.255671	-2.73658	C	-3.212	-0.66294	-3.61495
C	-3.49371	-1.2583	-3.34611	C	-3.22544	-0.41082	-3.67868	H	-3.52927	-0.47751	-4.63628
H	-3.87224	-1.26285	-4.3636	H	-3.56302	-0.13742	-4.67477	C	-2.45037	-1.82524	-3.31138
C	-2.72715	-2.35859	-2.87208	C	-2.42348	-1.54731	-3.48412	H	-2.1864	-2.51753	-4.1046
H	-2.51922	-3.19419	-3.5331	H	-2.12621	-2.1609	-4.33067	C	-2.04815	-2.07571	-2.02361
C	-2.24793	-2.36702	-1.58609	C	-2.00014	-1.88765	-2.2031	H	-1.46339	-2.96541	-1.82644
H	-1.65626	-3.21036	-1.25326	H	-1.36682	-2.7598	-2.08364	C	-2.37447	-1.18403	-0.94762
C	-2.49583	-1.27924	-0.6845	C	-2.35729	-1.12231	-1.05375	C	0.99896	-1.48454	0.307405
C	0.984466	-1.43211	0.524089	C	1.033524	-1.50017	0.197003	H	0.423878	-0.57076	0.228546
H	0.481146	-0.47291	0.497819	H	0.439197	-0.59685	0.123202	C	0.288115	-2.67428	0.548137
C	0.228059	-2.56074	0.830377	C	0.350132	-2.69905	0.375625	C	1.001935	-3.90236	0.648892
C	0.882972	-3.80539	0.858854	C	1.112701	-3.87907	0.460135	H	0.454016	-4.82115	0.837064
H	0.320011	-4.70709	1.087951	H	0.612003	-4.83512	0.598713	C	2.360927	-3.92868	0.503225
C	2.242835	-3.89955	0.598674	C	2.497657	-3.84468	0.363704	H	2.926926	-4.8519	0.567332
H	2.750459	-4.85905	0.620159	H	3.085757	-4.75584	0.423397	C	3.121201	-2.72054	0.242756
C	3.000738	-2.75542	0.295073	C	3.177369	-2.62809	0.181909	C	2.381964	-1.44662	0.161963
C	2.367241	-1.48269	0.246579	C	2.440199	-1.41586	0.101216	C	3.083331	-0.16719	-0.07132
C	3.137183	-0.25397	-0.08771	C	3.125882	-0.10831	-0.07587	C	2.460222	1.070633	-0.07074
C	2.546922	1.009763	-0.18733	C	2.439709	1.110565	-0.08709	H	1.401122	1.124319	0.121259
H	1.486238	1.11924	-0.02209	H	1.368904	1.120194	0.044467	C	3.190156	2.273619	-0.30806
C	3.324532	2.14974	-0.50731	C	3.133434	2.332348	-0.26115	C	4.593968	2.141133	-0.54194
C	4.713611	1.932008	-0.72005	C	4.544963	2.245724	-0.41147	H	5.224931	2.997504	-0.72925
H	5.387439	2.740011	-0.97107	H	5.161675	3.1245	-0.54378	C	5.16512	0.896984	-0.52379
C	5.213276	0.648275	-0.60462	C	5.143307	0.999471	-0.38205	H	6.223959	0.742106	-0.6887
H	6.272191	0.46246	-0.76592	H	6.221813	0.914667	-0.49174	C	-4.21314	2.081939	-0.54734
C	-4.27531	2.04066	-0.80044	C	-4.3181	2.011853	-0.3274	N	-4.82672	3.039803	-0.80291
N	-4.90165	2.943138	-1.19271	N	-4.983	2.969126	-0.48939	N	2.582716	3.476258	-0.3084
N	2.76966	3.393053	-0.60814	N	2.481126	3.532285	-0.28155	H	4.85479	-1.15208	-0.25787
C	1.337174	3.581236	-0.39767	C	1.035463	3.589276	-0.08041	C	3.359902	4.697321	-0.54805
C	3.601599	4.542663	-0.95365	C	3.235952	4.774978	-0.41216	C	1.140897	3.588094	-0.06243
H	0.744092	3.010647	-1.12326	H	0.502611	3.013706	-0.84625	H	3.837729	4.67229	-1.53284
H	1.096445	4.636512	-0.51843	H	0.708365	4.625895	-0.14957	H	4.12871	4.831833	0.220194
H	1.03615	3.276684	0.612138	H	0.747113	3.203605	0.905809	H	2.688764	5.552751	-0.51526
H	4.065102	4.42365	-1.94093	H	3.813359	4.796259	-1.34399	H	0.568733	3.040964	-0.81888
H	4.39599	4.70053	-0.21416	H	3.927705	4.921139	0.427655	H	0.856775	4.637013	-0.11239
H	2.979231	5.436149	-0.97691	H	2.539742	5.612457	-0.42892	H	0.879289	3.208246	0.930794
3 in DMF / -1358.148896 Ha				**3** rad.anion DMF / -1358.261741 Ha				**3** rad.cation DMF / -1357.958801 Ha			
O	4.292307	-2.9592	0.05709	O	4.517648	-2.69216	0.099729	O	4.326025	-2.86289	0.11594
H	4.663019	-2.03173	-0.14683	H	4.814853	-1.73269	-0.05972	N	4.422358	-0.30141	-0.40284
N	4.464532	-0.46848	-0.32613	N	4.481179	-0.18118	-0.23153	C	-1.23684	-2.61271	0.919861
C	-1.27123	-2.45073	1.230061	C	-1.18628	-2.75356	0.511514	H	-1.66217	-3.48583	0.415012
H	-1.76454	-3.36395	0.884564	H	-1.5459	-3.52146	-0.18416	H	-1.41304	-2.8175	1.981689
H	-1.37869	-2.47901	2.317835	H	-1.43304	-3.15063	1.503591	C	-1.98506	-1.36248	0.499033
C	-2.01847	-1.25016	0.679173	C	-1.94972	-1.46783	0.279819	C	-2.25275	-0.33947	1.442658
C	-2.23478	-0.10358	1.485557	C	-2.26298	-0.61256	1.385756	C	-1.7829	-0.39692	2.797842
C	-1.70712	0.012372	2.81583	C	-1.79847	-0.86894	2.709909	H	-1.18886	-1.2405	3.126218

H	-1.10511	-0.78969	3.22371	H	-1.15875	-1.72561	2.890818	C	-2.05468	0.603696	3.696441
C	-1.92949	1.126224	3.585438	C	-2.12485	-0.04857	3.78524	H	-1.68263	0.532435	4.713578
H	-1.51261	1.184837	4.585965	H	-1.74761	-0.28425	4.776908	C	-2.82033	1.736141	3.30345
C	-2.70169	2.207985	3.078478	C	-2.93281	1.082584	3.583705	H	-3.03382	2.519479	4.023867
H	-2.87694	3.082701	3.697124	H	-3.19569	1.728596	4.417007	C	-3.2851	1.841202	2.017026
C	-3.21942	2.150077	1.809356	C	-3.39171	1.378632	2.301801	H	-3.8652	2.708077	1.718283
H	-3.8024	2.979605	1.422749	H	-4.01047	2.258598	2.147692	C	-3.0154	0.823689	1.051013
C	-3.00064	1.010691	0.974905	C	-3.07439	0.566641	1.187101	C	-3.47254	0.9244	-0.28453
C	-3.512	0.944332	-0.34333	C	-3.534	0.876041	-0.14408	C	-3.1889	-0.07532	-1.24562
C	-3.27524	-0.17754	-1.17491	C	-3.1753	0.05393	-1.2733	C	-3.63511	0.031919	-2.59855
C	-3.7719	-0.24237	-2.51299	C	-3.59077	0.359548	-2.59092	H	-4.2141	0.900824	-2.89354
H	-4.35155	0.58959	-2.89946	H	-4.20606	1.240481	-2.75324	C	-3.33905	-0.94087	-3.51952
C	-3.5226	-1.33329	-3.3074	C	-3.2326	-0.43412	-3.67889	H	-3.68496	-0.84269	-4.54369
H	-3.90607	-1.36456	-4.32255	H	-3.56932	-0.16994	-4.67768	C	-2.57656	-2.07904	-3.1371
C	-2.7594	-2.42378	-2.80615	C	-2.43068	-1.56877	-3.47323	H	-2.34056	-2.84069	-3.8735
H	-2.55949	-3.27905	-3.44406	H	-2.13324	-2.1903	-4.3138	C	-2.13795	-2.219	-1.84446
C	-2.27378	-2.39815	-1.52269	C	-2.00812	-1.89708	-2.18883	H	-1.55378	-3.09346	-1.58662
H	-1.68568	-3.2353	-1.16875	H	-1.37575	-2.76868	-2.06074	C	-2.42575	-1.2329	-0.84254
C	-2.51154	-1.28396	-0.65113	C	-2.36595	-1.12099	-1.0468	C	0.989596	-1.46566	0.37955
C	0.977803	-1.42307	0.548793	C	1.028572	-1.49718	0.208719	H	0.432095	-0.54401	0.270855
H	0.484851	-0.45865	0.516535	H	0.440387	-0.59001	0.131021	C	0.261949	-2.62719	0.695547
C	0.212083	-2.54018	0.874933	C	0.338576	-2.69152	0.394735	C	0.952566	-3.86493	0.833309
C	0.853344	-3.79158	0.910374	C	1.094005	-3.87582	0.484199	H	0.391299	-4.76147	1.08004
H	0.282939	-4.68439	1.154944	H	0.587889	-4.82802	0.628726	C	2.305376	-3.92851	0.64793
C	2.209527	-3.90372	0.636716	C	2.478862	-3.85023	0.384688	H	2.852699	-4.86093	0.736552
H	2.705909	-4.86903	0.663119	H	3.06104	-4.76497	0.447887	C	3.082289	-2.75126	0.308324
C	2.976343	-2.77155	0.312631	C	3.165333	-2.63869	0.194614	C	2.368756	-1.46523	0.196035
C	2.357066	-1.49209	0.258177	C	2.435706	-1.42202	0.109679	C	3.090428	-0.21216	-0.107
C	3.138424	-0.27547	-0.09486	C	3.13111	-0.1202	-0.07568	C	2.500747	1.041564	-0.10153
C	2.564916	0.995872	-0.1901	C	2.456722	1.104947	-0.08501	H	1.456773	1.128234	0.151546
H	1.509147	1.121934	-0.0062	H	1.38704	1.125506	0.055045	C	3.247524	2.218822	-0.4061
C	3.353726	2.12354	-0.52824	C	3.161631	2.319903	-0.26793	C	4.632203	2.043146	-0.71336
C	4.7363	1.884524	-0.76197	C	4.571283	2.2183	-0.42873	H	5.273959	2.877527	-0.95544
H	5.417661	2.681739	-1.0267	H	5.195671	3.09052	-0.56772	C	5.171394	0.784796	-0.6956
C	5.219404	0.594535	-0.6487	C	5.157764	0.966801	-0.39987	H	6.215385	0.597648	-0.91305
H	6.272917	0.393002	-0.8255	H	6.23445	0.871016	-0.51687	C	-4.23302	2.06993	-0.67551
C	-4.27836	2.038096	-0.85015	C	-4.33395	2.014156	-0.34853	N	-4.85342	3.00441	-0.99446
N	-4.90484	2.930874	-1.26422	N	-5.00358	2.967074	-0.51917	N	2.672382	3.437071	-0.40088
N	2.815619	3.373409	-0.6261	N	2.52247	3.525881	-0.28681	H	4.826885	-1.24571	-0.35365
C	1.390352	3.584448	-0.388	C	1.079427	3.599407	-0.07384	C	3.46686	4.631041	-0.70976
C	3.660284	4.51142	-0.98092	C	3.28891	4.760703	-0.43267	C	1.248678	3.59311	-0.08397
H	0.77522	3.014684	-1.09536	H	0.533689	3.030807	-0.83601	H	3.878773	4.578312	-1.7229
H	1.162296	4.641583	-0.51583	H	0.763994	4.639819	-0.13878	H	4.287641	4.752456	0.004737
H	1.10591	3.2948	0.630973	H	0.79536	3.216036	0.914495	H	2.824157	5.506325	-0.646
H	4.111812	4.384532	-1.97253	H	3.859769	4.768059	-1.36844	H	0.624534	3.042662	-0.79544
H	4.464067	4.658591	-0.24949	H	3.987355	4.906255	0.401377	H	0.989332	4.647666	-0.14696
H	3.050054	5.413237	-0.99906	H	2.600742	5.604581	-0.45178	H	1.029635	3.244869	0.930804

Table S8. Cartesian coordinates for optimized geometries for **4**.

4 in CH_2Cl_2 / -1316.473307 Ha				**4** rad.anion CH_2Cl_2 / -1316.582636 Ha				**4** rad.cation CH_2Cl_2 / -1316.254544 Ha			
O	4.780722	-2.12362	0.137376	O	4.849378	-2.03941	0.184273	O	4.697773	-2.17499	0.107954
H	5.032272	-1.20179	-0.16815	H	5.077809	-1.11265	-0.12083	N	4.545235	0.332061	-0.51186
N	4.572164	0.351172	-0.50079	N	4.57635	0.42712	-0.4753	C	-0.81631	-2.29731	1.353136
C	-0.79882	-2.30509	1.326859	C	-0.77602	-2.39639	1.143528	H	-1.1992	-3.28747	1.084177
H	-1.16316	-3.29045	1.02262	H	-1.10549	-3.35759	0.731175	H	-0.88719	-2.27605	2.447727
H	-0.89874	-2.3033	2.415957	H	-0.90731	-2.50643	2.227126	C	-1.70537	-1.22153	0.751714
C	-1.70314	-1.2399	0.73486	C	-1.678	-1.29257	0.635681	C	-2.01504	-0.05205	1.494953
C	-2.04428	-0.08778	1.487988	C	-2.01612	-0.19304	1.488923	C	-1.46431	0.207352	2.796861
C	-1.50536	0.164642	2.794547	C	-1.44942	-0.02429	2.787234	H	-0.77211	-0.49773	3.238261
H	-0.79831	-0.53319	3.225094	H	-0.7111	-0.73578	3.140624	C	-1.78279	1.345187	3.500089
C	-1.84806	1.282778	3.511889	C	-1.79829	1.034501	3.619676	H	-1.35056	1.514475	4.480156
H	-1.41906	1.44716	4.495393	H	-1.34006	1.121612	4.60144	C	-2.677	2.306597	2.950358
C	-2.76122	2.231253	2.973118	C	-2.73375	1.988393	3.186115	H	-2.92329	3.197596	3.517182

H	-3.03009	3.110123	3.550868	H	-3.01425	2.818216	3.829183	C	-3.22286	2.107829	1.70476
C	-3.29687	2.040191	1.724827	C	-3.29698	1.870034	1.917463	H	-3.89993	2.842909	1.284184
H	-3.98799	2.768274	1.312981	H	-4.01434	2.613474	1.580667	C	-2.91072	0.94077	0.93888
C	-2.9556	0.892965	0.943875	C	-2.961	0.807173	1.04569	C	-3.45582	0.731927	-0.35301
C	-3.4848	0.691348	-0.35311	C	-3.53106	0.686637	-0.27228	C	-3.13061	-0.41787	-1.1162
C	-3.12646	-0.43483	-1.13322	C	-3.14881	-0.38093	-1.16183	C	-3.66625	-0.6258	-2.42643
C	-3.64168	-0.63293	-2.45111	C	-3.67101	-0.49435	-2.47221	H	-4.34216	0.115338	-2.83817
H	-4.33188	0.097477	-2.86043	H	-4.38867	0.246657	-2.8137	C	-3.33477	-1.73997	-3.15886
C	-3.27257	-1.72335	-3.19773	C	-3.28863	-1.52303	-3.3304	H	-3.74887	-1.88285	-4.15082
H	-3.67223	-1.85663	-4.19824	H	-3.7087	-1.5791	-4.33104	C	-2.44412	-2.71139	-2.61944
C	-2.36339	-2.67943	-2.66631	C	-2.35462	-2.47719	-2.89464	H	-2.18396	-3.58429	-3.20805
H	-2.06895	-3.53405	-3.26743	H	-2.03752	-3.27783	-3.55786	C	-1.91389	-2.54834	-1.36174
C	-1.85604	-2.52529	-1.4005	C	-1.82639	-2.39535	-1.60988	H	-1.23224	-3.29854	-0.98263
H	-1.15633	-3.26091	-1.02443	H	-1.09408	-3.13464	-1.30486	C	-2.23398	-1.40464	-0.55429
C	-2.21584	-1.40674	-0.57752	C	-2.20286	-1.36798	-0.69557	C	1.257894	-1.03875	0.536506
C	1.277715	-1.0283	0.533484	C	1.295221	-1.06192	0.448986	H	0.620597	-0.17024	0.438804
H	0.648978	-0.1541	0.41524	H	0.631813	-0.21762	0.302244	C	0.653354	-2.23729	0.98201
C	0.682753	-2.20719	0.968735	C	0.721079	-2.25795	0.863563	C	1.45003	-3.40753	1.117157
C	1.500887	-3.34435	1.112595	C	1.573589	-3.36455	1.043342	H	0.987372	-4.32809	1.455506
H	1.065135	-4.28277	1.446465	H	1.156243	-4.31671	1.363465	C	2.792718	-3.37564	0.824803
C	2.857581	-3.28871	0.832337	C	2.938485	-3.2664	0.812558	H	3.422086	-4.25194	0.921035
H	3.487665	-4.1659	0.940031	H	3.592798	-4.1227	0.944602	C	3.432009	-2.16464	0.371929
C	3.453479	-2.09424	0.394148	C	3.510161	-2.0541	0.393909	C	2.612358	-0.95597	0.228903
C	2.655979	-0.92739	0.236278	C	2.680998	-0.91414	0.206691	C	3.205741	0.309494	-0.22531
C	3.245462	0.348906	-0.22405	C	3.24415	0.381679	-0.22695	C	2.500095	1.511998	-0.38861
C	2.497388	1.533585	-0.37813	C	2.464515	1.547044	-0.38271	H	1.443052	1.562085	-0.17772
H	1.438658	1.566662	-0.16233	H	1.401606	1.544749	-0.18554	C	3.166263	2.664465	-0.82724
C	3.141066	2.691646	-0.81706	C	3.08232	2.727988	-0.79541	C	4.548085	2.626187	-1.10663
C	4.51708	2.672127	-1.10063	C	4.4643	2.752218	-1.0519	H	5.078916	3.504408	-1.44493
H	5.039693	3.556835	-1.4424	H	4.966729	3.65601	-1.37342	C	5.216046	1.426015	-0.93563
C	5.182137	1.465984	-0.92167	C	5.160712	1.564667	-0.87151	H	6.272693	1.306586	-1.12549
H	6.246316	1.384593	-1.12182	H	6.23099	1.517452	-1.04976	C	-4.3439	1.705497	-0.90159
C	-4.3958	1.651417	-0.89204	C	-4.46829	1.642152	-0.70713	N	-5.07455	2.508224	-1.3543
N	-5.13995	2.434294	-1.33213	N	-5.25281	2.43988	-1.07079	C	2.436603	3.886199	-0.99113
C	2.389595	3.907118	-0.97731	C	2.302659	3.925566	-0.95615	N	1.841352	4.886806	-1.12565
N	1.78709	4.893163	-1.10843	N	1.683159	4.90086	-1.08912	H	5.027561	-0.58074	-0.37585

Table S9. Cartesian coordinates for optimized geometries for **5**.

5 in CH_2Cl_2 / -1171.272918 Ha				**5** rad.anion CH_2Cl_2 / -1171.359585 Ha				**5** rad.cation CH_2Cl_2 / -1171.071019 Ha			
O	-4.31128	-2.24059	-0.68756	O	-4.33695	-2.23834	-0.69115	O	-4.07851	-2.47758	-0.5802
H	-4.65532	-1.40525	-0.23575	H	-4.66999	-1.41473	-0.2139	N	-4.33023	-0.11029	0.490511
N	-4.37957	0.065432	0.395371	N	-4.37784	0.042175	0.457775	C	1.343346	-1.46717	-1.72266
C	1.31065	-1.70258	-1.53479	C	1.305939	-1.73045	-1.48537	H	1.859237	-2.43186	-1.77603
H	1.756745	-2.6929	-1.39948	H	1.743894	-2.7207	-1.30796	H	1.390941	-1.08439	-2.74921
H	1.456813	-1.48264	-2.59708	H	1.459133	-1.55178	-2.55816	C	2.078799	-0.53656	-0.77367
C	2.077245	-0.69196	-0.70027	C	2.062753	-0.68866	-0.68942	C	2.275827	0.827009	-1.10894
C	2.335024	0.609856	-1.1996	C	2.256655	0.620489	-1.23271	C	1.761861	1.427937	-2.30727
C	1.848853	1.072306	-2.47006	C	1.692545	1.051088	-2.46982	H	1.176678	0.837959	-3.00378
H	1.241446	0.416815	-3.08287	H	1.05602	0.373587	-3.03004	C	1.980845	2.753707	-2.59943
C	2.119066	2.338407	-2.92764	C	1.918613	2.330053	-2.98837	H	1.576821	3.17512	-3.51601
H	1.732367	2.656108	-3.89157	H	1.4684	2.611868	-3.93739	C	2.728191	3.582835	-1.71587
C	2.898993	3.244645	-2.15059	C	2.715935	3.248042	-2.28371	H	2.893738	4.627137	-1.9655
H	3.106157	4.240663	-2.53037	H	2.894422	4.242887	-2.68507	C	3.231575	3.056664	-0.55269
C	3.377418	2.854006	-0.92697	C	3.272128	2.876139	-1.05965	H	3.801439	3.677554	0.134493
H	3.968102	3.535593	-0.32043	H	3.885676	3.583093	-0.50366	C	3.021422	1.683563	-0.20949
C	3.111617	1.544264	-0.41014	C	3.06311	1.584241	-0.49998	C	3.526167	1.157967	0.985092
C	3.588475	1.15754	0.846505	C	3.61722	1.21029	0.744471	C	3.321436	-0.17952	1.341514
C	3.32067	-0.11332	1.367812	C	3.400839	-0.06389	1.316158	C	3.83728	-0.70011	2.571523
C	3.80066	-0.49632	2.661921	C	3.949304	-0.42601	2.578359	H	4.395573	-0.02965	3.220582
H	4.384945	0.224254	3.228259	H	4.556859	0.30871	3.104096	C	3.635191	-2.00929	2.926054
C	3.530096	-1.73681	3.179587	C	3.725891	-1.68047	3.145969	H	4.030551	-2.39453	3.861805
H	3.897986	-2.01495	4.162704	H	4.157747	-1.92703	4.113115	C	2.901225	-2.87034	2.060149
C	2.757093	-2.6664	2.424196	C	2.934109	-2.61833	2.461706	H	2.740979	-3.90645	2.346107

H	2.537789	-3.64431	2.842815	H	2.742379	-3.59543	2.899013	C	2.392968	-2.40731	0.870213
C	2.284797	-2.3379	1.176934	C	2.382045	-2.29824	1.217259	H	1.833257	-3.09302	0.243915
H	1.689652	-3.06378	0.635717	H	1.759828	-3.03795	0.723939	C	2.57986	-1.04792	0.453235
C	2.547167	-1.05524	0.587956	C	2.596916	-1.03507	0.592735	C	-0.89967	-0.74027	-0.74751
C	-0.91791	-0.79408	-0.6525	C	-0.92407	-0.82999	-0.61146	H	-0.41067	0.189672	-0.48392
H	-0.38342	0.093536	-0.33596	H	-0.36976	0.03609	-0.26954	C	-0.1112	-1.72207	-1.38546
C	-0.18832	-1.81154	-1.26085	C	-0.20039	-1.83854	-1.24089	C	-0.708	-2.96283	-1.73645
C	-0.88262	-2.96775	-1.66291	C	-0.90836	-2.9742	-1.67625	H	-0.10422	-3.72384	-2.22373
H	-0.34168	-3.78414	-2.13568	H	-0.37398	-3.78446	-2.16803	C	-2.02996	-3.20267	-1.46815
C	-2.25106	-3.08543	-1.46311	C	-2.28003	-3.08455	-1.48303	H	-2.50661	-4.14188	-1.73095
H	-2.78639	-3.97857	-1.77048	H	-2.82324	-3.96547	-1.81235	C	-2.86504	-2.21366	-0.81448
C	-2.98044	-2.05245	-0.85136	C	-3.00029	-2.06001	-0.84868	C	-2.24402	-0.92728	-0.45137
C	-2.31027	-0.87181	-0.42826	C	-2.31936	-0.89642	-0.39705	C	-3.0211	0.13529	0.208192
C	-3.04617	0.237336	0.226775	C	-3.04449	0.207242	0.276201	C	-2.51796	1.391074	0.572605
C	-2.42902	1.426065	0.664464	C	-2.41573	1.389266	0.718349	H	-1.48427	1.636496	0.368554
H	-1.36415	1.573074	0.533587	H	-1.35219	1.531261	0.572604	C	-3.32509	2.346103	1.198542
C	-3.1759	2.434932	1.272637	C	-3.14893	2.395324	1.346219	C	-4.67006	2.017886	1.45966
C	-4.55665	2.222154	1.431193	C	-4.5294	2.1892	1.519364	H	-5.33583	2.723987	1.943355
H	-5.18916	2.971429	1.89674	H	-5.15195	2.937398	2.000045	C	-5.14623	0.776994	1.091818
C	-5.10548	1.030385	0.979544	C	-5.09035	1.005935	1.060425	H	-6.16632	0.452139	1.257099
H	-6.16847	0.829601	1.084068	H	-6.15377	0.811358	1.17407	C	-2.78002	3.693121	1.582808
C	-2.53027	3.710858	1.749703	C	-2.48891	3.661239	1.83079	H	-2.92625	3.873834	2.653961
H	-2.64557	3.82028	2.833892	H	-2.55803	3.739005	2.921847	H	-3.31512	4.485906	1.046324
H	-3.00397	4.582773	1.285688	H	-2.98498	4.543733	1.412532	H	-1.71472	3.778542	1.35601
H	-1.46341	3.732899	1.514959	H	-1.43288	3.694531	1.552608	H	4.087073	1.806321	1.655011
H	4.174386	1.861173	1.433092	H	4.224677	1.933247	1.287354	H	-4.66843	-1.04517	0.201998

Table S10. Cartesian coordinates for optimized geometries for **6**.

6 in CH_2Cl_2 / -1131.974620 Ha				**6** rad.anion CH_2Cl_2 / -1132.061474 Ha				**6** rad.cation CH_2Cl_2 / -1131.770926 Ha			
O	-4.59058	-1.47201	-0.9946	O	-4.59374	-1.53014	-0.96777	O	-4.30777	-2.00016	-0.55957
H	-4.85365	-0.77119	-0.31875	H	-4.85498	-0.8456	-0.27691	N	-4.42244	0.248201	0.707483
N	-4.43311	0.432971	0.698218	N	-4.43508	0.352286	0.757427	C	1.07998	-1.05302	-1.90929
C	1.051529	-1.21666	-1.84138	C	1.053321	-1.2068	-1.82645	H	1.53696	-2.00899	-2.18069
H	1.411165	-2.2443	-1.95414	H	1.420168	-2.23519	-1.93504	H	1.08952	-0.47414	-2.83892
H	1.2069	-0.76616	-2.82689	H	1.195004	-0.75959	-2.81948	C	1.912925	-0.36194	-0.84352
C	1.911276	-0.49742	-0.81762	C	1.903095	-0.46689	-0.8156	C	2.175873	1.029832	-0.92489
C	2.262366	0.864163	-0.99999	C	2.180783	0.924297	-1.00066	C	1.647789	1.872165	-1.95893
C	1.788907	1.653936	-2.10276	C	1.62248	1.70535	-2.05526	H	1.00029	1.456275	-2.72153
H	1.118059	1.212082	-2.83006	H	0.925671	1.244932	-2.74843	C	1.932348	3.217596	-2.00739
C	2.150653	2.969873	-2.25421	C	1.929999	3.058987	-2.2251	H	1.516054	3.824998	-2.80533
H	1.771005	3.538637	-3.09799	H	1.480508	3.612757	-3.04609	C	2.763213	3.823625	-1.0251
C	3.016882	3.601787	-1.31419	C	2.808324	3.701444	-1.33584	H	2.979032	4.88596	-1.08111
H	3.295649	4.642148	-1.45244	H	3.050052	4.753723	-1.466	C	3.284795	3.059877	-0.01015
C	3.487423	2.893132	-0.23939	C	3.363174	2.980703	-0.2783	H	3.91926	3.508613	0.749183
H	4.14339	3.362851	0.488891	H	4.038973	3.472123	0.419665	C	3.009248	1.659714	0.077729
C	3.127398	1.520531	-0.04089	C	3.072556	1.602584	-0.07294	C	3.534866	0.890279	1.122212
C	3.596813	0.807496	1.067069	C	3.625427	0.874637	1.004037	C	3.26968	-0.47962	1.22862
C	3.237705	-0.52835	1.279223	C	3.327974	-0.48882	1.226961	C	3.812777	-1.25069	2.305098
C	3.710757	-1.24665	2.424691	C	3.875721	-1.20945	2.324973	H	4.438529	-0.74571	3.035784
H	4.362439	-0.72907	3.123812	H	4.547745	-0.68303	3.000705	C	3.553773	-2.59314	2.414317
C	3.351044	-2.55193	2.641007	C	3.571959	-2.55218	2.549914	H	3.970295	-3.16956	3.23444
H	3.714677	-3.08542	3.514133	H	4.005566	-3.07548	3.398901	C	2.732805	-3.23465	1.443981
C	2.490503	-3.21215	1.715821	C	2.697015	-3.21921	1.675674	H	2.52828	-4.29717	1.534909
H	2.201078	-4.24323	1.896818	H	2.442461	-4.26256	1.84705	C	2.195002	-2.52668	0.395415
C	2.021818	-2.5586	0.602373	C	2.142847	-2.54351	0.583836	H	1.568178	-3.05117	-0.3156
H	1.359213	-3.08653	-0.07313	H	1.456064	-3.08216	-0.06106	C	2.438441	-1.12388	0.235884
C	2.375493	-1.19469	0.327113	C	2.438002	-1.17683	0.306443	C	-1.07693	-0.36006	-0.74451
C	-1.07496	-0.40253	-0.66184	C	-1.08127	-0.43443	-0.64606	H	-0.54733	0.530234	-0.42924
H	-0.45765	0.308675	-0.12619	H	-0.45545	0.266299	-0.10605	C	-0.3602	-1.30168	-1.51406
C	-0.44915	-1.26307	-1.55865	C	-0.45093	-1.27662	-1.55696	C	-1.01731	-2.48927	-1.93254
C	-1.25248	-2.19051	-2.24868	C	-1.25313	-2.19829	-2.25547	H	-0.46882	-3.22127	-2.51828
H	-0.79426	-2.88156	-2.95234	H	-0.7931	-2.87582	-2.97186	C	-2.33137	-2.71323	-1.6128
C	-2.6242	-2.23937	-2.04486	C	-2.62473	-2.26427	-2.04322	H	-2.85303	-3.60916	-1.93232

H	-3.24355	-2.95562	-2.57597	H	-3.24088	-2.98083	-2.57837	C	-3.09474	-1.76116	-0.83231
C	-3.24869	-1.36427	-1.14058	C	-3.2506	-1.40766	-1.12389	C	-2.40835	-0.53715	-0.38908
C	-2.467	-0.41975	-0.42099	C	-2.47251	-0.46445	-0.39856	C	-3.11357	0.475945	0.408242
C	-3.08725	0.512718	0.550472	C	-3.09287	0.453315	0.584941	C	-2.54947	1.666123	0.893282
C	-2.3551	1.45118	1.306363	C	-2.36219	1.402993	1.330017	H	-1.51385	1.902515	0.692665
H	-1.28032	1.529837	1.207155	H	-1.29132	1.499869	1.207953	C	-3.32205	2.550223	1.639139
C	-3.02123	2.288199	2.194328	C	-3.0245	2.225837	2.233148	C	-4.66504	2.264017	1.915136
C	-4.40999	2.190517	2.330285	C	-4.40915	2.105039	2.3957	H	-5.2843	2.937582	2.493837
H	-4.96205	2.826629	3.013108	H	-4.95841	2.729894	3.091188	C	-5.19423	1.083116	1.427378
C	-5.07	1.241669	1.556504	C	-5.06786	1.148598	1.630513	H	-6.21856	0.770795	1.586955
H	-6.14773	1.116467	1.618387	H	-6.14243	1.006715	1.711804	H	-2.87537	3.466989	2.0087
H	-2.46048	3.0121	2.777727	H	-2.46431	2.95748	2.8075	H	4.161019	1.369458	1.870572
H	4.249355	1.303372	1.781759	H	4.296386	1.385294	1.693567	H	-4.78844	-0.65038	0.328922

Table S11. Cartesian coordinates for optimized geometries for **7**.

7 in CH_2Cl_2 / -1469.032780 Ha				**7** rad.anion CH_2Cl_2 / -1469.126157 Ha				**7** rad.cation CH_2Cl_2 / -1468.822740 Ha			
O	-3.28536	3.736381	-0.07614	O	-2.68206	4.072165	-0.34515	O	-2.00164	4.257851	-0.1541
H	-3.85096	2.907618	-0.04806	H	-3.35214	3.326342	-0.06065	N	-3.373	2.193623	0.397072
N	-3.94126	1.258687	-0.00712	N	-3.74592	1.887571	0.230445	C	2.322612	1.021078	-1.8308
C	2.236621	2.287285	-0.22224	C	2.295292	1.51494	-1.51384	H	2.120083	0.607337	-2.82176
H	2.648608	2.696839	-1.15014	H	2.298284	1.266341	-2.57982	H	3.196839	1.662432	-1.96807
H	2.739464	2.852828	0.568652	H	3.085707	2.264759	-1.40678	C	2.635966	-0.08142	-0.83736
C	2.615641	0.822319	-0.10855	C	2.670402	0.281911	-0.70895	C	3.378524	0.218449	0.345695
C	2.839671	0.242999	1.16641	C	3.264611	0.433441	0.570989	C	3.858376	1.525841	0.653157
C	2.665342	0.968144	2.393574	C	3.489198	1.716995	1.17267	H	3.644523	2.352925	-0.0117
H	2.332339	1.998931	2.364559	H	3.178751	2.613174	0.648963	C	4.590809	1.774025	1.795813
C	2.894579	0.381877	3.614217	C	4.072363	1.839289	2.410745	H	4.941535	2.781374	1.997228
H	2.749638	0.957633	4.523679	H	4.224087	2.825518	2.839912	C	4.889985	0.732367	2.71033
C	3.317699	-0.97671	3.703498	C	4.476664	0.685103	3.142729	H	5.466927	0.946137	3.604202
H	3.497682	-1.42243	4.677204	H	4.938049	0.799784	4.119189	C	4.447664	-0.54488	2.454813
C	3.490127	-1.7127	2.559821	C	4.276251	-0.5635	2.611563	H	4.672635	-1.35615	3.140977
H	3.80716	-2.75096	2.612332	H	4.575297	-1.45272	3.160597	C	3.688877	-0.83653	1.28177
C	3.25413	-1.14036	1.267937	C	3.666577	-0.7328	1.326699	C	3.245802	-2.14097	1.025652
C	3.416648	-1.89916	0.103693	C	3.453898	-2.00852	0.791032	C	2.50835	-2.45477	-0.12519
C	3.171842	-1.35413	-1.16128	C	2.849856	-2.18104	-0.45844	C	2.072968	-3.78973	-0.36522
C	3.323698	-2.14467	-2.34639	C	2.623037	-3.49201	-0.9908	H	2.330315	-4.55727	0.358785
H	3.643868	-3.17764	-2.23803	H	2.939093	-4.34796	-0.40004	C	1.34292	-4.10654	-1.49073
C	3.068689	-1.61939	-3.58665	C	2.018807	-3.66963	-2.20837	H	1.016135	-5.12672	-1.66369
H	3.185448	-2.22934	-4.47742	H	1.850009	-4.66894	-2.59861	C	1.019002	-3.09275	-2.42388
C	2.642155	-0.26424	-3.70755	C	1.602786	-2.53447	-2.96403	H	0.442515	-3.34164	-3.30922
H	2.430838	0.14407	-4.69154	H	1.11359	-2.67967	-3.92283	C	1.426197	-1.78766	-2.22283
C	2.492688	0.527703	-2.59565	C	1.807948	-1.26176	-2.49058	H	1.145043	-1.04521	-2.95913
H	2.154276	1.548966	-2.72503	H	1.464364	-0.42451	-3.08625	C	2.18956	-1.4128	-1.07498
C	2.756074	0.028285	-1.27504	C	2.443801	-1.01963	-1.22496	C	-0.02945	1.285733	-0.8922
C	-0.2448	1.641882	-0.11677	C	-0.14331	1.42481	-0.74628	H	-0.07582	0.204602	-0.84862
H	0.066332	0.604358	-0.1045	H	-0.02026	0.352476	-0.64111	C	1.152888	1.872681	-1.37221
C	0.7453	2.615409	-0.17172	C	0.961759	2.17094	-1.15741	C	1.238998	3.289224	-1.40939
C	0.340035	3.964718	-0.18894	C	0.814991	3.562769	-1.28395	H	2.149273	3.756432	-1.77471
H	1.090196	4.750985	-0.22926	H	1.658492	4.174117	-1.59664	C	0.186406	4.075509	-1.01084
C	-1.00238	4.309718	-0.15661	C	-0.41197	4.168033	-1.00847	H	0.239507	5.158346	-1.0539
H	-1.31395	5.349454	-0.17109	H	-0.53272	5.244199	-1.10003	C	-1.04481	3.501697	-0.52212
C	-1.99822	3.319619	-0.10365	C	-1.5204	3.414579	-0.60022	C	-1.12979	2.040226	-0.47607
C	-1.625	1.948336	-0.07871	C	-1.40663	1.994741	-0.45509	C	-2.34816	1.392083	-0.0012
C	-2.64238	0.877096	-0.013	C	-2.55643	1.183652	-0.02072	C	-2.55884	0.000354	0.080909
C	-2.31539	-0.4957	0.045962	C	-2.50944	-0.1997	0.141853	H	-1.78478	-0.68908	-0.22259
H	-1.28664	-0.82605	0.049257	H	-1.59027	-0.73843	-0.05321	C	-3.76701	-0.48355	0.553719
C	-3.33662	-1.43241	0.10547	C	-3.64329	-0.92131	0.55819	C	-4.79307	0.389774	0.954966
C	-4.67537	-1.02066	0.108054	C	-4.85806	-0.18158	0.815685	H	-5.74233	0.028341	1.329171
H	-5.49437	-1.72865	0.154759	H	-5.76615	-0.67744	1.141131	C	-4.55509	1.744774	0.859388
C	-4.91928	0.345205	0.051352	C	-4.83284	1.180806	0.634881	H	-5.27982	2.497931	1.141375
H	-5.9349	0.729631	0.052949	H	-5.73007	1.76986	0.818821	C	-4.01439	-1.9769	0.630592
C	-3.02564	-2.90894	0.156975	C	-3.61796	-2.37294	0.737748	F	-4.44919	-2.33686	1.860672
F	-3.62391	-3.50872	1.218904	F	-3.93352	-2.78986	2.028251	F	-2.90745	-2.69977	0.363295

F	-1.70213	-3.16704	0.249467	F	-2.4182	-2.95046	0.452617	F	-4.96863	-2.35443	-0.25449
F	-3.47856	-3.55101	-0.95269	F	-4.55305	-3.0544	-0.03542	H	3.478255	-2.92939	1.736538
H	3.732926	-2.93644	0.184288	H	3.75926	-2.88334	1.360313	H	-3.14108	3.218962	0.302316

Table S12. Cartesian coordinates for optimized geometries for **8**.

8 in CH_2Cl_2 / -1469.033023 Ha				**8** rad.anion CH_2Cl_2 / -1469.120008 Ha				**8** rad.cation CH_2Cl_2 / -1468.817399 Ha			
O	-3.2691	-2.05874	-1.48871	O	-3.22726	-2.2144	-1.32954	O	-2.94233	-2.36719	-0.87748
H	-3.68139	-1.34155	-0.93261	H	-3.65353	-1.49041	-0.79464	N	-3.43971	-0.03376	0.019423
N	-3.45649	0.016746	0.039427	N	-3.47173	-0.05135	0.070879	C	2.401963	-0.86895	-1.96558
C	2.408232	-1.45477	-1.59612	C	2.402868	-1.27431	-1.70365	H	2.959339	-1.76389	-2.25598
H	2.841454	-2.45321	-1.48018	H	2.890451	-2.25626	-1.71788	H	2.444229	-0.21638	-2.84157
H	2.677344	-1.16032	-2.61557	H	2.592699	-0.85971	-2.70284	C	3.057179	-0.21032	-0.76519
C	3.064005	-0.50742	-0.60816	C	3.054871	-0.39196	-0.65989	C	3.197225	1.206429	-0.70662
C	3.328971	0.837778	-0.96993	C	3.187239	1.012145	-0.89745	C	2.736235	2.082615	-1.73661
C	2.948565	1.39652	-2.23747	C	2.65869	1.66944	-2.04814	H	2.238022	1.684656	-2.61247
H	2.419868	0.782935	-2.95733	H	2.103847	1.095073	-2.78309	C	2.901551	3.451933	-1.64806
C	3.222854	2.702779	-2.56009	C	2.820973	3.041111	-2.26375	H	2.541258	4.086258	-2.45285
H	2.917714	3.093875	-3.5263	H	2.402503	3.497261	-3.15783	C	3.53262	4.036518	-0.52385
C	3.900972	3.555235	-1.63996	C	3.514538	3.827268	-1.32724	H	3.655601	5.114088	-0.46988
H	4.1129	4.584375	-1.91404	H	3.642568	4.894318	-1.49328	C	3.988573	3.230328	0.497181
C	4.276339	3.071184	-0.4137	C	4.033204	3.230124	-0.17916	H	4.477298	3.663791	1.365774
H	4.788559	3.710435	0.300658	H	4.56681	3.832415	0.554098	C	3.834587	1.81524	0.439415
C	4.002196	1.716625	-0.03574	C	3.887832	1.836772	0.074791	C	4.299896	1.004965	1.485213
C	4.372579	1.232542	1.223237	C	4.405668	1.232617	1.241053	C	4.167181	-0.38946	1.450263
C	4.093938	-0.08344	1.608802	C	4.255643	-0.14693	1.507716	C	4.660586	-1.19217	2.522174
C	4.463083	-0.56561	2.906148	C	4.771401	-0.7444	2.691917	H	5.139136	-0.69669	3.362859
H	4.972987	0.115715	3.582239	H	5.300216	-0.10832	3.399649	C	4.540034	-2.56244	2.492306
C	4.179536	-1.85033	3.291913	C	4.612561	-2.1032	2.959608	H	4.918581	-3.16657	3.311443
H	4.462709	-2.20379	4.278856	H	5.016556	-2.53077	3.874172	C	3.919334	-3.18686	1.380749
C	3.504739	-2.7271	2.392788	C	3.922464	-2.91343	2.04112	H	3.825849	-4.2688	1.356204
H	3.274013	-3.74095	2.706657	H	3.782917	-3.97273	2.243494	C	3.430139	-2.43907	0.328984
C	3.141141	-2.30353	1.13786	C	3.40681	-2.36164	0.865157	H	2.953943	-2.95799	-0.49376
H	2.618578	-2.993	0.485402	H	2.864498	-3.01138	0.186045	C	3.531598	-1.01652	0.31507
C	3.422204	-0.97079	0.683668	C	3.556885	-0.98083	0.544471	C	0.070453	-0.3331	-1.09457
C	0.093071	-0.69715	-0.7938	C	0.07573	-0.61317	-0.88456	H	0.442901	0.658943	-0.86884
H	0.586875	0.100213	-0.25218	H	0.552632	0.238309	-0.41484	C	0.963847	-1.25385	-1.66775
C	0.887915	-1.58076	-1.51486	C	0.897235	-1.50315	-1.56985	C	0.496651	-2.56397	-1.94957
C	0.245818	-2.6202	-2.21541	C	0.290923	-2.62384	-2.16615	H	1.177044	-3.2874	-2.39221
H	0.838488	-3.33137	-2.78579	H	0.903692	-3.34271	-2.70571	C	-0.8031	-2.9252	-1.69211
C	-1.13408	-2.7542	-2.18972	C	-1.07968	-2.83698	-2.07062	H	-1.17152	-3.92022	-1.92236
H	-1.62916	-3.55604	-2.72843	H	-1.54404	-3.70926	-2.52066	C	-1.7458	-1.9992	-1.11064
C	-1.9303	-1.85528	-1.46101	C	-1.89922	-1.93285	-1.38018	C	-1.26199	-0.64865	-0.81469
C	-1.31651	-0.79727	-0.73797	C	-1.32373	-0.7845	-0.76852	C	-2.15942	0.348042	-0.23755
C	-2.11373	0.169387	0.049605	C	-2.14614	0.199253	-0.03545	C	-1.81991	1.682339	0.078022
C	-1.54089	1.224217	0.797933	C	-1.61479	1.375976	0.54701	H	-0.81759	2.046493	-0.10247
H	-0.46921	1.367961	0.825398	H	-0.56014	1.603478	0.470346	C	-2.76761	2.532666	0.618521
C	-2.3583	2.088306	1.509381	C	-2.45092	2.251747	1.21958	C	-4.07993	2.085315	0.865319
C	-3.74866	1.914614	1.486204	C	-3.8218	1.973206	1.321878	H	-4.83178	2.738495	1.289085
H	-4.41398	2.571873	2.031005	H	-4.50129	2.637095	1.84047	C	-4.37964	0.780427	0.548741
C	-4.23408	0.85766	0.731075	C	-4.26708	0.80431	0.722845	H	4.77537	1.471185	2.344993
H	4.881786	1.894683	1.919471	H	4.933503	1.852945	1.96407	H	-2.49819	3.556559	0.855883
H	-1.92143	2.898195	2.084234	H	-2.045	3.153775	1.665737	C	-5.74377	0.155948	0.764306
C	-5.71776	0.568166	0.624932	C	-5.72426	0.392937	0.764775	F	-6.61702	1.045524	1.263707
F	-6.4589	1.428204	1.360162	F	-6.49325	1.297817	1.414126	F	-5.66908	-0.88651	1.623665
F	-6.01806	-0.68442	1.051306	F	-5.89473	-0.79817	1.394307	F	-6.24746	-0.32204	-0.39672
F	-6.15648	0.657274	-0.65652	F	-6.24494	0.248926	-0.48078	H	-3.62167	-1.03959	-0.24677

Table S13. Cartesian coordinates for optimized geometries for $(Me)_2$PhOH-py.

PhOH-py neutral – MeCN -633.075483 Ha				PhOH-py-rad.cation – MeCN -632.882275 Ha			
C	0.832626	-1.03128	0.001836	C	-0.84571	-1.07006	0.00351
C	2.246665	-1.0387	0.005885	C	-2.3111	-1.03698	0.009297
C	2.923239	0.177832	0.002516	C	-2.95809	0.178605	-0.00269

C	2.248614	1.413501	-0.00559	C	-2.25056	1.405186	-0.01855
C	0.858113	1.394101	-0.00793	C	-0.83672	1.386689	-0.0198
C	0.112872	0.192988	-0.00238	C	-0.10999	0.207045	-0.00323
C	2.981576	-2.35584	0.012689	C	-3.04445	-2.34304	0.022959
C	3.021233	2.713651	-0.01207	C	-2.99504	2.706442	-0.01223
C	-1.36983	0.215634	-0.0003	C	1.361601	0.233268	0.00158
C	-2.13029	1.403416	0.021465	C	2.148174	1.394457	0.032662
C	-3.51864	1.332094	0.019815	C	3.536135	1.29746	0.028838
C	-4.14943	0.083521	-0.00193	C	4.161664	0.045387	-0.0026
C	-3.34096	-1.0479	-0.0195	C	3.362217	-1.08304	-0.02631
H	4.011448	0.167736	0.004985	H	-4.0443	0.20348	-0.00277
H	0.33624	2.344622	-0.01642	H	-0.32943	2.343756	-0.03857
H	-1.64962	2.37275	0.041578	H	1.684032	2.370047	0.063032
H	-4.10597	2.24511	0.036336	H	4.133333	2.202493	0.052105
H	-5.22965	-0.00965	-0.0037	H	5.239656	-0.0536	-0.00598
H	-3.77039	-2.04606	-0.03462	H	3.748746	-2.09387	-0.04749
H	-0.77667	-2.04319	-0.00876	H	-2.7815	-2.94584	-0.85335
H	2.719573	-2.95504	0.892301	H	-4.12418	-2.18241	0.030117
H	4.062871	-2.19517	0.016168	H	-2.76805	-2.93499	0.902435
H	2.725978	-2.96044	-0.86512	H	-2.34581	3.548258	-0.26147
H	2.347331	3.57515	-0.01772	H	-3.42124	2.89039	0.983138
H	3.66946	2.789509	-0.89311	H	-3.83379	2.681415	-0.71531
H	3.667195	2.799419	0.869734	N	2.022691	-0.95644	-0.02365
N	-2.00195	-0.98454	-0.01892	O	-0.25266	-2.18471	0.001442
O	0.213879	-2.2389	0.002975	H	1.39611	-1.785	-0.03253

Table S14. Cartesian coordinates for optimized geometries for $(Me)_2$PhOH-py(Me).

PhOH-py(Me) neutral MeCN -672.373635 Ha				PhOH-py(Me) rad.cation – MeCN -672.182679 Ha			
C	-3.19016	0.545237	-0.00014	C	-3.22911	0.534301	-3.3E-05
C	-2.73595	-0.77068	-0.0001	C	-2.79686	-0.77256	-1E-06
C	-1.34223	-1.01022	-4.4E-05	C	-1.35773	-1.05356	0.00001
C	-0.41965	0.069737	-0.00002	C	-0.41643	0.080896	-1.1E-05
C	-3.68972	-1.93922	-0.00013	C	-3.74124	-1.93556	0.00002
C	1.044848	-0.1691	0.000042	C	1.039989	-0.14136	0.000004
C	1.999505	0.868145	0.000069	C	2.005607	0.873352	-4E-06
C	-0.94424	1.382128	-5.7E-05	C	-0.93436	1.366531	-4.4E-05
C	3.364611	0.581948	0.000129	C	3.371909	0.576237	0.000014
C	-2.3102	1.644044	-0.00011	C	-2.32372	1.624105	-5.6E-05
C	4.397528	1.679791	0.00017	C	4.405519	1.666378	0.00004
C	-2.84367	3.05933	-0.00015	C	-2.84091	3.031565	-8.5E-05
C	2.764493	-1.74615	0.000131	C	2.794764	-1.75975	0.000039
C	3.750587	-0.77029	0.00016	C	3.76222	-0.77732	0.000033
H	0.068041	-2.28496	0.000025	H	0.740269	-2.14071	0.000031
H	-4.26354	0.724966	-0.00018	H	-4.29573	0.74218	-4.2E-05
H	1.685256	1.904424	0.000043	H	1.697603	1.909853	-2.5E-05
H	-0.26473	2.227165	-0.00004	H	-0.27258	2.224048	-6.2E-05
H	5.044204	1.602905	-0.88086	H	5.050279	1.577219	-0.88076
H	5.043962	1.603058	0.881389	H	5.049828	1.577571	0.881209
H	3.932606	2.668519	0.000024	H	3.947981	2.65707	-0.00026
H	3.022771	-2.80184	0.000153	H	3.017595	-2.81916	0.000053
H	4.798262	-1.05393	0.000204	H	4.808714	-1.05833	0.000041
H	-4.72631	-1.59203	-0.00016	H	-4.77795	-1.59353	0.000031
H	-3.54029	-2.57716	0.878619	H	-3.5774	-2.57001	0.878023
H	-3.54024	-2.57717	-0.87886	H	-3.57743	-2.57002	-0.87798
H	-2.02944	3.789711	-0.00012	H	-2.03174	3.76424	-0.00016
H	-3.46676	3.252243	0.88122	H	-3.47206	3.20797	0.879316
H	-3.46668	3.252225	-0.88159	H	-3.47217	3.207898	-0.87942
N	1.453336	-1.4614	0.000075	N	1.490313	-1.42484	0.000026
O	-0.94313	-2.30707	-1.4E-05	O	-0.96316	-2.25274	0.000034

Table S15. Cartesian coordinates for optimized geometries for $(Me)_2$PhOH-py(NMe_2).

PhOH-py(4NMe_2) neutral – MeCN -766.995996 Ha	PhOH-py(4NMe_2) rad.cation – MeCN -766.811624 Ha

C	2.108310	-0.955700	0.000003	C	2.132330	-1.003243	0.009465
C	3.448861	-0.503063	0.000004	C	3.510327	-0.502011	0.023588
C	3.695830	0.867005	0.000000	C	3.736225	0.854547	0.009292
C	2.656716	1.816086	-0.000004	C	2.671789	1.790138	-0.018982
C	1.347282	1.345611	-0.000005	C	1.341274	1.321056	-0.028253
C	1.029819	-0.031034	-0.000001	C	1.024452	-0.029639	-0.010578
C	4.572287	-1.509804	0.000008	C	4.623905	-1.505220	0.050168
C	2.964801	3.297059	-0.000007	C	2.968252	3.260512	-0.040675
C	-0.383510	-0.497729	-0.000003	C	-0.386094	-0.475328	-0.012933
C	-1.472615	0.380230	0.000001	C	-1.472674	0.384982	0.007266
C	-2.801503	-0.110235	0.000000	C	-2.812046	-0.104277	0.000464
C	-2.957432	-1.524040	-0.000005	C	-2.982402	-1.523389	-0.024941
C	-1.826787	-2.319038	-0.000008	C	-1.878320	-2.332655	-0.040233
C	-3.684260	2.176825	0.000012	C	-3.669511	2.186785	0.049871
C	-5.233539	0.186568	0.000000	C	-5.234933	0.203316	0.011093
H	4.728681	1.210253	0.000001	H	4.757187	1.226749	0.017923
H	0.546345	2.077087	-0.000009	H	0.556367	2.067667	-0.052058
H	-1.299949	1.445155	0.000004	H	-1.298525	1.448009	0.031455
H	-3.932358	-1.992539	-0.000005	H	-3.960518	-1.981499	-0.030078
H	-1.926050	-3.401690	-0.000010	H	-1.949308	-3.412998	-0.057044
H	-3.135775	2.509798	0.889887	H	-3.126062	2.491869	0.950497
H	-4.657992	2.664605	0.000018	H	-4.642528	2.673354	0.056814
H	-3.135780	2.509811	-0.889861	H	-3.120395	2.529320	-0.833547
H	-5.945177	1.010952	-0.000004	H	-5.934785	1.036090	0.022569
H	-5.421773	-0.426438	0.889881	H	-5.421978	-0.416636	0.894201
H	-5.421768	-0.426442	-0.889879	H	-5.421546	-0.391260	-0.889274
H	0.903158	-2.425860	0.000000	H	4.548157	-2.149103	0.933228
H	4.524147	-2.163432	0.878658	H	5.595147	-1.006565	0.059976
H	5.542688	-1.006211	0.000007	H	4.574684	-2.165813	-0.822401
H	4.524149	-2.163437	-0.878639	H	3.557998	3.519507	-0.928492
H	2.047393	3.892797	-0.000018	H	3.571722	3.543828	0.829988
H	3.550487	3.584600	-0.881335	H	2.056811	3.861239	-0.042774
H	3.550469	3.584607	0.881330	N	-0.627749	-1.820470	-0.035173
N	-0.570178	-1.845127	-0.000006	N	-3.867713	0.734238	0.018412
N	-3.877522	0.729630	0.000002	O	1.934861	-2.250766	0.013045
O	1.913433	-2.298448	0.000005	H	0.211471	-2.417450	-0.035688

Table S16. Cartesian coordinates for optimized geometries for AN.

AN neutral – MeCN -539.410658 Ha				AN rad.anion – MeCN -539.501297 Ha			
C	-0.000001	1.406999	0.000002	C	0.000000	1.407010	0.000001
C	-1.224960	0.723357	0.000001	C	-1.243650	0.726657	0.000003
C	-2.482209	1.410075	-0.000001	C	-2.496048	1.401256	0.000000
H	-2.480962	2.496944	-0.000001	H	-2.497979	2.490064	-0.000001
C	-3.665491	0.714328	0.000000	C	-3.707105	0.703650	-0.000002
H	-4.611525	1.247694	0.000001	H	-4.647625	1.249580	-0.000004
C	-3.665491	-0.714329	0.000000	C	-3.707105	-0.703650	0.000001
H	-4.611525	-1.247694	0.000001	H	-4.647625	-1.249580	0.000000
C	-2.482209	-1.410075	-0.000001	C	-2.496048	-1.401256	-0.000001
H	-2.480960	-2.496944	-0.000001	H	-2.497979	-2.490064	-0.000002
C	-1.224960	-0.723356	0.000000	C	-1.243650	-0.726657	0.000001
C	-0.000001	-1.406999	0.000002	C	0.000000	-1.407010	0.000000
C	1.224961	-0.723356	0.000001	C	1.243650	-0.726657	0.000001
C	2.482208	-1.410074	-0.000001	C	2.496048	-1.401256	0.000000
H	2.480961	-2.496943	-0.000001	H	2.497979	-2.490064	-0.000001
C	3.665491	-0.714328	0.000000	C	3.707105	-0.703650	0.000000
H	4.611525	-1.247695	0.000001	H	4.647625	-1.249580	-0.000001
C	3.665491	0.714327	0.000000	C	3.707105	0.703650	-0.000001
H	4.611525	1.247695	0.000001	H	4.647625	1.249580	-0.000003
C	2.482208	1.410074	-0.000001	C	2.496048	1.401256	-0.000001
H	2.480963	2.496943	-0.000001	H	2.497979	2.490064	-0.000002
C	1.224961	0.723356	0.000000	C	1.243650	0.726657	0.000001
H	0.000001	2.494580	0.000002	H	0.000000	-2.496419	-0.000003
H	0.000001	-2.494579	0.000002	H	0.000000	2.496419	-0.000002

Table S17. Cartesian coordinates for optimized geometries for 9-Me-AN.

9-Me-AN rad.neutral – MeCN -578.700314 Ha				9-Me-AN rad.anion – MeCN -578.790256 Ha			
C	0.059356	2.726046	0.000001	C	0.00017	2.717242	-0.095738
H	0.592643	3.101151	0.881096	H	-0.877232	3.105373	-0.62216
H	-0.925185	3.189066	-0.000029	H	0.876806	3.105064	-0.623709
C	0.002695	1.213302	0.00001	C	0.000008	1.205968	-0.045699
C	-1.228654	0.509516	0.000006	C	1.242612	0.498035	-0.006711
C	-2.511335	1.158259	-0.000007	C	2.513489	1.143411	0.054855
H	-2.567585	2.239577	-0.000014	H	2.559629	2.226383	0.102798
C	-3.683798	0.443596	-0.000008	C	3.715299	0.427	0.066158
H	-4.634095	0.96958	-0.000016	H	4.660135	0.963686	0.111818
C	-3.670137	-0.98222	-0.000001	C	3.701316	-0.977419	0.024629
H	-4.607064	-1.531263	-0.000001	H	4.633667	-1.537199	0.031463
C	-2.473196	-1.649543	0.000003	C	2.479765	-1.651211	-0.016533
H	-2.445777	-2.736136	0.000005	H	2.459846	-2.739561	-0.040003
C	-1.226896	-0.941648	0.000005	C	1.237314	-0.956864	-0.025549
C	-0.012871	-1.635828	0.000005	C	-0.000035	-1.638446	-0.052055
C	1.211578	-0.95778	0.000002	C	-1.23736	-0.956815	-0.025558
C	2.453945	-1.670322	-0.000005	C	-2.479819	-1.651147	-0.016558
H	2.424809	-2.756882	-0.000009	H	-2.459903	-2.739498	-0.040043
C	3.653253	-1.004406	-0.000007	C	-3.701366	-0.977356	0.02461
H	4.58838	-1.556583	-0.000012	H	-4.633721	-1.537128	0.031431
C	3.673298	0.420921	-0.000004	C	-3.715328	0.427064	0.066168
H	4.625989	0.942575	-0.000004	H	-4.660155	0.963764	0.111845
C	2.501449	1.138819	0.000001	C	-2.513518	1.143461	0.054882
H	2.549359	2.221422	0.000004	H	-2.559678	2.226431	0.102862
C	1.222444	0.487872	0.000006	C	-1.242631	0.498096	-0.006705
H	0.592692	3.101143	-0.881068	H	0.001164	3.184149	0.903109
H	-0.020944	-2.723154	0.000003	H	-0.00006	-2.727576	-0.070578

Table S18. Cartesian coordinates for optimized geometries for 9-CN-AN.

9-CN-AN neutral – MeCN -631.663696 Ha				9-CN-AN rad.anion – MeCN -631.775623 Ha			
C	0.000001	-1.785245	0.000000	C	0.000003	-1.790941	0.000000
C	1.226698	-1.107684	0.000000	C	1.242455	-1.108430	-0.000001
C	2.471011	-1.814949	-0.000001	C	2.484029	-1.803773	0.000000
H	2.448440	-2.900953	-0.000001	H	2.464749	-2.891573	0.000001
C	3.664338	-1.138395	0.000000	C	3.699803	-1.129396	0.000001
H	4.603452	-1.682645	0.000000	H	4.632265	-1.687734	0.000001
C	3.676424	0.286895	0.000000	C	3.716669	0.277703	0.000001
H	4.626699	0.812076	0.000001	H	4.661889	0.813783	0.000002
C	2.503352	1.002845	0.000000	C	2.516451	0.990042	0.000000
H	2.529503	2.087769	0.000000	H	2.542292	2.076652	0.000001
C	1.241230	0.334803	0.000000	C	1.263318	0.334951	-0.000001
C	0.000000	1.023830	0.000000	C	0.000000	1.039813	-0.000002
C	-1.241230	0.334802	0.000000	C	-1.263316	0.334948	-0.000001
C	-2.503352	1.002843	0.000000	C	-2.516451	0.990038	0.000000
H	-2.529504	2.087767	0.000000	H	-2.542294	2.076647	0.000000
C	-3.676423	0.286892	0.000000	C	-3.716668	0.277696	0.000001
H	-4.626699	0.812073	0.000001	H	-4.661889	0.813775	0.000002
C	-3.664336	-1.138397	0.000000	C	-3.699799	-1.129403	0.000001
H	-4.603449	-1.682650	0.000000	H	-4.632260	-1.687743	0.000001
C	-2.471008	-1.814951	-0.000001	C	-2.484024	-1.803778	0.000000
H	-2.448438	-2.900955	-0.000001	H	-2.464742	-2.891578	0.000001
C	-1.226697	-1.107684	0.000000	C	-1.242452	-1.108433	-0.000001
C	-0.000001	2.452340	0.000000	C	-0.000001	2.445238	0.000000
N	-0.000006	3.618874	0.000000	N	-0.000016	3.622713	0.000001
H	0.000001	-2.872265	0.000000	H	0.000004	-2.878860	0.000002

7. Theoretical modeling of CPET-CR for 1 and 3 in CH_2Cl_2.

Calculation of CPET-CR reaction free energies by (C)DFT

The reaction free energies between the ground state (GS) and the charge-separated state (CSS) were estimated using density functional theory (DFT). The GS geometry was optimized with conventional DFT, and the CSS geometry was optimized with constrained DFT (CDFT), where the Becke charges of the phenoxyl-pyridinium and cyanoanthracene motifs within the triad were constrained to reflect charges of +1 and −1, respectively. For both types of calculations, the geometries were optimized in the gas phase using the B3LYP (*38,39*) functional and the 6-31+G** basis set (*40-42*), followed by a Hessian calculation to obtain the zero-point energy and entropic contributions and then calculation of the solvation free energy using the conductor-like polarizable continuum model (C-PCM) (*43*). The reaction free energy for CPET-CR was determined to be the difference in free energies between the product GS and the reactant CSS.

The resulting reaction free energies are given in Table S19. Alternative approaches for determining the reaction free energies were considered, including optimizing in solvent, constraining the spins rather than or in addition to the Becke charges, and only allowing the transferring proton to be optimized from the otherwise GS geometry for calculations of the CSS. All of these procedures yielded the qualitatively correct ordering of reaction free energies for **1**, **2**, and **3** and would subsequently give qualitative agreement in the ratio of rate constants.

Table S19. Reaction free energies in eV for CPET-CR computed with DFT and CDFT for the GS and CSS, respectively, for triads **1**, **2**, and **3**.

Triad	Solvent	ΔG^o
1	CH_2Cl_2	-2.54
	n-BuCN	-2.48
	DMF	-2.46
	MeCN	-2.42
2	CH_2Cl_2	-2.53
	n-BuCN	-2.43
	DMF	-2.41
3	CH_2Cl_2	-2.36
	DMF	-2.29
	MeCN	-2.29

The reaction free energies in Table S19 are in agreement with those obtained via the Weller method (see Section S6 above). Moreover, they fully reproduce the expected trend based on substituent effect (the pyridine's pK_a) and solvent polarity. The reaction free energies of CPET-CS for **1**-**3** were estimated from these reaction free energies combined with the experimental excitation energy, as discussed above, using: $\Delta G^{o\prime}_{\text{CPET-CS}} = -(\Delta G^{o\prime}_{\text{CPET-CR}} + E_{0\text{-}0})$. For **4**-**8**, no minimum was found in which the proton was localized on the donor N of the CSS using charge-constrained CDFT. This observation correlates with the lack of CSS accumulation for these triads observed by visible transient absorption (Section S3). The reaction free energies of CPET-CS and CPET-CR for **4**-**8** were obtained from the Weller method (Table S4).

Table S20. Reaction free energies in eV for CPET-CR computed with DFT and CDFT for the GS and CSS, respectively, for triads **1**, **2**, and **3** and with multiple exchange-correlation functionals and CDFT constraints.

Triad	Solvent	ΔG^{o} *	ΔG^{o} †	ΔG^{o} ‡	ΔG^{o} §
1	CH_2Cl_2	-2.54	-2.52	-2.51	-2.63
	n-BuCN	-2.48	-2.44	-2.43	-2.55
	DMF	-2.46	-2.41	-2.40	-2.52
	MeCN	-2.42	-2.41	-2.40	-2.52
2	CH_2Cl_2	-2.53	-2.44	-2.46	-2.65
	n-BuCN	-2.43	-2.35	-2.37	-2.56
	DMF	-2.41	-2.32	-2.34	-2.53
3	CH_2Cl_2	-2.36	-2.24	-2.40	-2.35
	DMF	-2.29	-2.14	-2.30	-2.25

*B3LYP functional with charge constrained for CDFT calculations of the CSS.
†B3LYP functional with spin and charge constrained for CDFT calculations of the CSS.
‡CAM-B3LYP functional (*47*) with spin and charge constrained for CDFT calculations of the CSS.
§ωB97X functional (*48*) with spin and charge constrained for CDFT calculations of the CSS.

Table S20 provides results of benchmarking several methods for computing the reaction free energies for CPET-CR in each triad and solvent for which this reaction was observed experimentally. Each method shown demonstrates the same trend in CPET-CR driving forces, and all of these levels of theory can reproduce the qualitative inverted region behavior. If the restriction that the reorganization energy and electronic coupling are identical for triads **1** and **3** were removed, the experimental observations could be reproduced with any of these data sets. Given this restriction, however, the B3LYP functional with the charge constrained for the CDFT calculations of the CSS provides the best agreement with the experimental data. Moreover, the B3LYP functional was used for the proton potentials, and thus for consistency this functional is also used for the driving forces. Overall, these calculations should be viewed as a proof of concept providing a qualitative explanation of the inverted region behavior rather than as quantitatively meaningful.

Reorganization energies

The reorganization energies and proton potentials for **1** and **3** were estimated using separate fragments of the overall triads for computational simplicity. The triads were fragmented such that the phenol-pyridine and 9-cyanoanthracene motifs were studied separately. The structures of all fragments are shown in Fig. S54. The GS was represented by the (reduced) neutral phenol-pyridine and (oxidized) neutral 9-cyanoanthracene fragments, whereas the CSS was represented by the (oxidized) phenoxyl-pyridinium cation and (reduced) radical anion 9-cyanoanthracene fragments. These DFT calculations were performed with the same computational methods described above but with the 6-31G** basis set. The reduced and oxidized fragments provide the correct qualitative electronic structures of each motif in both states and avoided the use of CDFT.

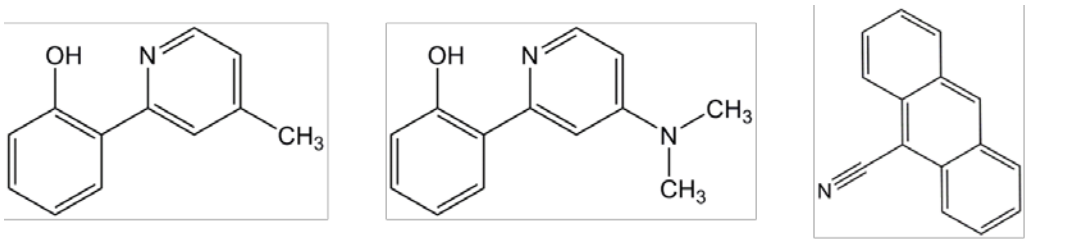

Fragment **1** (GS/reduced) Fragment **3** (GS/reduced) 9-Cyanoanthracene fragment (GS/oxidized)

Figure S54. Structures of triad fragments used for calculating reorganization energies and proton potentials. In Fragments **1** and **3**, the CSS was represented by oxidizing the motif and allowing the proton to transfer from O to N. In 9-cyanoanthracene, the CSS was represented by reduction of the species to produce the radical anion.

The total reorganization energy λ is the sum of the inner-sphere (solute) and outer-sphere (solvent) reorganization energies. The inner-sphere reorganization energy λ_i was calculated using a four-point scheme (*49,50*) given by

$$\lambda_i = \frac{1}{2}\left[E_{\mathrm{CSS}}\left(R_{\mathrm{eq}}^{\mathrm{GS}}\right) - E_{\mathrm{CSS}}\left(R_{\mathrm{eq}}^{\mathrm{CSS}}\right) + E_{\mathrm{GS}}\left(R_{\mathrm{eq}}^{\mathrm{CSS}}\right) - E_{\mathrm{GS}}\left(R_{\mathrm{eq}}^{\mathrm{GS}}\right)\right] \quad \text{(S7)}$$

In this expression, the first (third) term is the energy calculated at the optimized GS (CSS) geometry in the CSS (GS) redox state with the transferring hydrogen optimized for the CSS (GS). The second and fourth terms are the energies of the CSS and GS, respectively, at their equilibrium geometries. All of these calculations were performed by optimizing the molecules in the gas phase and considering only the electronic energies.

This four-point procedure was performed for the full triad molecules using charge CDFT for the CSS and standard DFT for the GS, as well as for the aforementioned fragments using standard DFT by assigning the appropriate charges to each fragment. The total inner-sphere reorganization energy for CPET-CR as determined with the fragments is the sum of the values for 9-cyanoanthracene and either Fragment **1** or Fragment **3**. The inner-sphere reorganization energies computed with both approaches are given in Table S21. Note that the inner-sphere reorganization energy is significantly larger when computed for the full triad rather than the sum of the fragments, presumably due to geometrical changes at the interface between the fragments.

Table S21. Inner-sphere (solute) reorganization energies for the three fragments computed with standard DFT (left) and for the full triads computed with charge CDFT for the CSS and standard DFT for the GS (right).

Fragment	λ_i (eV)	Triad	λ_i (eV)
9-Cyanoanthracene	0.10	**1**	1.15
Fragment **1**	0.28	**3**	1.08
Fragment **3**	0.31		

The outer-sphere, or solvent, reorganization energy was determined using the Marcus two-sphere model, given by

$$\lambda_s = \frac{(\Delta q)^2}{2}\left(\frac{1}{\varepsilon_\infty} - \frac{1}{\varepsilon_0}\right)\left(\frac{1}{R_D} + \frac{1}{R_A} - \frac{2}{R_{DA}}\right) \quad \text{(S8)}$$

In this model, Δq is the change in charge for each fragment between the GS and CSS and thus is ± 1, ε_∞ and ε_0 are the optical and static dielectric constants of the solvent, respectively, R_D is the radius of the electron donor, R_A is the radius of the electron acceptor, and R_{DA} is the distance between the donor and acceptor. The donor and acceptor radii were determined from the cavity volume obtained in the C-PCM calculation for the fragment geometries optimized in the gas phase, assuming a sphere with the same volume, and the spheres are assumed to be touching such that R_{DA} is the sum of R_D and R_A. The solvent reorganization energies for triads **1** and **3** were determined to be 0.68 eV and 0.66 eV, respectively. This approach is expected to overestimate the solvent reorganization energy due to the neglect of charge delocalization and screening effects.

The values for the total reorganization energy λ for **1** and **3** are both 1.06 eV with the inner-sphere component obtained from the fragment calculations and 1.83 eV and 1.74 eV, respectively, with the inner-sphere component obtained from the full triad calculations. The large discrepancy in inner-sphere and therefore total reorganization energies based on the choice of methodology led to the decision in this work to treat the reorganization energy as a fitting parameter to reproduce the experimental ratio of rate constants for CPET-CR in **1** and **3**. Its value is assumed to be equivalent for both triads, as the above calculations suggest. The resulting value of the reorganization energy, 1.40 eV, falls between the two calculated values for the total reorganization energy and yields not only the experimental ratio of CPET-CR rates between the two triads but also the appropriate KIE of nearly unity for each triad (see below). While alternative methodologies for computing both components of the reorganization energy could also be considered, the qualitative rate constant ordering, which implicates inverted region behavior, holds for any reasonable value of λ.

Average geometries and proton potentials

Calculation of the rate constants of CPET-CR for triads **1** and **3** also required the proton potentials at different proton donor-acceptor distances. For this purpose, we first generated average structures for the reduced and oxidized phenol-pyridine fragment in which the proton transfers. These average structures represent the crossing point between the diabatic curves corresponding to the reduced and oxidized states along an inner-sphere solute coordinate. Moreover, these average structures must be obtained for a series of different proton donor-acceptor (O—N) distances. First, geometry optimizations with the proton donor-acceptor distance constrained to a series of specified values were performed in the reduced and oxidized states, corresponding to the GS and CSS, respectively. Then, at each proton donor-acceptor distance, the GS and CSS structures were aligned such that the donor N and acceptor O were superimposed, and the Cartesian coordinates of all other atoms were averaged.

For each average structure, the position of the transferring hydrogen atom was optimized in both the GS (reduced) and CSS (oxidized) states, with all other atoms frozen. The axis connecting the resulting positions of the hydrogen in both states was chosen to be the proton transfer coordinate. The transferring proton was subsequently placed at each of 24 grid points along this

axis, and a single-point DFT calculation in solution was performed at each grid point to generate the proton potential at that proton donor-acceptor distance in both the reduced and oxidized states. The energies obtained from these single-point calculations were then interpolated to yield the proton potential energy curves for the reduced and oxidized states, corresponding to the GS and CSS, respectively. The resulting proton potentials are shown in Figures S55 and S56.

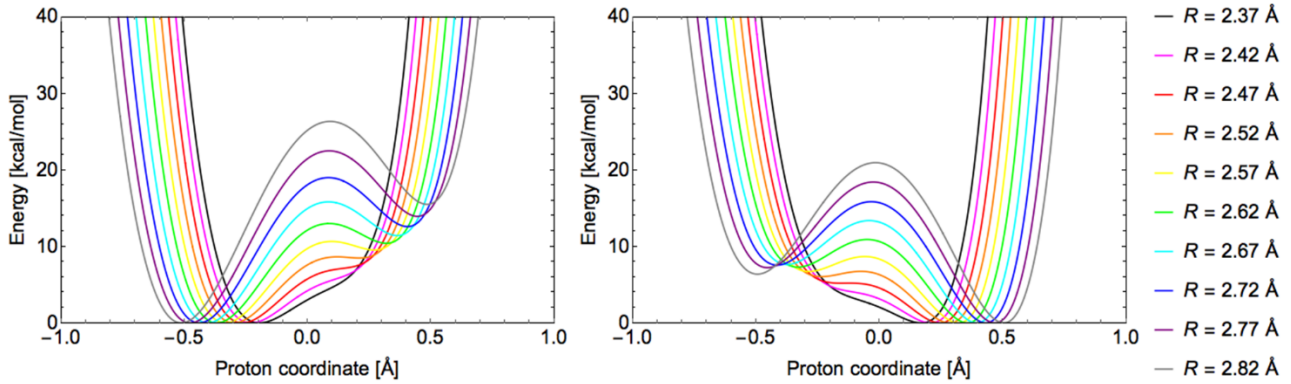

Figure S55. Proton potentials for **1** in the reactant CSS (left) and product GS (right) for all proton donor-acceptor distances considered.

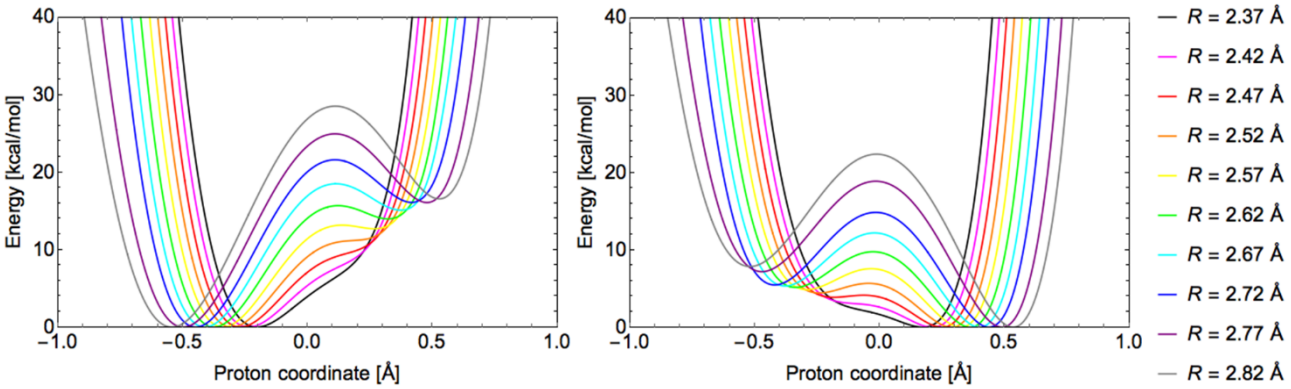

Figure S56. Proton potentials for **3** in the reactant CSS (left) and product GS (right) for all proton donor-acceptor distances considered.

Probability distribution function for proton donor-acceptor distances

The rate constant for CPET-CR is calculated by thermal averaging along the proton donor-acceptor distance R. This thermal averaging is performed using a probability distribution function for a harmonic potential with an effective force constant k_{eff}:

$$P(R) = \frac{\exp\left[-k_{\text{eff}}\left(R-\overline{R}\right)^2 / 2k_{\text{B}}T\right]}{\int_{-\infty}^{\infty}\exp\left[-k_{\text{eff}}\left(R-\overline{R}\right)^2 / 2k_{\text{B}}T\right]dR} \tag{S6}$$

In this expression, $\overline{R}$ is the average equilibrium proton donor-acceptor distance, and k_{eff} is the effective force constant. The effective force constants are determined for the phenol-pyridine fragments in both the neutral and cationic states, corresponding to the GS and CSS, respectively. At the optimized geometry of each state in the gas phase, this effective force constant was determined

by projecting all normal modes onto the proton donor-acceptor axis and performing a weighted sum of the force constants associated with these harmonic motions (*50,51*). The effective force constant k_{eff} utilized in the probability distribution function is the average of the resulting two values. The calculated effective force constants, as well as the equilibrium proton donor-acceptor distances, are given in Table S22.

Table S22. Equilibrium proton donor-acceptor distances and effective force constants for the phenol-pyridine fragments **1** and **3**.

Fragment	State	R (Å)	$\overline{R}$ (Å)	k_{eff} (au)	Average k_{eff} (au)
1	CSS	2.57	2.57	0.0516	0.0514
	GS	2.57		0.0512	
3	CSS	2.58	2.57	0.0519	0.0484
	GS	2.56		0.0450	

CPET-CR rate constants, kinetic isotope effects, and reactant/product vibronic state pair contributions

With all of the input quantities calculated as described above, the rate constants of CPET-CR for **1** and **3** were computed according to Equations 1 and 2 in the main text. The reactant and product vibronic states can be viewed as proton vibrational states within their respective diabatic electronic states. The one-dimensional Schrödinger equation was solved for each of the calculated proton potentials at each proton donor-acceptor distance in order to obtain the proton (or deuteron) vibrational wavefunctions. These nuclear wavefunctions were used to compute the overlap integrals $S_{\mu\nu}$ that enter the rate constant expression. The calculated rate constants for both triads with either H or D are given in Table S23, assuming an electronic coupling of 1 kcal/mol. These absolute rate constants are not meaningful given that the actual electronic coupling is unknown. However, the electronic coupling cancels exactly when computing the H/D kinetic isotope effect (KIE) for each triad, as well as when computing the ratio of the rate constants for **1** and **3**, because it is assumed to be the same for both triads.

Table S23. CPET-CR rate constants (in s^{-1}), assuming an electronic coupling of 1 kcal/mol, KIEs, and ratio of rate constants for **1** and **3**.*

	1	**3**	k_3/k_1
k^{H}	2.40×10^{11}	6.62×10^{11}	2.76
k^{D}	2.22×10^{11}	6.17×10^{11}	
KIE	1.08	1.07	

* The absolute magnitudes of the individual rate constants are not meaningful because the electronic coupling for these systems is unknown.

The calculated ratio of rate constants for **1** and **3** of 2.76 is in agreement with the experimentally determined value and demonstrates that, despite being more exoergic, CPET-CR is slower for **1** than for **3**, implicating the Marcus inverted region. In addition, both calculated KIEs

are in good agreement with the experimentally observed KIEs of unity. (As discussed above, the reorganization energy was varied to reproduce the experimental ratio of rate constants, but the KIEs were computed without further parameterization.) Analysis of the contributions to the rate constant (Tables S24–S27) indicates that the KIE of unity is the result of large contributions from highly excited proton vibrational wavefunctions in the product state. These vibrational wavefunctions for the product (GS) are delocalized for both H and D (Figure 4), leading to significant overlap with the ground state vibrational wavefunctions for the reactant (CSS) with only small differences between H and D.

To further elucidate these data, we analyzed the dominant contributions to the rate constants for each triad and isotope in terms of reactant/product vibronic state pairs. This analysis was performed at the dominant proton donor-acceptor distance, which is the distance corresponding to the maximum of $k(R)P(R)$. For both triads for both H and D, the dominant proton donor-acceptor distance was the equilibrium distance, 2.57 Å. These data are given in Tables S24–S27. While these tables only show the data for one reactant and nine product vibronic states, the calculations performed included three reactant and twelve product vibronic states. As is clear from the percent contributions, the states shown herein represent all non-negligible contributions to the rate constant. These data include the Marcus free energy barrier for each reactant/product vibronic state pair, $\Delta G^{\dagger}_{\mu\nu}$, defined as follows:

$$\Delta G^{\dagger}_{\mu\nu} = \frac{\left(\Delta G^{\circ}_{\mu\nu} + \lambda\right)^2}{4\lambda} \tag{S7}$$

For both triads and both isotopes, the dominant contributions to the rate constant are from the ground reactant (CSS) state to the excited product (GS) states. This observation is expected because for exoergic reactions such as this CPET-CR, these reactant/product vibronic state pairs have small free energy barriers, $\Delta G^{\dagger}_{\mu\nu}$, and large overlap integrals. Although the dominant contributing vibronic state pairs are less exoergic than ΔG°_{00}, which is the reaction free energy for the reactant and product ground vibronic states, their effective reaction free energies, $\Delta G^{\circ}_{\mu\nu}$, are still greater in magnitude than the reorganization energy, λ = 32.28 kcal/mol. Moreover, the higher product vibronic states do not contribute significantly due to smaller overlap integrals arising from oscillations of the associated proton vibrational wavefunctions (Figure 4). As a result, the CPET-CR process for these systems exhibits inverted region behavior.

Table S24. Main contributions to the rate constant for **1** with hydrogen at R = 2.57 Å.*

(μ,ν)	P_μ	$\Delta G^{\circ}_{\mu\nu}$	$\Delta G^{\dagger}_{\mu\nu}$	$S^2_{\mu\nu}$	$\exp\left[-\Delta G^{\dagger}_{\mu\nu} / k_B T\right]$	% Contrib.
(0,0)	1.00	-58.49	5.32	1.03E-03	1.27E-04	0.00
(0,1)	1.00	-53.60	3.52	4.53E-01	2.64E-03	13.12
(0,2)	1.00	-52.19	3.07	4.24E-01	5.63E-03	26.19
(0,3)	1.00	-48.80	2.11	1.03E-01	2.84E-02	31.98
(0,4)	1.00	-45.10	1.27	1.73E-02	1.17E-01	22.15
(0,5)	1.00	-40.83	0.57	1.45E-03	3.85E-01	6.11
(0,6)	1.00	-36.11	0.11	4.99E-05	8.26E-01	0.45
(0,7)	1.00	-31.01	0.01	4.78E-08	9.79E-01	0.00

(0,8)	1.00	-25.57	0.35	1.41E-07	5.54E-01	0.00

* Free energies in kcal/mol.

Table S25. Main contributions to the rate constant for **1** with deuterium at $R = 2.57$ Å.*

(μ,ν)	P_μ	$\Delta G^{o}_{\mu\nu}$	$\Delta G^{\dagger}_{\mu\nu}$	$S^2_{\mu\nu}$	$\exp\left[-\Delta G^{\dagger}_{\mu\nu}/k_B T\right]$	% Contrib.
(0,0)	1.00	-58.49	5.32	1.01E-05	1.27E-04	0.00
(0,1)	1.00	-54.09	3.68	9.36E-03	2.00E-03	0.22
(0,2)	1.00	-52.73	3.24	7.38E-01	4.24E-03	37.25
(0,3)	1.00	-50.95	2.70	1.56E-01	1.05E-02	19.54
(0,4)	1.00	-48.96	2.15	7.88E-02	2.64E-02	24.77
(0,5)	1.00	-46.50	1.56	1.56E-02	7.14E-02	13.25
(0,6)	1.00	-43.75	1.02	1.98E-03	1.80E-01	4.23
(0,7)	1.00	-40.74	0.55	1.39E-04	3.93E-01	0.65
(0,8)	1.00	-37.51	0.21	3.65E-06	7.00E-01	0.03

* Free energies in kcal/mol.

Table S26. Main contributions to the rate constant for **3** with hydrogen at $R = 2.57$ Å. *

(μ,ν)	P_μ	$\Delta G^{o}_{\mu\nu}$	$\Delta G^{\dagger}_{\mu\nu}$	$S^2_{\mu\nu}$	$\exp\left[-\Delta G^{\dagger}_{\mu\nu}/k_B T\right]$	% Contrib.
(0,0)	1.00	-54.54	3.84	1.32E-03	1.55E-03	0.01
(0,1)	1.00	-50.90	2.68	7.02E-01	1.08E-02	30.07
(0,2)	1.00	-49.03	2.17	1.95E-01	2.56E-02	19.72
(0,3)	1.00	-45.88	1.43	8.59E-02	8.93E-02	30.37
(0,4)	1.00	-42.20	0.76	1.47E-02	2.76E-01	16.05
(0,5)	1.00	-37.99	0.25	1.38E-03	6.53E-01	3.56
(0,6)	1.00	-33.35	0.01	5.57E-05	9.85E-01	0.22
(0,7)	1.00	-28.32	0.12	1.64E-07	8.14E-01	0.00
(0,8)	1.00	-22.96	0.67	1.20E-07	3.21E-01	0.00

* Free energies in kcal/mol.

Table S27. Main contributions to the rate constant for **3** with deuterium at $R = 2.57$ Å.*

(μ,ν)	P_μ	$\Delta G^{o}_{\mu\nu}$	$\Delta G^{\dagger}_{\mu\nu}$	$S^2_{\mu\nu}$	$\exp\left[-\Delta G^{\dagger}_{\mu\nu}/k_B T\right]$	% Contrib.
(0,0)	1.00	-54.54	3.84	1.26E-05	1.55E-03	0.00
(0,1)	1.00	-50.59	2.60	4.30E-01	1.25E-02	22.85
(0,2)	1.00	-50.21	2.49	3.73E-01	1.50E-02	23.72
(0,3)	1.00	-47.96	1.90	1.29E-01	4.04E-02	22.14
(0,4)	1.00	-46.06	1.47	5.40E-02	8.38E-02	19.20
(0,5)	1.00	-43.61	0.99	1.16E-02	1.87E-01	9.17
(0,6)	1.00	-40.90	0.58	1.57E-03	3.79E-01	2.53

(0,7)	1.00	-37.94	0.25	1.22E-04	6.59E-01	0.34
(0,8)	1.00	-34.75	0.05	3.86E-06	9.24E-01	0.02

* Free energies in kcal/mol.

Geometries and energies for relevant species

Table S28. Cartesian coordinates for optimized geometries for **1**.

1-GS / -1263.875304 Ha				**1**-CSS / -1263.797642			
O	4.849938	-1.896554	0.157935	O	3.759234	-2.477474	-1.270268
H	5.078676	-0.987998	-0.197599	H	4.251828	-1.139610	-1.722255
N	4.583053	0.549267	-0.582722	N	4.195006	-0.062096	-1.629469
C	-0.697270	-2.114807	1.463220	C	-0.484224	-1.247262	2.195681
H	-1.039909	-3.137257	1.279455	H	-0.912052	-2.153156	2.664970
H	-0.786156	-1.987755	2.547163	H	-0.207455	-0.580123	3.034157
C	1.343089	-0.847218	0.577794	C	1.571658	-0.549981	0.923083
H	0.696778	0.009468	0.430663	H	1.321321	0.474982	1.182599
C	0.775360	-2.018072	1.068591	C	0.806749	-1.584268	1.482454
C	1.616076	-3.133225	1.242534	C	1.161018	-2.937843	1.194464
H	1.203693	-4.065539	1.622565	H	0.599426	-3.745127	1.661988
C	2.965529	-3.064626	0.934189	C	2.150365	-3.229905	0.283910
H	3.617491	-3.922948	1.060556	H	2.413887	-4.252648	0.032851
C	3.533969	-1.877579	0.438919	C	2.871976	-2.187739	-0.400840
C	2.712363	-0.730268	0.256202	C	2.562242	-0.799147	-0.032060
C	3.269874	0.544151	-0.253235	C	3.271194	0.296169	-0.696984
C	2.505262	1.720928	-0.396629	C	3.072616	1.671189	-0.476451
H	1.456626	1.730538	-0.125128	H	2.337624	1.997822	0.247886
C	3.081948	2.892051	-0.883238	C	3.792397	2.626183	-1.191842
C	4.446408	2.859017	-1.218941	C	4.735878	2.182046	-2.144961
H	4.951559	3.740628	-1.602010	H	5.316956	2.888970	-2.726693
C	5.145366	1.672285	-1.048980	C	4.910294	0.828810	-2.340188
H	6.202933	1.607244	-1.293277	H	5.611644	0.418051	-3.057719
C	2.273910	4.154930	-1.048789	C	3.563519	4.097881	-0.974926
H	2.723787	4.983729	-0.490844	H	4.504498	4.609409	-0.745908
H	1.247370	4.024503	-0.697255	H	2.861474	4.281947	-0.159036
H	2.235455	4.456594	-2.101828	H	3.157239	4.557903	-1.882992
C	-1.637724	-1.145025	0.771777	C	-1.540038	-0.596178	1.270525
C	-1.958153	0.094409	1.380716	C	-2.563084	0.224573	1.843566
C	-1.364948	0.519614	2.616872	C	-2.573705	0.524707	3.237671
H	-0.628798	-0.112831	3.097535	H	-1.764375	0.117263	3.825633
C	-1.685140	1.721786	3.194162	C	-3.547923	1.300988	3.830971
H	-1.212627	2.016013	4.126472	H	-3.509496	1.505555	4.897522
C	-2.630358	2.587431	2.577198	C	-4.590480	1.834544	3.039680
H	-2.883653	3.533411	3.046196	H	-5.359937	2.452495	3.494086
C	-3.217367	2.231784	1.390194	C	-4.630820	1.569197	1.685391
H	-3.934480	2.892168	0.913459	H	-5.434104	1.974879	1.077757
C	-2.899556	0.992446	0.752771	C	-3.644515	0.759887	1.052388
C	-3.481508	0.623084	-0.481950	C	-3.713087	0.433775	-0.330049
C	-3.144978	-0.593600	-1.120887	C	-2.712794	-0.379432	-0.936196
C	-3.716263	-0.962481	-2.377518	C	-2.793167	-0.768006	-2.303126
H	-4.432464	-0.291585	-2.840782	H	-3.641064	-0.425725	-2.888710
C	-3.368406	-2.137163	-2.993301	C	-1.829062	-1.568764	-2.885568
H	-3.811263	-2.400473	-3.949088	H	-1.921944	-1.853574	-3.930593
C	-2.423089	-3.009475	-2.387006	C	-0.703936	-1.974501	-2.132286
H	-2.140567	-3.930071	-2.888610	H	0.093319	-2.551122	-2.596745
C	-1.861446	-2.691563	-1.176588	C	-0.577232	-1.588938	-0.814482
H	-1.129100	-3.362455	-0.745234	H	0.297626	-1.833768	-0.185792
C	-2.200248	-1.481290	-0.485792	C	-1.599214	-0.843622	-0.138868
C	-4.422114	1.504624	-1.103119	C	-4.799756	0.913822	-1.111096
N	-5.185646	2.225606	-1.608667	N	-5.688385	1.317908	-1.755231

Table S29. Cartesian coordinates for optimized geometries for **2**.

2-GS / -1339.0651786744 Ha				**2**-CSS / -1338.9478785989			
O	4.8865888	-1.742206	0.920422	O	3.7116988	-2.3741064	-1.2179359
H	5.1104659	-0.8416605	0.5410732	H	4.2070654	-0.9978515	-1.5565444
N	4.58875	0.6074023	-0.0673939	N	4.1649233	0.064263	-1.3547947
C	-0.7728888	-2.3565349	1.2718106	C	-0.6173241	-1.415599	2.2165631
H	-1.0323414	-3.2836279	0.7501473	H	-1.0565007	-2.346366	2.6222359
H	-1.0131224	-2.5592865	2.3203678	H	-0.3771834	-0.7858	3.0946848
C	1.2934394	-0.9650501	0.6456709	C	1.5002503	-0.6372544	1.1080159
H	0.6244401	-0.17551	0.3243805	H	1.246946	0.3637204	1.4477993
C	0.7338874	-2.1331238	1.1488806	C	0.7041861	-1.707928	1.5397285
C	1.6092625	-3.154387	1.5671227	C	1.0568017	-3.0330568	1.1415646
H	1.2034357	-4.082116	1.9654155	H	0.4675188	-3.8720823	1.5075322
C	2.9821081	-2.9973466	1.4803518	C	2.071047	-3.2514602	0.2368519
H	3.6616043	-3.780135	1.8018272	H	2.3299969	-4.2497566	-0.1019948
C	3.5432126	-1.8122033	0.9695846	C	2.8161218	-2.158321	-0.3340478
C	2.6872069	-0.7635534	0.5350667	C	2.5170841	-0.8098931	0.1638508
C	3.2330755	0.4981753	-0.0180376	C	3.2528833	0.3382595	-0.3732389
C	2.4241476	1.5446831	-0.4801315	C	3.0909003	1.6684455	0.0149271
H	1.3439082	1.4920472	-0.4600994	H	2.3828187	1.9533515	0.7814411
C	3.0102276	2.7056124	-0.9919422	C	3.8352383	2.6796218	-0.6069972
C	4.4094611	2.804717	-1.0366679	C	4.7586129	2.3463062	-1.6240562
H	4.9236397	3.6757599	-1.4211171	H	5.3517909	3.0909653	-2.1360038
C	5.1383599	1.7198748	-0.5587404	C	4.8888555	1.0155132	-1.9642361
H	6.2254208	1.7478072	-0.5726798	H	5.5746995	0.6776238	-2.7330374
O	2.154525	3.6666601	-1.4151573	O	3.6027316	3.9263385	-0.1765248
C	2.6868792	4.8747596	-1.9583524	C	4.2767296	5.0340241	-0.793059
H	3.2805451	4.6757032	-2.8581203	H	4.0295406	5.0942054	-1.8578326
H	1.8216272	5.4836933	-2.2200743	H	3.902682	5.9183871	-0.2796102
H	3.2979758	5.4062389	-1.2195621	H	5.3602773	4.9578336	-0.6549103
C	-1.6694677	-1.2427499	0.7671472	C	-1.6416026	-0.7141151	1.2887497
C	-2.1031607	-0.2235084	1.651756	C	-2.7201395	0.018682	1.8792852
C	-1.6583687	-0.1498196	3.013878	C	-2.8283036	0.1555997	3.2946394
H	-0.9434752	-0.8763673	3.380364	H	-2.0505523	-0.3061088	3.8852435
C	-2.0960476	0.8360139	3.861049	C	-3.8555831	0.8455394	3.9047796
H	-1.7358461	0.8683477	4.8849144	H	-3.892449	0.9261318	4.9878544
C	-3.0146634	1.821178	3.4048602	C	-4.8541108	1.4539825	3.11051
H	-3.3604062	2.5937255	4.0851877	H	-5.6630435	2.0076233	3.5791791
C	-3.4586416	1.8019788	2.1077922	C	-4.8005866	1.3447656	1.735351
H	-4.1529564	2.558405	1.7559992	H	-5.5696103	1.8081771	1.1246845
C	-3.0166755	0.7966704	1.1932587	C	-3.7590279	0.6246226	1.0833564
C	-3.4497839	0.7764142	-0.153027	C	-3.7297409	0.4576751	-0.3283791
C	-2.9914908	-0.2075244	-1.060203	C	-2.6795238	-0.2744521	-0.9523991
C	-3.404523	-0.216273	-2.4282386	C	-2.6653567	-0.5050055	-2.3571222
H	-4.0946301	0.5488766	-2.7690315	H	-3.4780613	-0.1038216	-2.9549863
C	-2.9380844	-1.1658452	-3.300423	C	-1.653889	-1.226637	-2.9616551
H	-3.2600779	-1.1557274	-4.3373892	H	-1.6747168	-1.3912881	-4.0360651
C	-2.0276402	-2.162028	-2.8520236	C	-0.5759588	-1.7092426	-2.1853695
H	-1.6515868	-2.9023328	-3.55184	H	0.258904	-2.2249204	-2.6555631
C	-1.6176981	-2.1901054	-1.5434252	C	-0.5407728	-1.4763194	-0.8271729
H	-0.9104939	-2.9498214	-1.2331662	H	0.2974762	-1.7850757	-0.1806686
C	-2.0820799	-1.2250871	-0.5889654	C	-1.6115567	-0.8143081	-0.1394619
C	-4.3618562	1.7793204	-0.6105114	C	-4.7690082	1.0150454	-1.1225218
N	-5.1043362	2.5964898	-0.9837505	N	-5.6193962	1.4823499	-1.7754434

Table S30. Cartesian coordinates for optimized geometries for **3**.

3-GS / -1358.539374 Ha				**3**-CSS / -1358.467278			
O	4.291555	-2.952644	-0.085720	O	3.55757598	-3.1463923	-1.1575834
H	4.682517	-2.035305	-0.223300	H	4.29358154	-1.6965832	-1.2653799
N	4.471616	-0.410219	-0.289125	N	4.15214501	-0.6703811	-1.0883185
C	-1.246364	-2.476084	1.184863	C	-1.0923299	-2.1224277	1.85771827
H	-1.746433	-3.393601	0.859909	H	-1.7093224	-3.0381255	1.90813154
H	-1.337397	-2.486706	2.275635	H	-0.8807172	-1.8700107	2.91092731
C	0.996121	-1.434788	0.533323	C	1.12661765	-1.3894791	0.89814602
H	0.504486	-0.470404	0.570047	H	0.93442718	-0.4090979	1.32261671
C	0.229623	-2.564927	0.799901	C	0.23418929	-2.4351906	1.19671202
C	0.866701	-3.818015	0.747472	C	0.52127728	-3.7427186	0.70222902
H	0.297103	-4.723842	0.944894	H	-0.1517564	-4.5633239	0.9463432
C	2.217100	-3.916274	0.449966	C	1.6203331	-3.9711374	-0.0927835
H	2.716683	-4.878825	0.407553	H	1.86157346	-4.9614583	-0.4657421
C	2.987944	-2.768592	0.189767	C	2.52400053	-2.9041822	-0.4626193
C	2.369816	-1.487059	0.221305	C	2.20383279	-1.5572457	0.03119656
C	3.142534	-0.250795	-0.062979	C	2.9923644	-0.4010654	-0.416056
C	2.551393	1.018460	-0.103012	C	2.61044024	0.9263593	-0.2552731
H	1.490326	1.117796	0.064437	H	1.66538447	1.13851033	0.21914178
C	3.324857	2.170533	-0.363880	C	3.40459947	1.99013601	-0.7582268
C	4.710270	1.967531	-0.593247	C	4.61095052	1.63254601	-1.4404302
H	5.382296	2.786928	-0.810475	H	5.26863747	2.37761078	-1.8649885
C	5.209977	0.677590	-0.545226	C	4.93258997	0.3087369	-1.5907953
H	6.267970	0.500772	-0.724876	H	5.82166899	-0.0137144	-2.1202003
N	2.761571	3.422680	-0.394194	N	3.02905999	3.28327498	-0.6139531
C	1.316716	3.575646	-0.276912	C	1.76598053	3.62122106	0.05147833
C	3.571393	4.577932	-0.757696	C	3.84322074	4.35812831	-1.1826251
H	0.781233	3.082880	-1.100566	H	0.90667711	3.19372844	-0.4763426
H	1.067391	4.636744	-0.296171	H	1.65214732	4.70374672	0.06360174
H	0.947505	3.163200	0.669296	H	1.75994082	3.26664202	1.0879528
H	3.956750	4.509138	-1.785158	H	3.89716882	4.28562937	-2.2755858
H	4.422784	4.695444	-0.077044	H	4.86025704	4.34436361	-0.7748514
H	2.960397	5.477979	-0.683963	H	3.39173177	5.31550123	-0.9280546
C	-2.000655	-1.280699	0.630860	C	-1.863341	-1.0138952	1.11730869
C	-2.174379	-0.112305	1.414997	C	-2.6013044	-0.0190857	1.83498896
C	-1.596636	0.030127	2.721659	C	-2.5743165	0.05563724	3.25882628
H	-0.985430	-0.768239	3.124153	H	-1.9648066	-0.6703002	3.77702457
C	-1.775330	1.166268	3.469089	C	-3.2781631	1.00481422	3.97708829
H	-1.320053	1.244147	4.451835	H	-3.2220071	1.01854145	5.06238694
C	-2.551302	2.245757	2.963228	C	-4.0628035	1.95551723	3.29152419
H	-2.694906	3.137019	3.566934	H	-4.6181505	2.70881645	3.84370987
C	-3.113867	2.164478	1.715307	C	-4.1249676	1.92684444	1.90976909
H	-3.701969	2.989266	1.325676	H	-4.7323603	2.65547064	1.38102916
C	-2.939835	1.001187	0.902706	C	-3.419901	0.95470849	1.14747665
C	-3.497481	0.914107	-0.393915	C	-3.5171333	0.90017043	-0.2734814
C	-3.306062	-0.231467	-1.202167	C	-2.790394	-0.0794118	-1.0184874
C	-3.854938	-0.319956	-2.518460	C	-2.8993633	-0.1843949	-2.4313854
H	-4.440468	0.511620	-2.897221	H	-3.5669662	0.49675399	-2.9508061
C	-3.647071	-1.430574	-3.295650	C	-2.1813682	-1.1275508	-3.1480696
H	-4.070274	-1.481186	-4.294425	H	-2.2896799	-1.1841247	-4.2281502
C	-2.870901	-2.514536	-2.801207	C	-1.2760584	-1.9766621	-2.4762393
H	-2.695900	-3.382248	-3.430148	H	-0.6524396	-2.669038	-3.0376722
C	-2.335505	-2.466263	-1.539209	C	-1.13338	-1.8841177	-1.1052959
H	-1.727525	-3.293213	-1.194918	H	-0.3785492	-2.4525751	-0.5412539
C	-2.536474	-1.335236	-0.681147	C	-1.9255447	-0.9939775	-0.3152131
C	-4.257079	2.013743	-0.903981	C	-4.3362724	1.83511178	-0.9575133
N	-4.869404	2.913991	-1.320266	N	-4.9959916	2.61810502	-1.5253968

Table S31. Cartesian coordinates for optimized geometries for Fragment-**1**.

Fragment 1 –GS (Reduced) -593.914907 Ha				Fragment 1 CSS (Oxidized) -593.663426 Ha			
O	4.848389	-1.922453	0.176943	O	4.77040967	-1.8835368	0.1845294
H	5.081036	-1.015357	-0.175613	H	5.03916819	-0.3477875	-0.3855474
N	4.605769	0.517782	-0.578259	N	4.5517842	0.55600415	-0.5775235
C	1.354583	-0.843864	0.598650	C	1.33157398	-0.8369152	0.60099696
H	0.703622	0.012275	0.460013	H	0.65399237	-0.0005038	0.47365252
C	0.803501	-2.009362	1.108305	C	0.80068611	-2.0333922	1.11654364
C	1.622749	-3.130350	1.297324	C	1.61270981	-3.1691971	1.31350533
H	1.205271	-4.050740	1.695812	H	1.17949974	-4.0802242	1.71247231
C	2.968894	-3.069976	0.976902	C	2.94847899	-3.1101807	0.99706502
H	3.625938	-3.922473	1.113101	H	3.61854284	-3.9529384	1.12818758
C	3.536783	-1.891811	0.459356	C	3.54163533	-1.8991876	0.46284213
C	2.719800	-0.739509	0.259318	C	2.67319869	-0.7200069	0.26401189
C	3.284188	0.515430	-0.283155	C	3.22480543	0.53300829	-0.2749467
C	2.518652	1.679887	-0.499473	C	2.4972997	1.7072046	-0.5034134
H	1.460806	1.689895	-0.267327	H	1.43947471	1.73554355	-0.2776955
C	3.102191	2.833971	-1.012736	C	3.10840225	2.85415365	-1.0203626
C	4.474984	2.798700	-1.306754	C	4.48675044	2.80117543	-1.3091082
H	4.984900	3.668429	-1.709213	H	5.00608172	3.66360283	-1.7110948
C	5.172926	1.624682	-1.072239	C	5.18374199	1.63478139	-1.0764305
H	6.236950	1.557340	-1.286855	H	6.24307415	1.52202626	-1.2743898
C	2.294156	4.085075	-1.248219	C	2.32667577	4.11300158	-1.2648924
H	2.692303	4.923250	-0.665742	H	2.74672011	4.94213066	-0.6854959
H	1.246581	3.946532	-0.970158	H	1.27571237	4.00070028	-0.9940286
H	2.329617	4.380992	-2.302493	H	2.38333337	4.39884825	-2.320674
H	-0.252046	-2.048451	1.356895	H	-0.2546399	-2.0750661	1.36489265

Table S32. Cartesian coordinates for optimized geometries for Fragment-**3**.

Fragment 3 GS (Reduced) -688.572446 Ha				Fragment 3 CSS (Oxidized) -688.336207 Ha			
O	4.358436	-2.909575	0.306648	O	4.29964645	-2.858983	0.44447547
H	4.730473	-1.990044	0.151343	H	4.81151216	-1.3054649	0.02462104
N	4.485896	-0.382762	-0.060247	N	4.43402066	-0.3580423	-0.1603557
C	0.981901	-1.466188	0.529093	C	0.9529186	-1.4808706	0.45384333
H	0.454369	-0.520055	0.471692	H	0.38218282	-0.5730495	0.29597156
C	0.249587	-2.607588	0.820575	C	0.24106631	-2.6415055	0.79893929
C	0.910395	-3.838705	0.920192	C	0.9034161	-3.866541	1.02238326
H	0.351226	-4.742448	1.146080	H	0.33229156	-4.749806	1.28799097
C	2.282234	-3.907238	0.739875	C	2.26944118	-3.9263547	0.90017302
H	2.820986	-4.845622	0.819919	H	2.8314503	-4.8401274	1.05983292
C	3.033679	-2.753164	0.451780	C	3.04790565	-2.7547919	0.54554589
C	2.376377	-1.493454	0.325859	C	2.33525184	-1.4802051	0.31603937
C	3.134653	-0.264370	-0.010123	C	3.07589982	-0.2553239	-0.0466378
C	2.511493	0.961491	-0.276975	C	2.48943182	0.97936251	-0.276894
H	1.434187	1.021915	-0.264749	H	1.41897268	1.07377349	-0.1900519
C	3.272179	2.109086	-0.579605	C	3.26781996	2.12199937	-0.6243522
C	4.679630	1.949708	-0.619637	C	4.68068097	1.93302616	-0.7236067
H	5.342950	2.771088	-0.854642	H	5.34604545	2.74383761	-0.981545
C	5.211311	0.700416	-0.359778	C	5.21293998	0.69505728	-0.4867966
H	6.288833	0.554712	-0.393703	H	6.27683917	0.49988156	-0.5488712
N	2.679167	3.323951	-0.827435	N	2.69874405	3.32389565	-0.8486043
C	1.229267	3.438046	-0.848376	C	1.24709753	3.49594016	-0.7405431
C	3.493015	4.463163	-1.223139	C	3.52790616	4.48107022	-1.2049655
H	0.775124	2.829617	-1.642828	H	0.71773147	2.86090319	-1.4591283
H	0.954693	4.478953	-1.020263	H	0.99616289	4.53203805	-0.9579646
H	0.790974	3.130268	0.108653	H	0.89466203	3.26684267	0.27097323
H	4.023714	4.286592	-2.168874	H	4.07065215	4.30605031	-2.1397312
H	4.236996	4.710485	-0.456218	H	4.24558735	4.71318215	-0.4111816
H	2.849879	5.333518	-1.354370	H	2.88476927	5.34753975	-1.3440162
H	-0.822952	-2.542009	0.972896	H	-0.8384392	-2.5870998	0.89354601

Table S33. Cartesian coordinates for optimized geometries for 9-cyanoanthracene fragment.

9-cyanoanthracene fragment - GS (oxidized) -631.788948 Ha				9-cyanoanthracene fragment - CSS (reduced) -631.821585 Ha			
C	-9.509052	-2.485110	-0.010925	C	-9.543692	-2.4951675	-0.0111007
C	-8.140171	-2.468214	-0.000863	C	-8.1554822	-2.4633657	-0.0010112
C	-7.421519	-1.232606	-0.005434	C	-7.4346079	-1.2396796	-0.0054703
C	-8.163007	0.003689	-0.020884	C	-8.1820732	-0.0041462	-0.0209605
C	-9.588925	-0.055529	-0.031030	C	-9.5930322	-0.0730774	-0.0309255
C	-10.239009	-1.262613	-0.026179	C	-10.266641	-1.2921266	-0.0261548
C	-6.022434	-1.194665	0.004678	C	-6.0215417	-1.1961834	0.00470121
C	-7.445923	1.225736	-0.025358	C	-7.453816	1.23915638	-0.0255137
C	-6.029429	1.258550	-0.015084	C	-6.0133118	1.27140201	-0.0150634
C	-5.309334	0.009679	0.000305	C	-5.2967896	0.01767847	0.00033481
C	-3.880228	0.037282	0.010712	C	-3.8770216	0.05301995	0.01060532
H	-3.345618	-0.908518	0.022282	H	-3.3413633	-0.8949318	0.02219799
C	-3.200204	1.225461	0.006222	C	-3.1745808	1.25084856	0.00620307
C	-3.913845	2.457552	-0.008980	C	-3.8746239	2.46735942	-0.0087691
C	-5.284698	2.476008	-0.019321	C	-5.2673681	2.4710684	-0.0191496
H	-5.471168	-2.132016	0.016313	H	-5.469602	-2.1346825	0.01634913
H	-10.045078	-3.429158	-0.007341	H	-10.066796	-3.4494323	-0.007338
H	-7.573420	-3.395110	0.010798	H	-7.5873573	-3.3922221	0.01067875
H	-10.151077	0.872620	-0.042667	H	-10.155708	0.85655006	-0.0425835
H	-11.324402	-1.289812	-0.034046	H	-11.354343	-1.3069814	-0.0341432
H	-2.114659	1.235139	0.014213	H	-2.0863875	1.24426743	0.01434213
H	-3.362583	3.392955	-0.012389	H	-3.3330274	3.41077857	-0.0123146
H	-5.822658	3.418384	-0.030882	H	-5.8063774	3.4146128	-0.030723
C	-8.170992	2.458665	-0.040640	C	-8.1702755	2.45745684	-0.0406091
N	-8.761458	3.462819	-0.053083	N	-8.7650734	3.46898573	-0.0531644

8. Mechanistic analysis of PCET recombination.

CSS → GS recombination could in principle proceed by CPET, or by the stepwise mechanisms of initial PT followed by ET (PT-ET mechanism), or initial ET followed by PT (ET-PT mechanism). These are depicted in Figure S57. The stepwise mechanisms for the CSS recombination implicate intermediates that resemble those proposed for ET-PT and PT-ET in thermally activated, bimolecular oxidations of phenol-base compounds. In the latter systems, such intermediates have been shown to typically be higher in energy than the reactant and product states, and often no local minimum on the GS potential energy surfaces was found for the proton transferred species (Intermediate 1 at the top of Figure S57) *(18,45,52-58)*.

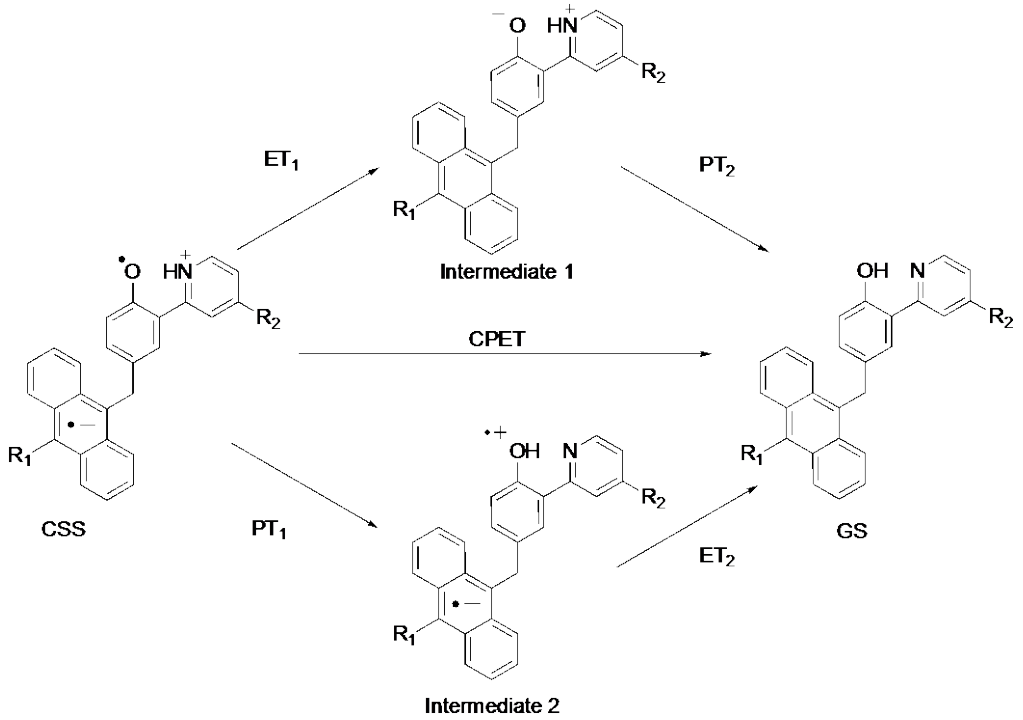

Figure S57. PCET mechanistic pathways for CSS recombination.

Initial PT_1 from the CSS ($An^{\bullet-}$–$PhO^{\bullet}$–pyH^{+}, a zwitterionic biradical) would give another zwitterion with an anthracene radical anion and phenol radical cation ($An^{\bullet-}$–$PhOH^{\bullet+}$–py). This species would then undergo ET_2 to repopulate the GS (PT-ET mechanism). Initial PT_1 from the CSS is estimated to be endergonic. The pK_as of the reactant free pyridiniums in MeCN are: *p*-Me-pyridinium, ~13; *p*-MeO-pyridinium, 14.2; *p*-NMe_2-pyridinium, 17.7; and the pK_a of the product protonated phenoxyl radical in MeCN is ~ 0, based on the pK_a of $^{t}Bu_3PhOH^{\bullet+}$ in MeCN (*3,59*). Using these values, initial PT_1 is estimated to be endergonic by ca. 0.9 ± 0.1 eV. The following ET_2 is therefore estimated to be highly exergonic by > 3 eV. While this value in MeCN is only an approximate estimate of the intramolecular PT_1 in CH_2Cl_2, it is not possible for a reaction that is even close to this endoergic to occur on the sub-ns timescale. In addition, the most acidic pyridinium (*p*-Me-pyridinium in **1**) would show the fastest CSS recombination, however, the opposite trend is observed (Table S1).

Initial ET_1 from the CSS would form a zwitterion localized on the phenol-pyridine portion ($An–PhO^{-}–pyH^{+}$), which would then undergo PT_2 to repopulate the GS (ET-PT mechanism). First, we analyze the energetics of the steps in this possible mechanism. Initial ET_1 from the CSS is

estimated to be exergonic by ca. -1.1 eV, based on the reduction potentials of the cyanoanthracene ($An/An^{\bullet-}$, $E°$ = -1.8 V vs Fc, Table S3 and Figure S51) and phenoxyl/phenoxide ($^tBu_3PhO^{\bullet}/^tBu_3PhO^-$, $E° \approx$ -0.7 V vs Fc) couples in MeCN. This estimated exoergicity using the separated molecules is a lower limit of ET_1 in the triads, because the nearby cationic pyridinium moiety in the triads will shift the phenoxyl/phenoxide couple towards more anodic potentials (easier to form the phenoxide). PT_2 is estimated to be exergonic by ca. -0.9 eV based on the pK_as of the independent *p*-(Me/MeO/NMe_2)-pyridinium cations and $^tBu_3PhOH$ in MeCN (28). These values of ET_1 and PT_2 sum to ~ -1.8 V, but they should sum to the calculated value of $\Delta G°_{CPET}$ (-2.45±0.18 eV for **1**-**3**) to close the thermochemical cycle, again indicating that these estimates with individual fragments underestimate the ET_1 driving force. In sum, both steps in the ET_1-PT_2 mechanism are clearly quite exergonic.

While the ET_1-PT_2 mechanism is energetically possible for **1**-**3**, it is not consistent with the pattern of rate constants. The differences in k_{CR} are up to the factor of 2.8 between **1** and **3** in CH_2Cl_2, while rate-limiting ET_1 should be quite insensitive to the pyridinium substituents since the proton is not moving in this step. There is a similar ratio of rate constants for the initial CS step for **1** and **3**, which has been identified as CPET (ET *with* proton movement). The $\Delta\Delta G°_{CPET}$ values of ~ 0.18 eV for **1**-**3** both in CS and CR are due primarily to the $\Delta\Delta G°_{PT}$ ~ 0.17 eV based on their ΔpK_a in CH_2Cl_2 (*22*). Thus, the differences in k_{CR} between **1** and **3** implicate proton transfer.

The ET_1 rate constant could be affected by the differences in the O•…HN^+ hydrogen bonds in **1** vs. **3**, but the evidence is that this is a very small effect. Even large differences in H-bonding (presence *versus* absence of it) induce only small changes in the $E°$ of in phenoxyl radicals (*18*). Differences in H-bonding in such molecules are indicated by changes of multiple ppm in the ^1H NMR chemical shifts of the phenolic proton, but these differences are relatively small for **1**-**3**: δ O*H*···N for **1** (14.36 ppm), **2** (14.39 ppm), and **3** (14.80 ppm). It is expected that similar small differences affect the CSSs. Thus, the small differences in H-bond strength in **1**-**3** are expected to be too small to move the reduction potentials ($E°$) of the phenoxyl/phenoxide couples to induce sufficient differences in the ET_1 rate constant to account for the observed variation on CSS decays.

In addition, we have looked computationally at Intermediate I, the zwitterion localized on the phenol-pyridine portion $An–PhO^––pyH^+$ that is the product of ET_1. Despite extensive efforts, no minimum was found for this species on the GS potential energy surface in the DFT calculations, suggesting that it is not a stable state. This result is not so surprising for a strongly hydrogen-bonded adduct in which the proton tautomers differ in energy by ca. -0.9 eV (see above).

These various arguments together strongly implicate CPET as the mechanism for CSS decay.

9. X-ray crystallography.

Low-temperature diffraction data were collected on a Rigaku R-AXIS RAPID diffractometer coupled to an R-AXIS RAPID imaging plate detector with Mo Kα radiation (λ = 0.71073 Å) for the structures of **1** and **5**. Low-temperature data were collected on a Rigaku MicroMax-007HF diffractometer coupled to a Saturn994+ CCD detector with Cu Kα (λ = 1.54178 Å) for the structures of **3** and **12**. The diffraction images were processed and scaled using the Rigaku CrystalClear software (*40*) for **1** and **5**; Rigaku Oxford Diffraction software (*60*) for **3** and **12**. The structure was solved with SHELXT and was refined against F^2 on all data by full-matrix least squares with SHELXL (*51*). All non-hydrogen atoms were refined anisotropically. Unless stated otherwise, hydrogen atoms were included in the model at geometrically calculated positions and refined using a riding model. The isotropic displacement parameters of all hydrogen atoms were fixed to 1.2 times the U value of the atoms to which they are linked (1.5 times for methyl groups). The full numbering scheme of compounds **1**, **3**, **5** and **12** can be found in the full details of the X-ray structure determination (CIF). CCDC number 1877696 (**1**), 1877697 (**3**), 1877698 (**5**), and 1877699 (**12**) contains the supplementary crystallographic data for this paper.

Table S34. Details of X-Ray Crystal Structures **1**, **3**, **5**, and **12**

Compound	**1**	**3**	**5**	**12**
Data Code	spider-16085	007b-17022	spider-17017	007-17035
CCDC Number	1877696	1877697	1877698	1877699
Empirical Formula	$C_{28}H_{20}N_2O$	$C_{29}H_{23}N_3O$	$C_{27}H_{21}NO$	$C_{23}H_{16}BrCl_2NO$
Temperature (K)	93(2)	93(2)	93(2)	93(2)
Wavelength (Å)	0.71073	1.54184	0.71073	1.54184
FW	311.32	429.50	376.20	473.18
Crystal System	Triclinic	Triclinic	Triclinic	Monoclinic
Space Group	$P\bar{1}$	$P\bar{1}$	$P\bar{1}$	$P2_1/n$
***a* (Å)**	8.9585(6)	10.1843(8)	8.8682(6)	4.53170(10)
***b* (Å)**	11.2801(8)	10.6292(8)	9.9874(7)	23.7562(5)
***c* (Å)**	11.7621(8)	11.1285(7)	11.5922(8)	18.7351(4)
α (º)	100.230(2)	11.1285(7)	110.155(2)	90
β (º)	111.670(2)	67.717(7)	92.292(2)	93.715(2)
γ (º)	108.534(2)	73.040(7)	98.399(2)	90
***V* (Å^3)**	986.87(12)	1065.12(15)	948.99(11)	2012.71(8)
Z	2	2	2	4
ρ (g/cm^3)	1.348	1.339	1.314	1.562
μ (mm^{-1})	0.082	0.647	0.079	5.333
Completeness	100%	98%	100%	100%
Data / restraints / parameters	4526 / 0 / 285	3710 / 0 / 305	4336 / 0 / 267	3579 / 1 / 257
***R*1, w*R*2 (I > 2σ(I))**	0.0364, 0.0932	0.0407, 0.1071	0.0373, 0.0969	0.0275, 0.0678
***R*1, *wR*2 (all data)**	0.0547, 0.0978	0.0488, 0.1195	0.0542, 0.1008	0.0277, 0.0679
GOF	0.894	1.079	0.957	1.059
Largest Diff. Peak, Hole (e Å^{-3})	0.279, -0.219	0.264, -0.263	0.309, -0.289	0.507, -0.474

Refinement details for 10-(4-hydroxy-3-(4-methylpyridin-2-yl)benzyl)anthracene-9-carbonitrile (1). The phenolic hydrogen H3 was found in the difference map, and the position and thermal parameters were freely refined. See Table 33 and Figure S60 for information on atom H3.

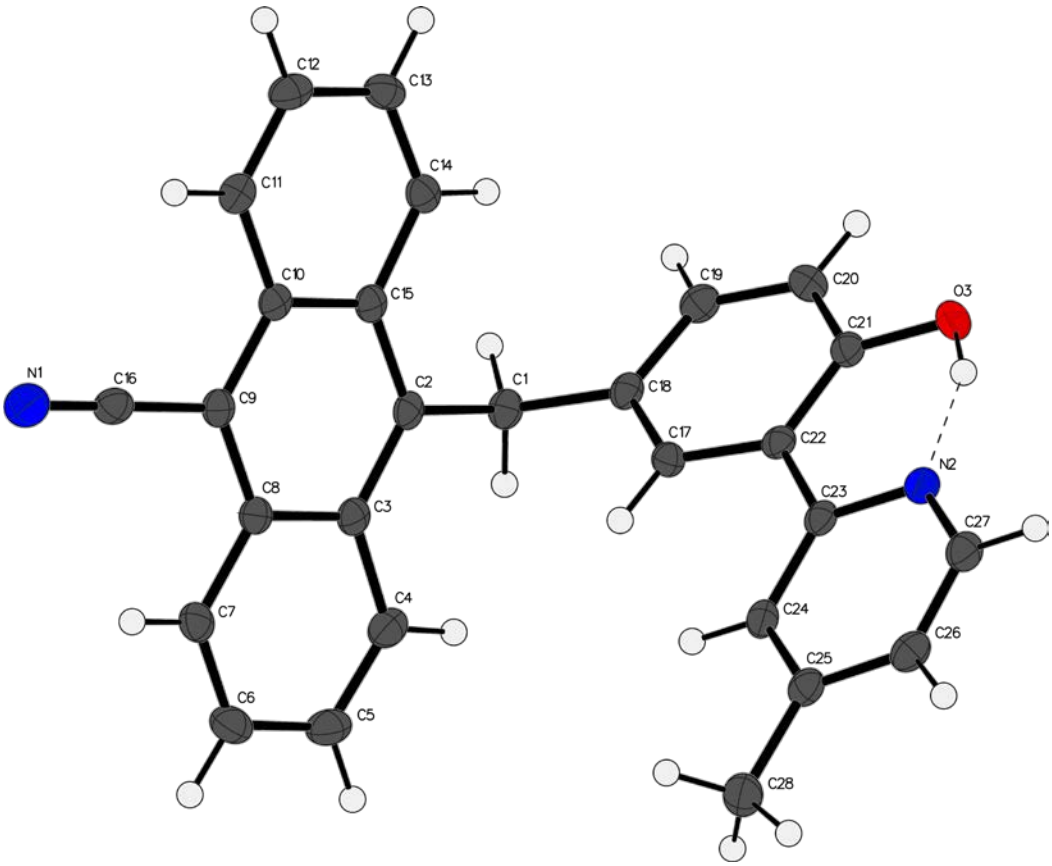

Figure S58. The complete numbering scheme of **1** with 50% thermal ellipsoid probability levels. The hydrogen atoms are shown as circles for clarity. Dashed lines highlight the hydrogen bond interaction.

Table S35. Hydrogen bonds for **1** [Å and °].

D-H...A	d(D-H)	d(H...A)	d(D...A)	<(DHA)
O(3)-H(3)...N(2)	0.955(18)	1.672(18)	2.5549(13)	151.9(16)

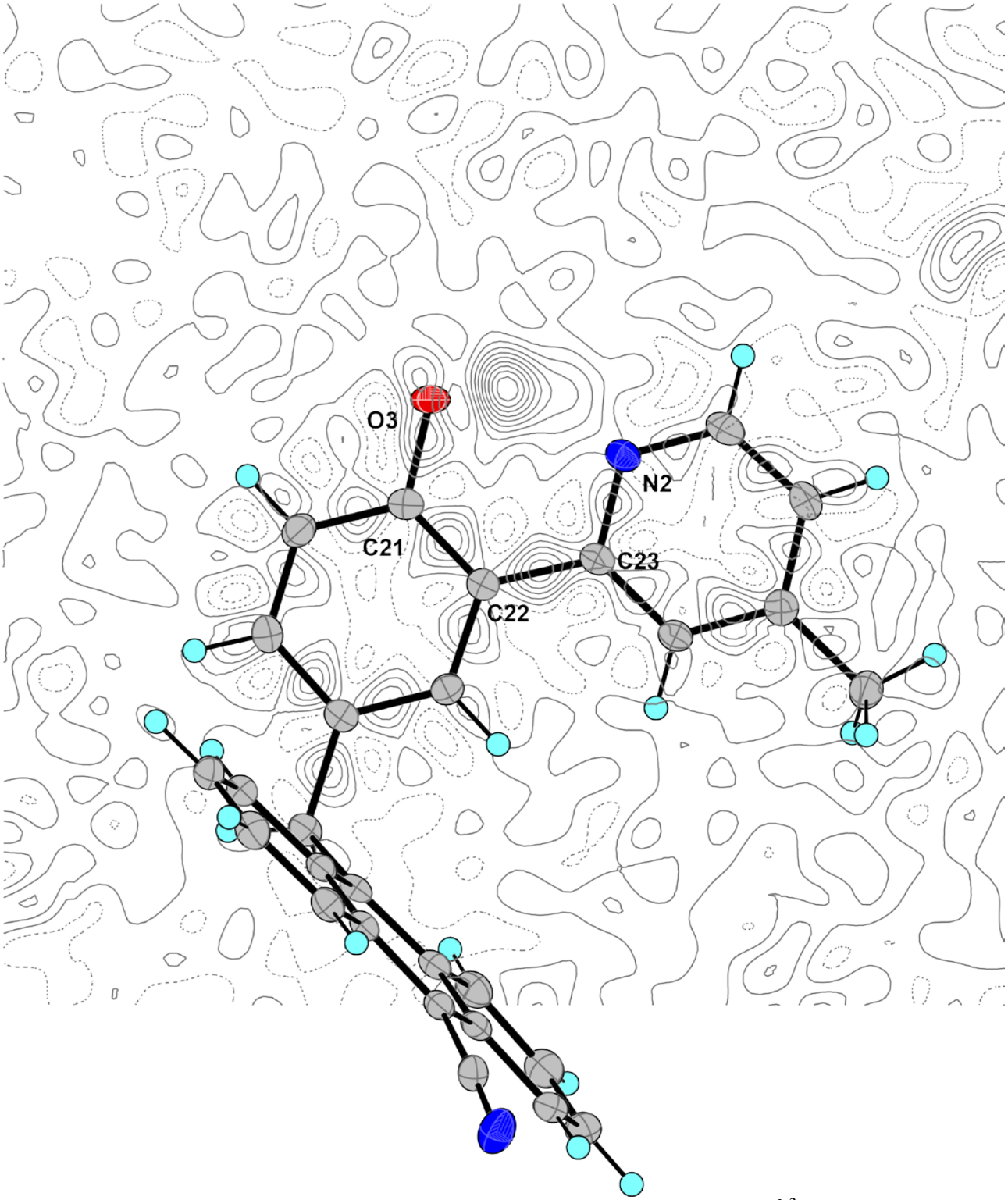

Figure S59. The Fourier difference map of total electron density in **1** (0.07 *e*/Å^3 isolines) highlights the plane of the amide {O3 C21 C22 C23 N2}, excluding contributions from H3 so as to show its effective position.

Refinement details for 10-(3-(4-(dimethylamino)pyridin-2-yl)-4-hydroxybenzyl)anthracene-9-carbonitrile (**3**): The phenolic hydrogen H1 was found in the difference map, and the position and thermal parameters were freely refined. See Table S34 and Figure S62 for information on atom H1. Several reflections were obscured by instrument artifacts and omitted from the least square refinement. X-ray extinction was also freely refined for in this model; the extinction converged at a value of 0.0053(6).

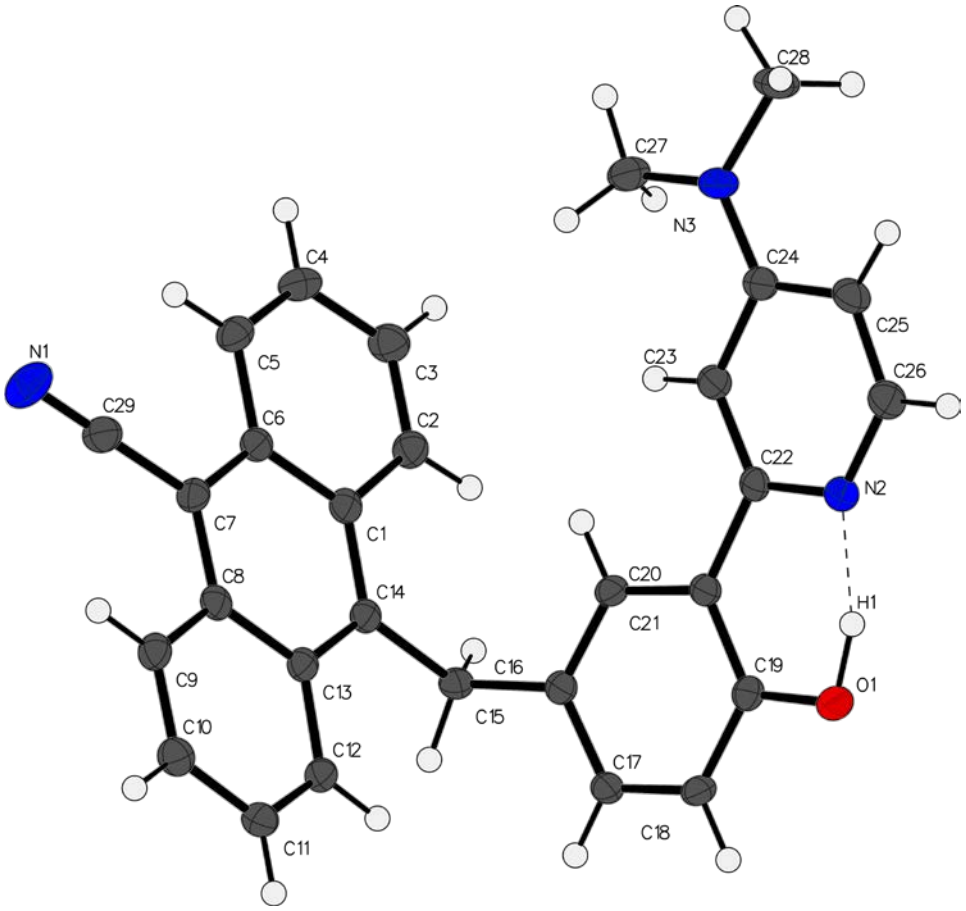

Figure S60. The complete numbering scheme of **3** with 50% thermal ellipsoid probability levels. The hydrogen atoms are shown as circles for clarity. Dashed lines highlight the hydrogen bond.

Table S36. Hydrogen bonds for **3** [Å and °].

D-H...A	d(D-H)	d(H...A)	d(D...A)	<(DHA)
O(1)-H(1)...N(2)	1.00(2)	1.59(2)	2.5338(15)	154(2)

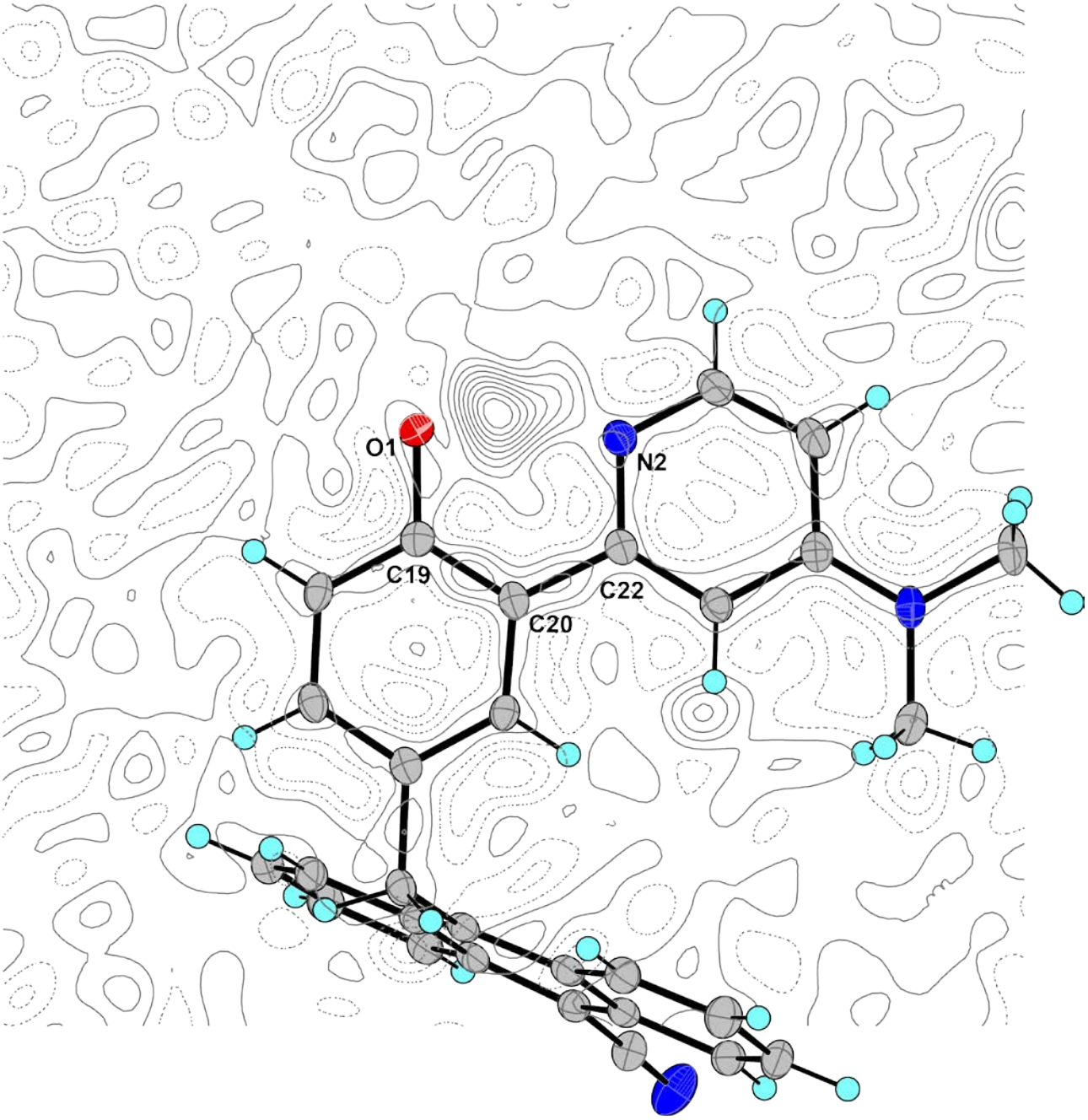

Figure S61. The Fourier difference map of total electron density in **3** (0.035 *e*/Å^3 isolines) highlights the plane of the amide {O1 C19 C20 C22 N2}, excluding contributions from H1 so as to show its effective position.

Refinement details for 4-(anthracen-9-yl-methyl)-2-(4-methylpyridin-2-yl)phenol (**5**): The phenolic hydrogen H1 was found in the difference map, and the position and thermal parameters were freely refined. See Table S35 and Figure S64 for information on atom H1

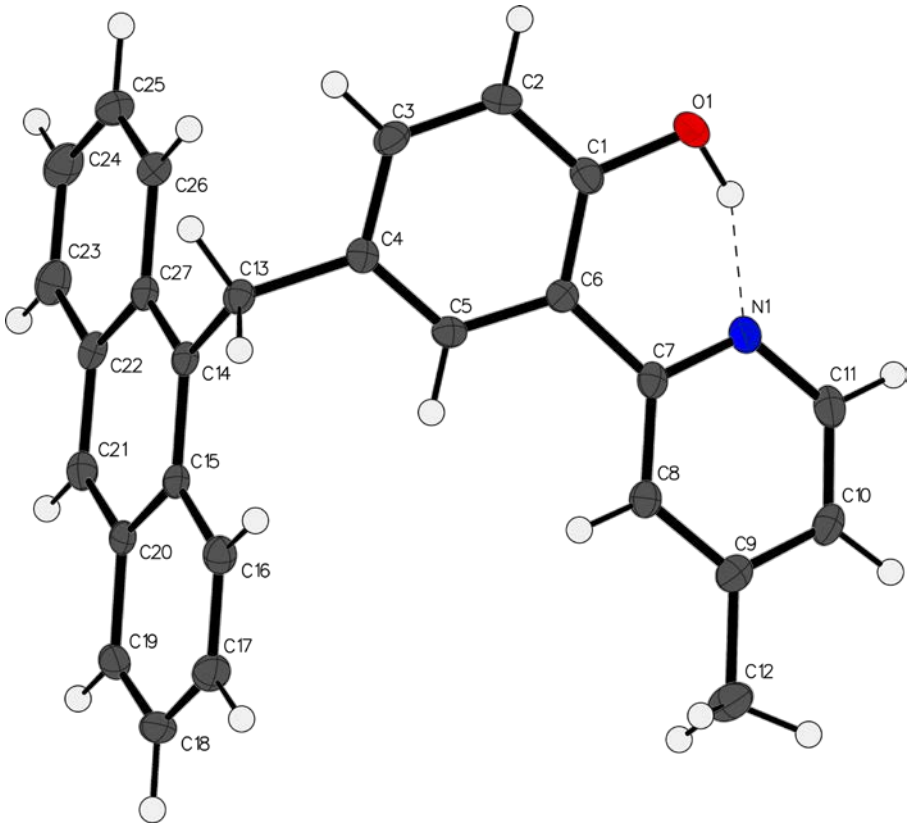

Figure S62. The complete numbering scheme of **5** with 50% thermal ellipsoid probability levels. The hydrogen atoms are shown as circles for clarity. Dashed bonds highlight the hydrogen bond

Table S37. Hydrogen bonds for spider-17017 [Å and °].

D-H...A	d(D-H)	d(H...A)	d(D...A)	<(DHA)
O(1)-H(1)...N(1)	0.98(2)	1.67(2)	2.5787(14)	152.8(18)

Symmetry transformations used to generate equivalent atoms:

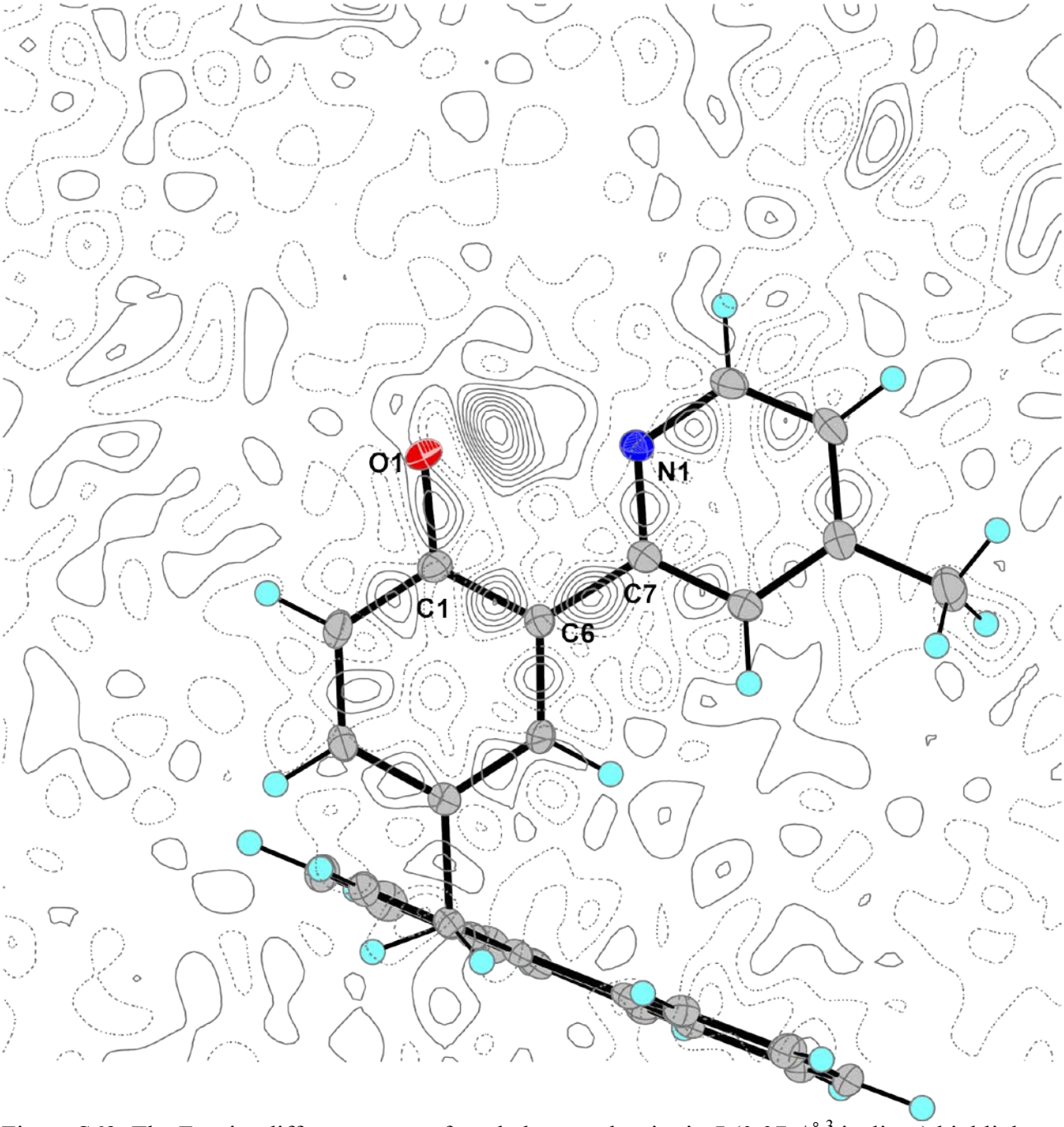

Figure S63. The Fourier difference map of total electron density in **5** (0.07*e*/Å^3 isolines) highlights the plane of the amide {O1 C1 C6 C7 N1}, excluding contributions from H1 so as to show its effective position.

Refinement details for 10-(3-bromo-4-hydroxybenzyl)anthracene-9-carbonitrile (12): The phenolic hydrogen H1 was found in the difference map and, and the thermal parameter was freely refined. The position parameters were semi-freely refined with an O-H distance restraint of 0.93(2) Å, as suggested by the difference map. See Table S36 and Figures S66 and S67 for information on atom H1.

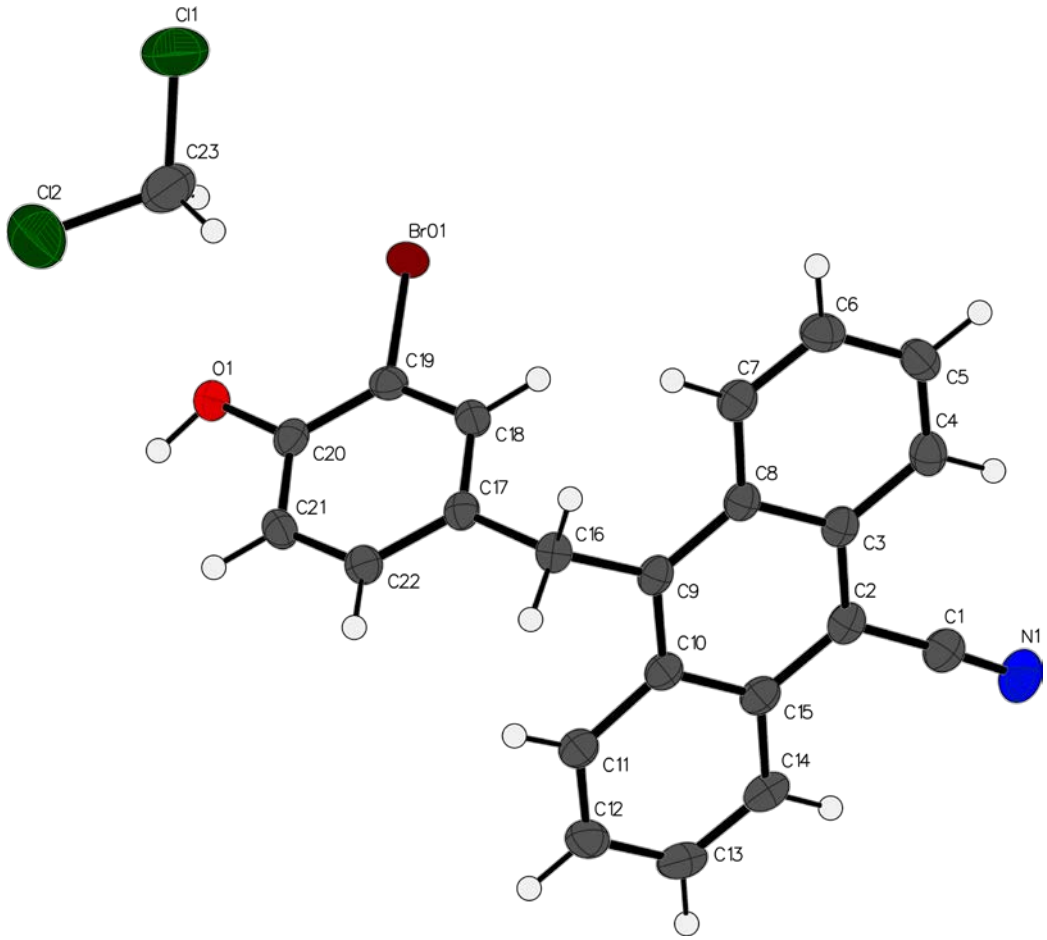

Figure S64. The complete numbering scheme of **12** with 50% thermal ellipsoid probability levels. The hydrogen atoms are shown as circles for clarity.

Table S38. Hydrogen bonds for **12** [Å and °].

D-H...A	d(D-H)	d(H...A)	d(D...A)	<(DHA)
O(1)-H(1)...N(1)#1	0.908(17)	1.904(18)	2.808(2)	173(3)

Symmetry transformations used to generate equivalent atoms:
#1 -x+1/2,y+1/2,-z+3/2

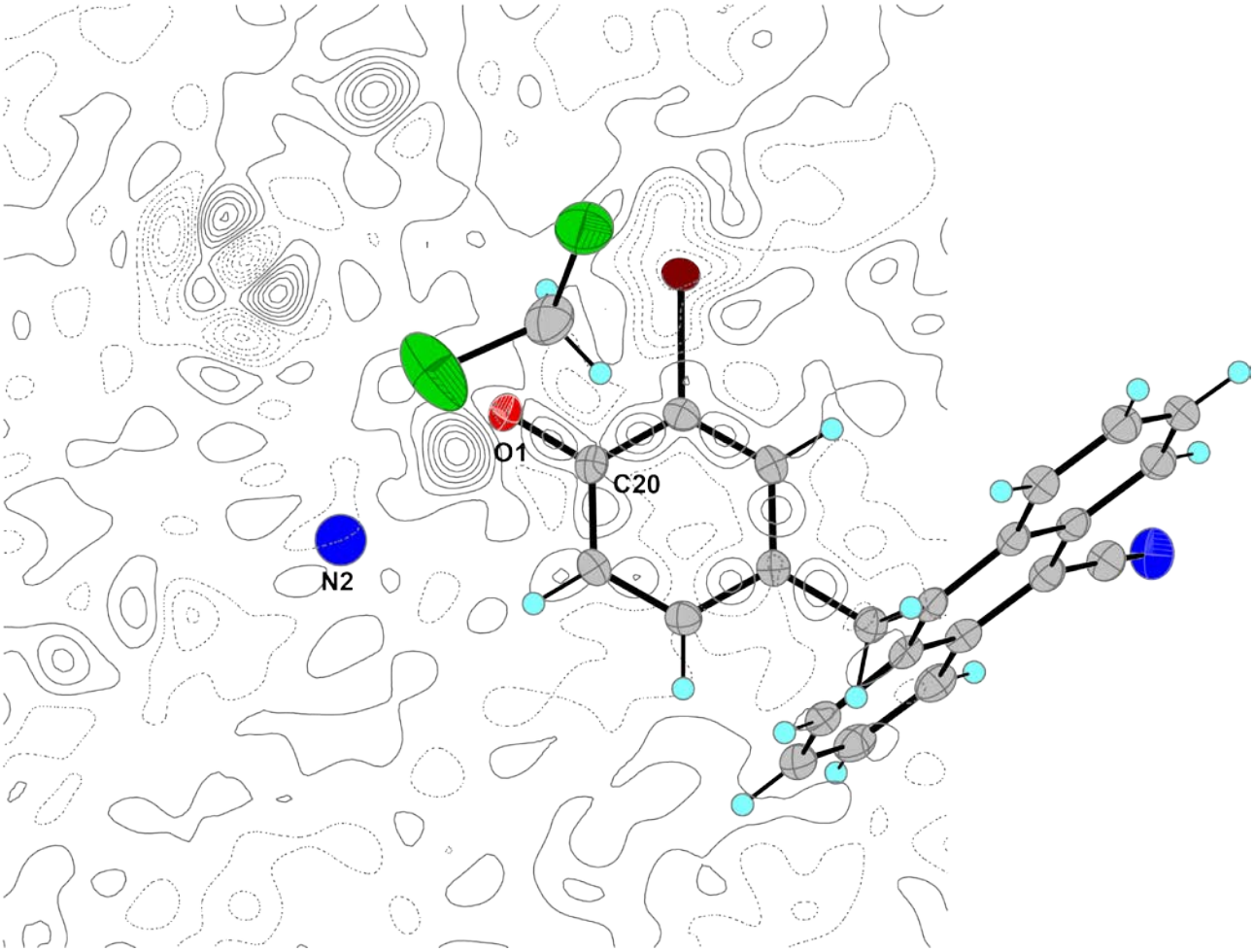

Figure S65. The Fourier difference map of total electron density in **12** (0.08*e*/Å^3 isolines) highlights the plane of {C20 O1 N2}, excluding contributions from H1 so as to show its effective position.

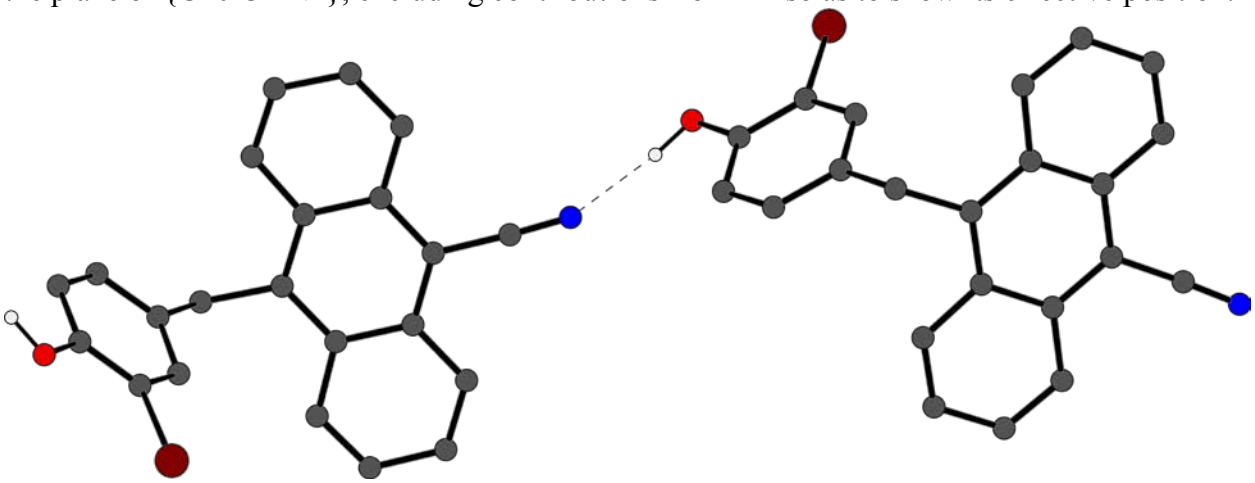

Figure S66. The hydrogen bonding in **12** with atoms and H1 shown as circles for clarity; most hydrogen atoms are omitted. The hydrogen bond interaction is highlighted with a dashed line.

Table S39. Summary of experimental and calculated structural parameters of the hydrogen bond in **1**-**8**.

	$d_{O\cdots N}$ / Å		d_{O-H} / Å		<(OHN) / º		δ(ppm)
	XDR	DFT*	XDR	DFT*	XDR	DFT*	O*H*···N‡
1	2.5549(13)	2.547	0.955(18)	1.011	151.9(16)	149.9	14.36
2	---	2.546	---	1.011	---	149.9	14.39
3	2.5338(15)	2.529	1.00(2)	1.018	154(2)	150.7	14.80
4	---	2.564	---	1.003	---	148.7	13.17
5	2.5787(14)	2.549	0.98(2)	1.01	152.8(18)	149.9	14.31
6	2.566(5)†	2.553	1.02(3)†	1.009	153(7)†	149.7	14.1
7	---	2.564	---	1.004	---	148.8	13.3
8	---	2.584	---	0.997	---	147.8	12.64

* Data from calculated geometry optimization using DFT (B3LYP/6-31++G**) CPCM of CH_2Cl_2. † Data from ref (*16*), ‡ triads **1**-**2**, **4**-**8** in $CDCl_3$, triad **3** in CD_2Cl_2.

Data S1. Triad 1 UV-VIS TA in CH_2Cl_2.

Transient absorption UV pump/Vis probe for triad 1 in CH_2Cl_2 shows spectral features and time evolution of the LES and CSS.

Data S2. Triad 1 mid-IR TA in CH_2Cl_2.

Transient absorption UV pump/mid-IR probe for triad 1 in CH_2Cl_2 shows spectral features and time evolution of the LES, CSS and GS.

References and Notes

1. D. R. Weinberg, C. J. Gagliardi, J. F. Hull, C. F. Murphy, C. A. Kent, B. C. Westlake, A. Paul, D. H. Ess, D. G. McCafferty, T. J. Meyer, Proton-coupled electron transfer. *Chem. Rev.* **112**, 4016–4093 (2012). doi:10.1021/cr200177j Medline

2. S. Hammes-Schiffer, A. A. Stuchebrukhov, Theory of coupled electron and proton transfer reactions. *Chem. Rev.* **110**, 6939–6960 (2010). doi:10.1021/cr1001436 Medline

3. J. J. Warren, T. A. Tronic, J. M. Mayer, Thermochemistry of proton-coupled electron transfer reagents and its implications. *Chem. Rev.* **110**, 6961–7001 (2010). doi:10.1021/cr100085k Medline

4. S. Y. Reece, D. G. Nocera, Proton-coupled electron transfer in biology: Results from synergistic studies in natural and model systems. *Annu. Rev. Biochem.* **78**, 673–699 (2009). doi:10.1146/annurev.biochem.78.080207.092132 Medline

5. Z. W. Seh, J. Kibsgaard, C. F. Dickens, I. Chorkendorff, J. K. Nørskov, T. F. Jaramillo, Combining theory and experiment in electrocatalysis: Insights into materials design. *Science* **355**, eaad4998 (2017). doi:10.1126/science.aad4998 Medline

6. D. C. Miller, K. T. Tarantino, R. R. Knowles, Proton-coupled electron transfer in organic synthesis: Fundamentals, applications, and opportunities. *Top. Curr. Chem.* **374**, 30 (2016). doi:10.1007/s41061-016-0030-6 Medline

7. J. C. Lennox, D. A. Kurtz, T. Huang, J. L. Dempsey, Excited-state proton-coupled electron transfer: Different avenues for promoting proton/electron movement with solar photons. *ACS Energy Lett.* **2**, 1246–1256 (2017). doi:10.1021/acsenergylett.7b00063

8. G. L. Closs, J. R. Miller, Intramolecular long-distance electron transfer in organic molecules. *Science* **240**, 440–447 (1988). doi:10.1126/science.240.4851.440 Medline

9. R. A. Marcus, Electron transfer reactions in chemistry: Theory and experiment (Nobel Lecture). *Angew. Chem. Int. Ed. Engl.* **32**, 1111–1121 (1993). doi:10.1002/anie.199311113

10. R. A. Marcus, N. Sutin, Electron transfers in chemistry and biology. *Biochim. Biophys. Acta* **811**, 265–322 (1985). doi:10.1016/0304-4173(85)90014-X

11. P. F. Barbara, T. J. Meyer, M. A. Ratner, Contemporary issues in electron transfer research. *J. Phys. Chem.* **100**, 13148–13168 (1996). doi:10.1021/jp9605663

12. K. S. Peters, A theory-experiment conundrum for proton transfer. *Acc. Chem. Res.* **42**, 89–96 (2009). doi:10.1021/ar8001156 Medline

13. P. Blowers, R. I. Masel, An extension of the marcus equation for atom transfer reactions. *J. Phys. Chem. A* **103**, 7047–7054 (1999). doi:10.1021/jp990039u

14. C. P. Andrieux, J. Gamby, P. Hapiot, J.-M. Savéant, Evidence for inverted region behavior in proton transfer to carbanions. *J. Am. Chem. Soc.* **125**, 10119–10124 (2003). doi:10.1021/ja035268f Medline

15. S. J. Edwards, A. V. Soudackov, S. Hammes-Schiffer, Driving force dependence of rates for nonadiabatic proton and proton-coupled electron transfer: Conditions for inverted region behavior. *J. Phys. Chem. B* **113**, 14545–14548 (2009). doi:10.1021/jp907808t Medline

16. M. A. Bowring, L. R. Bradshaw, G. A. Parada, T. P. Pollock, R. J. Fernández-Terán, S. S. Kolmar, B. Q. Mercado, C. W. Schlenker, D. R. Gamelin, J. M. Mayer, Activationless multiple-site concerted proton-electron tunneling. *J. Am. Chem. Soc.* **140**, 7449–7452 (2018). doi:10.1021/jacs.8b04455 Medline

17. Materials, methods, and additional information are available as supplementary materials.

18. I. J. Rhile, T. F. Markle, H. Nagao, A. G. DiPasquale, O. P. Lam, M. A. Lockwood, K. Rotter, J. M. Mayer, Concerted proton-electron transfer in the oxidation of hydrogen-bonded phenols. *J. Am. Chem. Soc.* **128**, 6075–6088 (2006). doi:10.1021/ja054167+ Medline

19. T. A. Gadosy, D. Shukla, L. J. Johnston, Generation, characterization, and deprotonation of phenol radical cations. *J. Phys. Chem. A* **103**, 8834–8839 (1999). doi:10.1021/jp992216x

20. S. D. Glover, C. Jorge, L. Liang, K. G. Valentine, L. Hammarström, C. Tommos, Photochemical tyrosine oxidation in the structurally well-defined α_3Y protein: Proton-coupled electron transfer and a long-lived tyrosine radical. *J. Am. Chem. Soc.* **136**, 14039–14051 (2014). doi:10.1021/ja503348d Medline

21. T. F. Markle, T. A. Tronic, A. G. DiPasquale, W. Kaminsky, J. M. Mayer, Effect of basic site substituents on concerted proton-electron transfer in hydrogen-bonded pyridyl-phenols. *J. Phys. Chem. A* **116**, 12249–12259 (2012). doi:10.1021/jp311388n Medline

22. W. D. Morris, J. M. Mayer, Separating proton and electron transfer effects in three-component concerted proton-coupled electron transfer reactions. *J. Am. Chem. Soc.* **139**, 10312–10319 (2017). doi:10.1021/jacs.7b03562 Medline

23. T. Asahi, M. Ohkohchi, R. Matsusaka, N. Mataga, R. P. Zhang, A. Osuka, K. Maruyama, Intramolecular photoinduced charge separation and charge recombination of the product ion pair states of a series of fixed-distance dyads of porphyrins and quinones: Energy gap and temperature dependences of the rate constants. *J. Am. Chem. Soc.* **115**, 5665–5674 (1993). doi:10.1021/ja00066a036

24. P. F. Barbara, G. C. Walker, T. P. Smith, Vibrational modes and the dynamic solvent effect in electron and proton transfer. *Science* **256**, 975–981 (1992). doi:10.1126/science.256.5059.975 Medline

25. J. Ulstrup, J. Jortner, The effect of intramolecular quantum modes on free energy relationships for electron transfer reactions. *J. Chem. Phys.* **63**, 4358–4368 (1975). doi:10.1063/1.431152

26. A. Soudackov, S. Hammes-Schiffer, Derivation of rate expressions for nonadiabatic proton-coupled electron transfer reactions in solution. *J. Chem. Phys.* **113**, 2385–2396 (2000). doi:10.1063/1.482053

27. A. Torrado, B. Imperiali, New synthetic amino acids for the design and synthesis of peptide-based metal ion sensors. *J. Org. Chem.* **61**, 8940–8948 (1996). doi:10.1021/jo961466w Medline

28. W. L. F. Armarego, C. Chai, "Purification of organic chemicals" in *Purification of Laboratory Chemicals* (Butterworth-Heinemann, ed. 7, 2013), chap. 4, pp. 103–554.

29. R. H. Goldsmith, J. Vura-Weis, A. M. Scott, S. Borkar, A. Sen, M. A. Ratner, M. R. Wasielewski, Unexpectedly similar charge transfer rates through benzo-annulated bicyclo[2.2.2]octanes. *J. Am. Chem. Soc.* **130**, 7659–7669 (2008). doi:10.1021/ja8004623 Medline

30. I. H. M. van Stokkum, D. S. Larsen, R. van Grondelle, Global and target analysis of time-resolved spectra. *Biochim. Biophys. Acta* **1657**, 82–104 (2004). doi:10.1016/j.bbabio.2004.04.011 Medline

31. K. M. Mullen, I. H. M. van Stokkum, TIMP: An R package for modeling multi-way spectroscopic measurements. *J. Stat. Softw.* **18**, 1–46 (2007). doi:10.18637/jss.v018.i03

32. J. J. Snellenburg, S. Laptenok, R. Seger, K. M. Mullen, I. H. M. van Stokkum, Glotaran: A Java-based graphical user interface for the R package TIMP. *J. Stat. Softw.* **49**, 22 (2012). doi:10.18637/jss.v049.i03

33. D. S. Kliger, A. C. Albrecht, Polarized spectroscopy of excited states of substituted anthracenes on a nanosecond time scale. *J. Chem. Phys.* **53**, 4059–4065 (1970). doi:10.1063/1.1673879

34. A. Weller, Electron-transfer and complex formation in the excited state. *Pure Appl. Chem.* **16**, 115–124 (1968). doi:10.1351/pac196816010115

35. C. Costentin, C. Louault, M. Robert, J.-M. Savéant, The electrochemical approach to concerted proton—Electron transfers in the oxidation of phenols in water. *Proc. Natl. Acad. Sci. U.S.A.* **106**, 18143–18148 (2009). doi:10.1073/pnas.0910065106 Medline

36. B. H. Solis, S. Hammes-Schiffer, Proton-coupled electron transfer in molecular electrocatalysis: Theoretical methods and design principles. *Inorg. Chem.* **53**, 6427–6443 (2014). doi:10.1021/ic5002896 Medline

37. M. J. Frisch, G. W. Trucks, H. B. Schlegel, G. E. Scuseria, M. A. Robb, J. R. Cheeseman, G. Scalmani, V. Barone, B. Mennucci, G. A. Petersson, H. Nakatsuji, M. Caricato, X. Li, H. P. Hratchian, A. F. Izmaylov, J. Bloino, G. Zheng, J. L. Sonnenberg, M. Hada, M. Ehara, K. Toyota, R. Fukuda, J. Hasegawa, M. Ishida, T. Nakajima, Y. Honda, O. Kitao, H. Nakai, T. Vreven, J. A. Montgomery Jr., J. E. Peralta, F. Ogliaro, M. Bearpark, J. J. Heyd, E. Brothers, K. N. Kudin, V. N. Staroverov, T. Keith, R. Kobayashi, J. Normand, K. Raghavachari, A. Rendell, J. C. Burant, S. S. Iyengar, J. Tomasi, M. Cossi, N. Rega, J. M. Millam, M. Klene, J. E. Knox, J. B. Cross, V. Bakken, C. Adamo, J. Jaramillo, R. Gomperts, R. E. Stratmann, O. Yazyev, A. J. Austin, R. Cammi, C. Pomelli, J. W. Ochterski, R. L. Martin, K. Morokuma, V. G. Zakrzewski, G. A. Voth, P. Salvador, J. J. Dannenberg, S. Dapprich, A. D. Daniels, O. Farkas, J. B. Foresman, J. V. Ortiz, J. Cioslowski, D. J. Fox, Gaussian 09, Gaussian, Inc. (2010).

38. A. D. Becke, Density-functional thermochemistry. III. The role of exact exchange. *J. Chem. Phys.* **98**, 5648–5652 (1993). doi:10.1063/1.464913

39. C. Lee, W. Yang, R. G. Parr, Development of the Colle-Salvetti correlation-energy formula into a functional of the electron density. *Phys. Rev. B* **37**, 785–789 (1988). doi:10.1103/PhysRevB.37.785 Medline

40. W. J. Hehre, R. Ditchfield, J. A. Pople, Self—consistent molecular orbital methods. XII. Further extensions of Gaussian—type basis sets for use in molecular orbital studies of organic molecules. *J. Chem. Phys.* **56**, 2257–2261 (1972). doi:10.1063/1.1677527

41. T. Clark, J. Chandrasekhar, G. W. Spitznagel, P. V. R. Schleyer, Efficient diffuse function-augmented basis sets for anion calculations. III. The 3-21+G basis set for first-row elements, Li-F. *J. Comput. Chem.* **4**, 294–301 (1983). doi:10.1002/jcc.540040303

42. P. C. Hariharan, J. A. Pople, The influence of polarization functions on molecular orbital hydrogenation energies. *Theor. Chim. Acta* **28**, 213–222 (1973). doi:10.1007/BF00533485

43. V. Barone, M. Cossi, Quantum calculation of molecular energies and energy gradients in solution by a conductor solvent model. *J. Phys. Chem. A* **102**, 1995–2001 (1998). doi:10.1021/jp9716997

44. M. Namazian, C. Y. Lin, M. L. Coote, Benchmark calculations of absolute reduction potential of Ferricinium/Ferrocene couple in nonaqueous solutions. *J. Chem. Theory Comput.* **6**, 2721–2725 (2010). doi:10.1021/ct1003252 Medline

45. J. N. Schrauben, M. Cattaneo, T. C. Day, A. L. Tenderholt, J. M. Mayer, Multiple-site concerted proton-electron transfer reactions of hydrogen-bonded phenols are nonadiabatic and well described by semiclassical Marcus theory. *J. Am. Chem. Soc.* **134**, 16635–16645 (2012). doi:10.1021/ja305668h Medline

46. A. P. Davis, A. J. Fry, Experimental and computed absolute redox potentials of polycyclic aromatic hydrocarbons are highly linearly correlated over a wide range of structures and potentials. *J. Phys. Chem. A* **114**, 12299–12304 (2010). doi:10.1021/jp106088n Medline

47. T. Yanai, D. P. Tew, N. C. Handy, A new hybrid exchange–correlation functional using the Coulomb-attenuating method (CAM-B3LYP). *Chem. Phys. Lett.* **393**, 51–57 (2004). doi:10.1016/j.cplett.2004.06.011

48. J.-D. Chai, M. Head-Gordon, Systematic optimization of long-range corrected hybrid density functionals. *J. Chem. Phys.* **128**, 084106 (2008). doi:10.1063/1.2834918 Medline

49. S. F. Nelsen, S. C. Blackstock, Y. Kim, Estimation of inner shell Marcus terms for amino nitrogen compounds by molecular orbital calculations. *J. Am. Chem. Soc.* **109**, 677–682 (1987). doi:10.1021/ja00237a007

50. B. Auer, L. E. Fernandez, S. Hammes-Schiffer, Theoretical analysis of proton relays in electrochemical proton-coupled electron transfer. *J. Am. Chem. Soc.* **133**, 8282–8292 (2011). doi:10.1021/ja201560v Medline

51. S. Horvath, L. E. Fernandez, A. V. Soudackov, S. Hammes-Schiffer, Insights into proton-coupled electron transfer mechanisms of electrocatalytic H_2 oxidation and production. *Proc. Natl. Acad. Sci. U.S.A.* **109**, 15663–15668 (2012). doi:10.1073/pnas.1118333109 Medline

52. L. Biczók, N. Gupta, H. Linschitz, Coupled Electron-Proton Transfer in Interactions of Triplet C_{60} with Hydrogen-Bonded Phenols: Effects of Solvation, Deuteration, and Redox Potentials. *J. Am. Chem. Soc.* **119**, 12601–12609 (1997). doi:10.1021/ja9727528

53. I. J. Rhile, J. M. Mayer, One-electron oxidation of a hydrogen-bonded phenol occurs by concerted proton-coupled electron transfer. *J. Am. Chem. Soc.* **126**, 12718–12719 (2004). doi:10.1021/ja031583q Medline

54. C. Costentin, M. Robert, J.-M. Savéant, Adiabatic and non-adiabatic concerted proton-electron transfers. Temperature effects in the oxidation of intramolecularly hydrogen-bonded phenols. *J. Am. Chem. Soc.* **129**, 9953–9963 (2007). doi:10.1021/ja071150d Medline

55. T. Irebo, O. Johansson, L. Hammarström, The rate ladder of proton-coupled tyrosine oxidation in water: A systematic dependence on hydrogen bonds and protonation state. *J. Am. Chem. Soc.* **130**, 9194–9195 (2008). doi:10.1021/ja802076v Medline

56. T. F. Markle, I. J. Rhile, J. M. Mayer, Kinetic effects of increased proton transfer distance on proton-coupled oxidations of phenol-amines. *J. Am. Chem. Soc.* **133**, 17341–17352 (2011). doi:10.1021/ja2056853 Medline

57. T. F. Markle, A. L. Tenderholt, J. M. Mayer, Probing quantum and dynamic effects in concerted proton-electron transfer reactions of phenol-base compounds. *J. Phys. Chem. B* **116**, 571–584 (2012). doi:10.1021/jp2091736 Medline

58. S. D. Glover, G. A. Parada, T. F. Markle, S. Ott, L. Hammarström, Isolating the effects of the proton tunneling distance on proton-coupled electron transfer in a series of homologous tyrosine-base model compounds. *J. Am. Chem. Soc.* **139**, 2090–2101 (2017). doi:10.1021/jacs.6b12531 Medline

59. I. Kaljurand, T. Rodima, I. Leito, I. A. Koppel, R. Schwesinger, Self-consistent spectrophotometric basicity scale in acetonitrile covering the range between pyridine and DBU. *J. Org. Chem.* **65**, 6202–6208 (2000). doi:10.1021/jo005521j Medline

60. J. Ho, Are thermodynamic cycles necessary for continuum solvent calculation of pK_as and reduction potentials? *Phys. Chem. Chem. Phys.* **17**, 2859–2868 (2015). doi:10.1039/C4CP04538F Medline